Investigation of the Properties of Nuclear Matter and Particle Structure at the Collider of Relativistic Nuclei and Polarized Protons

Project STAR (JINR Participation)

A. Aitbaev, A.A. Aparin, G.S. Averichev, H.N. Agakishiev, N.A. Balashov, T.G. Dedovich, I.Zh. Bunzarov, N.Y. Chankova-Bunzarova, V.B. Dunin, J. Fedorishin, P. Filip, A.O. Kechechian, O. Kenzhegulov, K.V. Klygina, V.V. Korenkov, A.A. Korobitsyn, R. Lednický, V.V. Lyuboshitz, S.I. Manukhov, V.V. Mitsyn, M.P. Osmachko, G.A. Ososkov, Yu.A. Panebrattsev, S.S. Panyushkina, E.A. Pervyshina, E.V. Potrebenikova, N.E. Sidorov, E. Shakhaliev, S.I. Snigirev, M.V. Tokarev, A. Tutebaeva, N.I. Vorontsova, S.F. Vokal, I. Zborovsky

Leaders: Richard Lednický, Yury Panebrattsev

JINR TOPIC: 02-0-1066-2007/2023

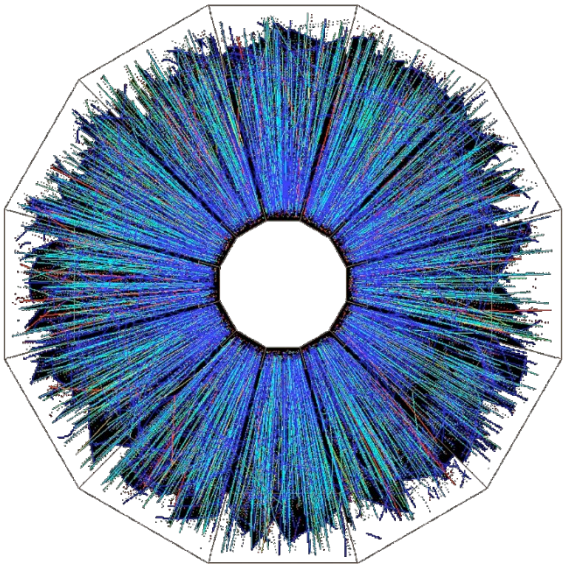

Dubna, 2021

INVESTIGATION OF THE PROPERTIES OF NUCLEAR MATTER AND PARTICLE STRUCTURE AT THE COLLIDER OF RELATIVISTIC NUCLEI AND POLARIZED PROTONS

PROJECT STAR (JINR PARTICIPATION)

CODE OF THEME: 02-0-1066-2007/2023

A. AITBAEV, A.A. APARIN, G.S. AVERICHEV, H.N. AGAKISHIEV, N.A. BALASHOV, T.G. DEDOVICH, I.ZH. BUNZAROV, N.Y. CHANKOVA-BUNZAROVA, V.B. DUNIN, J. FEDORISHIN, P. FILIP, A.O. KECHECHIAN, O. KENZHEGULOV, K.V. KLYGINA, V.V. KORENKOV, A.A. KOROBITSYN, R. LEDNICKÝ, V.V. LYUBOSHITZ, S.I. MANUKHOV, V.V. MITSYN, M.P. OSMACHKO, G.A. OSOSKOV, YU.A. PANEBRATTSEV, S.S. PANYUSHKINA, E.A. PERVYSHINA, E.V. POTREBENIKOVA, N.E. SIDOROV, E. SHAKHALIEV, S.I. SNIGIREV, M.V. TOKAREV, A. TUTEBAEVA, N.I. VORONTSOVA, S.F. VOKAL, I. ZBOROVSKY

NAMES OF PROJECT LEADERS: R. LEDNICKÝ, YU.A. PANEBRATTSEV

DATE OF SUBMISSION OF PROPOSAL OF PROJECT TO SOD _____

DATE OF THE LABORATORY STC _____ DOCUMENT NUMBER _____

STARTING DATE OF PROJECT _____

Form No. 25

PROJECT ENDORSEMENT LIST

INVESTIGATION OF THE PROPERTIES OF NUCLEAR MATTER
AND PARTICLE STRUCTURE
AT THE COLLIDER OF RELATIVISTIC NUCLEI AND POLARIZED PROTONS

PROJECT STAR (JINR PARTICIPATION)

CODE OF THEME: 02-0-1066-2007/2023

NAME OF PROJECT LEADERS: R. LEDNICKÝ, YU.A. PANEBRATTSEV

APPROVED BY JINR DIRECTOR		
	SIGNATURE	DATE
ENDORSED BY		
JINR VICE-DIRECTOR		
	SIGNATURE	DATE
CHIEF SCIENTIFIC SECRETARY		
	SIGNATURE	DATE
CHIEF ENGINEER		
	SIGNATURE	DATE
HEAD OF SCIENCE ORGANIZATION DEPARTMENT		
	SIGNATURE	DATE
LABORATORY DIRECTOR		
	SIGNATURE	DATE
LABORATORY CHIEF ENGINEER		
	SIGNATURE	DATE
PROJECT LEADER		
	SIGNATURE	DATE
PROJECT LEADER		
	SIGNATURE	DATE
ENDORSED		
RESPECTIVE PAC		
	SIGNATURE	DATE

Form No. 26

Schedule proposal and resources required for the implementation of the Project
STAR (JINR participation)
(Project title)

Expenditures, resources, financing sources			Costs (k$) Resource requirements	Proposals of the Laboratory on the distribution of finances and resources		
				2022	2023	2024
Expenditures		Main units of equipment, work towards its upgrade, adjustment etc.	30	10	10	10
		Materials	15	5	5	5
Required resources	Standard hour	Resources of – Laboratory design bureau; – JINR Experimental Workshop; – Laboratory experimental facilities division; – accelerator; – computer. Operating costs.				
		Payments for agreement-based research	45	15	15	15
ISTC		Travel allowance, including: a) Non-rouble zone countries b) rouble zone countries c) protocol-based	165	55	55	55
Financing sources	Budgetary resources	Budget expenditures including foreign-currency resources.	**255**	**85**	**85**	**85**
	External resources	Contributions by collaborators. Grants. Contributions by sponsors. Contracts. Other financial resources, etc.				

PROJECT LEADER

SIGNATURE

Form No. 29

Estimated expenditures for the Project STAR (JINR participation)

Investigation of the properties of nuclear matter and particle structure at the collider of relativistic nuclei and polarized protons

(full title of Project)

Expenditure items	Full cost	2022	2023	2024
Direct expenses for the Project				
1. Accelerator, reactor	–	–	–	–
2. Computers	–	–	–	–
3. Computer connection	–	–	–	–
4. Design bureau	–	–	–	–
5. Experimental Workshop	–	–	–	–
6. Materials	15	5	5	5
7. Equipment	30	10	10	10
8. Construction/repair of premises	–	–	–	–
9. Payments for agreement-based research	45	15	15	15
10. Travel allowance, including: a) non-rouble zone countries b) rouble zone countries c) protocol-based	165	55	55	55
Total direct expenses	**255**	**85**	**85**	**85**

PROJECT LEADER

LABORATORY DIRECTOR

LABORATORY CHIEF ENGINEER-ECONOMIST

Abstract

The goal of the STAR project (JINR participation) is to study the properties of nuclear matter at extreme densities and temperatures, to search for signatures of quark deconfinement and possible phase transitions in heavy ion collisions over a wide energy range at the Relativistic Heavy Ion Collider (RHIC). The research program also includes the study of the structure functions of quarks and gluons in collisions of transversely and longitudinally polarized protons.

The first section of this document is devoted to a discussion of the main results in the STAR experiment in 2019–2021, and the contribution of the JINR group to this research.

The following sections of the document are devoted to a discussion of the priority physical tasks of the STAR experiment in 2021–2025. First, this is the completion of studies under the BES-II program. There are also two new research programs for 2022–2025 with an expanded acceptance of the STAR facility in the direction of the forward angles – the HOT QCD Physics program in experiments with heavy ions and Cold QCD Physics programs in experiments on the collision of polarized protons and polarized protons with nuclei.
At the end of the document, the priority tasks in the STAR experiment for the JINR group are formulated.
Below is the Beam Use Request outlines the physics programs that compels the STAR collaboration to request data taking during the years 2021–2025.

STAR's **highest scientific priorities** for Run-21 and Run-22 are to complete second phase of the Beam Energy Scan (BES-II) program, and initiate the "must-do" Cold QCD forward physics program enabled by the newly completed suite of forward detectors via the collection of transversely polarized $p + p$ data at 510 GeV. From 2023–25 we will use a combination of soft and hard probes to explore the microstructure of the QGP and continue the forward physics program via the collection of high statistics Au + Au, p + Au and $p + p$ data at $\sqrt{s_{\mathrm{NN}}}$ = 200 GeV.

The BES-II program has so far been very successful. As shown in Table 1, we have recorded collisions at $\sqrt{s_{\mathrm{NN}}}$ = 9.2–27 GeV in collider mode, and $\sqrt{s_{\mathrm{NN}}}$ = 3–7.7 GeV in fixed target (FXT) mode. In Run-21, as shown in Table 2, our number one priority is to complete the BES-II by recording 100 M good events at $\sqrt{s_{\mathrm{NN}}}$ = 7.7 GeV.

Table 1. Summary of all BES-II and FXT Au + Au beam energies, equivalent chemical potential, event statistics, run times, and date collected.

Beam Energy (GeV/nucleon)	$\sqrt{s_{\mathrm{NN}}}$ (GeV)	μ_B (MeV)	Run Time	Number Events Requested (Recorded)	Date Collected
13.5	27	156	24 days	(560 M)	Run-18
9.8	19.6	206	36 days	400 M (582 M)	Run-19
7.3	14.6	262	60 days	300 M (324 M)	Run-19
5.75	11.5	316	54 days	230 M (235 M)	Run-20
4.59	9.2	373	102 days	160 M (162 M)[1]	Run-20 + 20b
31.2	7.7 (FXT)	420	0.5+1.1 days	100 M (50 M+112 M)	Run-19 + 20
19.5	6.2 (FXT)	487	1.4 days	100 M (118 M)	Run-20
13.5	5.2 (FXT)	541	1.0 day	100 M (103 M)	Run-20
9.8	4.5 (FXT)	589	0.9 days	100 M (108 M)	Run-20
7.3	3.9 (FXT)	633	1.1 days	100 M (117 M)	Run-20
5.75	3.5 (FXT)	666	0.9 days	100 M (116 M)	Run-20
4.59	3.2 (FXT)	699	2.0 days	100 M (200 M)	Run-19

3.85	3.0 (FXT)	721	4.6 days	100 M (259 M)	Run-18
3.85	7.7	420	11-20 weeks	100 M	Run-21[2]

[1]Run-20b data taking completed 7:30am Sept 1.

[2]Data not yet collected, Run-21 forms part of this year's BUR.

Table 2. Proposed Run-21 assuming 24–28 cryo-weeks, including an initial one week of cooldown, one week for CeC, a one week set-up time for each collider energy and 0.5 days for each FXT energy.

Single-Beam Energy (GeV/nucleon)	$\sqrt{s_{\mathrm{NN}}}$ (GeV)	Run Time	Species	Events (MinBias)	Priority
3.85	7.7	11-20 weeks	Au + Au	100 M	1
3.85	3 (FXT)	3 days	Au + Au	300 M	2
44.5	9.2 (FXT)	0.5 days	Au + Au	50 M	2
70	11.5 (FXT)	0.5 days	Au + Au	50 M	2
100	13.7 (FXT)	0.5 days	Au + Au	50 M	2
100	200	1 week	O + O	400 M 200 M (central)	3
8.35	17.1	2.5 weeks	Au + Au	250 M	3
3.85	3 (FXT)	3 weeks	Au + Au	2 B	3

Based on guidance from the Collider-Accelerator Department (CAD) and past experience we expect that the bulk of Run-21 will be devoted to Au + Au collisions at $\sqrt{s_{\mathrm{NN}}}$ = 7.7 GeV, the lowest collider energy of the program. Collection of these events is our highest priority. However, if we assume optimistic, but not overly so, rates and up-times, and 28 cryo-weeks, we project that the opportunity to collect of other exciting datasets will arise.

The **second highest priority** for Run-21 identified by the STAR collaboration is four short FXT runs; the collection of 300 M good events at $\sqrt{s_{\mathrm{NN}}}$ = 3 GeV and 50 M good events at each of three higher beam energies ($\sqrt{s_{\mathrm{NN}}}$ = 9.2, 11.5, and 13.7 GeV). In the second highest priority b the 3 GeV FXT system is listed first for reasons of logistics. It is recognized that the opportunity to address the topics listed as second and third priorities will be contingent on the performance of the 7.7 GeV collider run. Should it become evident early on in that run (in the first 4–8 weeks or so), that performance is exceeding the conservative projections and that time will be available at the end of Run-21, then it would beneficial to take three days to complete the 3 GeV FXT run. This system uses the same single beam energy (3.85 GeV) as the 7.7 GeV collider program, so there would be no time lost transitioning, and acquiring these data early in the run would give sufficient time to analyze the results of the ExpressStream production to investigate the acceptance and background for the search of the double-Λ hypernucleus and determine the statistics necessary to pursue this physics topic (currently estimated to be three weeks). 300 M events at 3 GeV with the enhanced iTPC and eTOF coverage gives access to the proton higher moments, precision φ, hypernuclei, and dilepton measurements. The higher $\sqrt{s_{\mathrm{NN}}}$ FXT data combined with the collider data at the same energy will provide full proton rapidity coverage allowing us to probe in detail the mechanisms of stopping at play in heavy-ion collisions. We estimate the total run time required to collect all these datasets is 6 days.

The STAR collaboration also finds important scientific opportunities are presented by the collection of our **third highest priority** datasets:

- O + O data at $\sqrt{s_{\mathrm{NN}}}$ = 200 GeV, in the context of understanding the early-time conditions of small systems. These data would allow for a direct comparison with a similarly proposed higher-energy O + O run at the LHC, and further motivate the case for a small system scan complementary to ongoing efforts by the NA61/SHINE collaboration at SPS energies, and other proposed light-ion species at the LHC.
- A sixth collider beam energy at $\sqrt{s_{\mathrm{NN}}}$ = 17.1 GeV. These data will provide for a finer scan in a range where the energy dependence of the net-proton kurtosis and neutron density fluctuations appear to undergo a sudden change.
- 2 B good events at $\sqrt{s_{\mathrm{NN}}}$ = 3 GeV in FXT mode. The enhanced statistics enables the measurements of mid-rapidity proton 5-th/6-th order moments/cumulants and the system size dependence of φ meson production. Furthermore, the large dataset has the potential to make the first measurement of (or put limits on) the production rate of the double-Λ hypernuclei.

The sequence with which we collect these datasets is currently somewhat fluid and are listed in the order of the requested run time; we do not want to take partial datasets. We expect to refine the ordering of our goals as Run-21 progresses. Collection of these data during future RHIC running periods is also of interest to the collaboration.

For Run-22, as shown in Table 3, we propose a dedicated 20 cryo-week transversely polarized $p + p$ run at $\sqrt{s}$ = 510 GeV. This run will take full advantage of STAR's new forward detection capabilities, consisting of a Forward Calorimeter System (FCS) and a Forward Tracking System (FTS) located between $2.5 < \eta < 4$, and further capitalizes on the recent BES-II detector upgrades.

Table 3. Proposed Run-22 assuming 20 cryo-weeks, including an initial one week of cool-down and a two weeks set-up time.

$\sqrt{s}$ (GeV)	Species	Polarization	Run Time	Sampled Luminosity	Priority
510	$p + p$	Transverse	16 weeks	400 pb^{-1}	1

These data will enable STAR to explore, with unprecedented precision, forward jet physics that probe both the high-x (largely valence quark) and low-*x* (primarily gluon) partonic regimes.

Looking further out, the STAR collaboration has determined that there is a compelling scientific program enabled by the first opportunity to capitalize on the combination of the BES-II and Forward Upgrades in the data collected from Au + Au, p + Au, and $p + p$ collisions at $\sqrt{s_{\mathrm{NN}}}$ = 200 GeV as outlined in Table 4.

Table 4. Proposed Run-23 – Run-25 assuming 24 (28) cryo-weeks of running every year, and 6 weeks set-up time to switch species in 2024. Sampled luminosities assume a "take all" triggers.

$\sqrt{s_{\mathrm{NN}}}$ (GeV)	Species	Number Events/ Sampled Luminosity	Date
200	Au + Au	10B / 38 nb^{-1}	2023
200	$p + p$	235 pb^{-1}	2024
200	p + Au	1.3 pb^{-1}	2024
200	Au + Au	10B / 52 nb^{-1}	2025

Significantly increased luminosities, the extended acceptance at mid-rapidity due to the iTPC, improved event plane and triggering capabilities of the EPD, and the ability to probe previously inaccessible forward region are all exploited in our Hot QCD program, that informs on the

microstructure of the QGP, and our Cold QCD program that will utilize transverse polarization setting the stage for related future measurements at the EIC.

Table of Contents

1. Issues Addressed and Main Goals of Researches

The goal of the STAR project (JINR participation) is to study the properties of nuclear matter at extreme densities and temperatures, to search for signatures of quark deconfinement and possible phase transitions in heavy ion collisions over a wide energy range at the Relativistic Heavy Ion Collider (RHIC). The research program also includes the study of the structure functions of quarks and gluons in collisions of transversely and longitudinally polarized protons.

The first section of this document is devoted to a discussion of the main results in the STAR experiment in 2019–2021, and the contribution of the JINR group to this research.

The following sections of the document are devoted to a discussion of the priority physical tasks of the STAR experiment in 2021–2025. First, this is the completion of studies under the BES-II program. There are also two new research programs for 2022–2025 with an expanded acceptance of the STAR facility in the direction of the forward angles – the HOT QCD Physics program in experiments with heavy ions and Cold QCD Physics programs in experiments on the collision of polarized protons and polarized protons with nuclei.

At the end of the document, the priority tasks in the STAR experiment for the JINR group are formulated.

2. Participation in the Heavy Ion and the Spin Physics program in STAR experiment at RHIC

This part of the project contains a short summary of the data obtained by the STAR Collabration and the JINR group during 2016–2020 and the first part of 2021, as well as proposal to continue of data tacking runs in the STAR experiment in the years 2021–2025.

In the **year 2016**, the run to study Heavy Flavor Physics has been hold at RHIC. At the present large statistics has been taken. The data processing is going on and the effects of suppression and collective flows in the events with open flavor (D_s, Λ_c, B, …) and quarkonia (J/ψ, Y) production are studied. One of main results of these researches is heavy quark suppression in gold-gold collisions at RHIC energy 200 GeV (Phys.Rev. C99(2019)034908).

In the **year 2017** the data taken run with polarized protons beams has been performed by STAR at RHIC. STAR's highest scientific priority is the first significant measurement of the sign change of the Sivers' function, when compared to the value measured in SIDIS, and evolution effects in transverse momentum distributions through measurements of single spin asymmetries in $W^{+/-}$, Z, direct photon and Drell-Yan pairs production in transversely polarized $p + p$ collisions at $\sqrt{s}$ = 510 GeV (arXiv:1607.01676).

One of the highlighted analyses from the STAR 2017 *pp* 510 GeV run is a measurement of the Z boson differential cross-section and its transverse single spin asymmetry A_N. The Z boson differential cross-section can be included in a global analysis to constrain the quark transverse momentum distribution (TMD) in the proton, the STAR data will especially constrain the TMDs at high x. The Z boson A_N is the cleanest observable to test the predicted non-universality of the Sivers function measures in deep inelastic scattering (DIS) and *pp* and TMD evolution effects, which are predicted to be large.

With the sample size (pp at $\sqrt{s}$ = 510 GeV, recorded luminosity 320 pb^{-1}, transverse polarization, average beam polarization 55 %) comparable to the previous 2011, 2012 and 2013 data combined, the 2017 Z boson differential cross-section $d\sigma/dp_T$ as a function of p_T has been extracted, and full

acceptance and efficiency corrections applied. The full systematic uncertainties for the 2017 results have been finished except for that due to the ongoing determination of the STAR 2017 barrel electro-magnetic calorimeter (BEMC) gain calibration. The currently measured Z boson A_N shows a hint of being away from zero in the positive direction, which favors the sign-change in the Sivers functions and small evolution effects. Howevere this analysis also requires the same BEMC gain calibration and its uncertainty mentioned in the above differential cross-section measurements.

In the **year 2018** the main task of the STAR collaboration was so call "the isobaric run" with ^{96}Zr and ^{96}Ru collisions. The study of isobaric collisions will provide enhanced clarity of the role of the magnetic field in the charge separation measurements. STAR scientific priority is the successful realization of the isobaric collision program. In 2018 there was two 3.5 week run with collisions of Ruthenium-96 (Ru + Ru) and Zirconium-96 (Zr + Zr) at $\sqrt{s_{\mathrm{NN}}}$ = 200 GeV. The following data analysis and comparison of results from these events will help clarify the interpretation of measurements related to the chiral magnetic effect. Since Ru nuclei have an atomic charge of 44 compared to 40 for Zr, Ru + Ru collisions will generate a magnetic field approximately 10 % larger than Zr + Zr collisions while all else remains essentially constant. Comparison of charge separation results will aid in determining the fraction of those measurements which are related to the chiral magnetic effect by isolating the magnetic field dependence. Our understanding of the chiral magnetic effect will thereby be greatly advanced and have a fundamental impact beyond the field of high-temperature QCD.

In this section, we briefly summarize the status of the production and analysis of the Isobar (^{96}Ru + ^{96}Ru and ^{96}Zr + ^{96}Zr) data collected in Run-18. The scientific goal that drove collection of this data was to clarify the interpretation of measurements related to the chiral magnetic effect. Comparison of charge separation results will aid in determining the fraction of those measurements which are related to the chiral magnetic effect by isolating the magnetic field dependence. STAR elected to perform blinded analyses on this dataset. This is the first known attempt of analysis blinding in the Heavy-Ion experimental community. We have implemented a detailed plan for how to ensure that we have successfully blinded all information that might reveal which isobar collision each event is the result of. To ensure transparency STAR plans to submit for publication a detailed description of the final blinding process prior to publication of the results.

In 2018 STAR's priority **also** was high statistics measurement and following data analysis of Au + Au collisions at $\sqrt{s_{\mathrm{NN}}}$ = 27 GeV which will allow to make statistically significant Λ and $\overline{\Lambda}$ global polarization measurements. These measurements used advantage of the newly installed Event Plane Detector's to improve reaction plane resolution. The JINR group participate in analyses of global polarization measurements at 27 GeV as well as energy dependence of this phenomena.

STAR's highest scientific priority for 2019–2021 is the commencement of the RHIC Beam Energy Scan II. BES-II is the research program to search for phase transition and critical point of QCD matter. The main goal of data tacking runs is dramatically enhancement of our understanding of the QCD phase diagram.

Three upgrades were completed prior to the BES-II. Both the inner Time Projection Chamber (iTPC) and the End-Cap Time of Flight (eTOF) were scheduled for full installation in Run 19; increasing the rapidity and low transverse momentum acceptance of STAR, and extending our particle identification capabilities. The Event Plane Detector (EPD) was fully installed for in 2018. The EPD provides enhanced event plane resolution and forward centrality measurements. JINR

physicists are have had participation in the work on the installation and preparation of the EPD (event plane detector) for these runs.

This program started with Run-19 in which the collaboration aims was to collect data from the two top collider energies of $\sqrt{s_{\mathrm{NN}}}$ =19.6 and 14.6 GeV as well as data from a subset of the fixed target (FXT) program. Collection of all the data outlined in Table 5 is STAR's highest scientific priority. BES-II will dramatically enhance our understanding of the QCD phase diagram. The proposed program involves dedicated low beam energy running and high precision measurements of the observables which have been proposed as sensitive to the phase structure of QCD matter. In addition to the five lower collider energies that have been put forward in past, STAR proposes a sixth collider beam energy at $\sqrt{s_{\mathrm{NN}}}$= 16.7 GeV. These data will provide for a finer scan in a range where the energy dependence of the net-proton kurtosis and neutron density fluctuations appears to undergo a sudden change.

Table 5. Summary of all BES-II and FXT Au + Au beam energies, equivalent chemical potential, requested event statistics, and run times.

Beam Energy (GeV/nucleon)	$\sqrt{s_{NN}}$ **(GeV)**	μ_B **(MeV)**	**Run time**	**Number Events**
9.8	19.6	205	4.5 weeks	400M
7.3	14.6	260	5.5 weeks	300M
8.35	16.7	235	5 weeks	250M
5.75	11.5	315	9.5 weeks	230M
4.55	9.1	370	9.5 weeks	160M
3.85	7.7	420	12 weeks	100M
31.2	7.7 (FXT)	420	2 days	100M
9.8	4.5 (FXT)	589	2 days	100M
7.3	3.9 (FXT)	633	2 days	100M
19.5	6.2 (FXT)	487	2 days	100M
13.5	5.2 (FXT)	541	2 days	100M
5.75	3.5 (FXT)	666	2 days	100M
4.55	3.2 (FXT)	699	2 days	100M
3.85	3.0 (FXT)	721	2 days	100M

With Run-19, the Collaboration will start its fixed-target (FXT) program which extends the reach of its BES-II program energy range down to lower center-of-mass energies. The proposed energies for both collider and fixed-target mode are summarized in Table 5.

As we have mentioned earlier three detector upgrades have been proposed for BES-II and have been successfully installed for Run-19. The upgrades increase STAR's acceptance both in rapidity and low transverse momentum, and extend its particle identification capabilities. The Event Plane Detector (EPD) was installed prior to Run-18. The inner Time Projection Chamber (iTPC) and the end-cap Time-of Flight (eTOF) commissioning have benefited from an extensive cosmic ray data taking campaign prior to Run-19. Following recommendations from the 2018 The STAR collaboration has commenced preparations to significantly improve its forward detection capabilities. A Forward Calorimeter System (FCS) and Forward Tracking System (FTS) will provide superior detection capabilities in the forward region between $2.5 < \eta < 4$.

STAR's **highest scientific priority for Run-20** was the continuation of the RHIC Beam Energy Scan II. The collaboration proposes to continue with the next two highest beam energies in collider mode (11.5and9.1GeV), as well as 6 FXT energies (7.7; 6.2; 5.2; 4.5; 3.94 3.5 GeV).

STAR's **highest scientific priority for Run-21** is the completion of the RHIC Beam Energy Scan II. The bulk of the 20-cryoweeks budget will be devoted to Au + Au collisions at the lowest collider energy of the program, at $\sqrt{s_{\mathrm{NN}}}$ = 7.7 GeV. We expect to refine our estimates of the projected run time for 7.7 GeV, currently 12 weeks, following some tests with C-AD towards the end of Run-19. The collaboration proposes to run the collider at $\sqrt{s_{\mathrm{NN}}}$ = 16.7 GeV to allow collection of an important data point between 14.6 and 19.6 GeV as is pointed out earlier in this summary. We list the Run-21 proposed priorities and sequence in Table 6. Depending on the availability of cryo-weeks in Run-20 and/or Run-21 the collaboration proposes to collect data set(s) in the context of a small system run using O + O collisions. These data would allow for a direct comparison with a similarly proposed higher-energy O + O run at the LHC around 2021–2022, and further motivate the case for a small system scan complementary to ongoing efforts by the NA61/SHINE collaboration at SPS energies, and other proposed light-ion species at the LHC.

Table 6. Proposed Run-21 assuming 20 cryo-weeks, including an initial one week of cool-down and a one week set-up time for each collider energy.

Beam Energy (GeV/nucleon)	$\sqrt{s_{\mathrm{NN}}}$ **(GeV)**	**μB (MeV)**	**Run time**	**Number Events**
3.85	7.7	Au + Au	12 weeks	100M
8.35	16.7	Au + Au	5 weeks	250M
100	200	O + O	1 week	400M

For Run-2022 period STAR Collaboration include a request for a dedicated 16-weeks pp run at 500 GeV. This run will take full advantage of STAR's new forward detection capabilities and further capitalize on the recent BES-II detector upgrades. We motivate a program that will use RHIC's unique ability to provide transverse and longitudinally polarized proton beams to exploit both an increased statistical power and kinematic reach from recent and planned detector upgrades as proposed.

3. Beam Energy Scan II Program. Search for QCD Critical Point

3.1. Physics objectives and Specific Observables

The BES-I scientific program has localized the most interesting regions and identified the observables which are likely to be the most discriminating for understanding the QCD phase structure. However, several of the key measurements were found to require higher statistics in order to provide a quantitative physics conclusion. Therefore, we propose to run a second phase of the beam energy scan (BES Phase-II) which is driven by the precision requirements of this suite of physics observables. The bullets below provide an overview of the observables key to achieving the goals of the BES Phase-II program. Following those bullets are subsections detailing the requirements and expected resolution that will be reached for each key observable.

- ***Onset of QGP***

Measurements to be carried out include: the nuclear modification factor as a function of p_T for produced hadrons, azimuthal anisotropy measurements as a function of p_T for identified hadrons with particular emphasis on the φ meson and the multi-strange hyperons, and the centrality dependence of charged particle correlations with respect to the reaction plane. Our current measurements show interesting trends in these measurements as a function of center-of-mass energies, and they point towards a possible turn-off of the signals of QGP below 19.6 GeV. The nuclear modification factor at high p_T having a value below unity is regarded as a signature of formation of hot and dense matter of quarks and gluons. Current measurements below 27 GeV do

not have sufficient event statistics to extend in p_T to 5 GeV/c, thereby preventing a quantitative conclusion on the turn-off of this signal of QGP. In the azimuthal anisotropy measurements, the v_2 of φ mesons plays a crucial role. Since generation of a large v_2 of φ mesons requires partonic interactions prior to the formation of φ, an absence or a low value of v_2 of φ mesons compared to other hadrons could indicate that the system created in heavy-ion collisions does not undergo the quark-hadron phase transition. Current measurements of v_2 of φ mesons versus p_T at 11.5 and 7.7 GeV provides such an indication, but with large statistical errors on the data points. A high statistics measurement of v_2 of φ mesons versus p_T is crucial in order to find out if a turn-off of partonic collectivity occurs below 19.6 GeV. The centrality dependence of a finite difference in charge correlations with respect to the reaction plane for same- and opposite-charge pairs is considered a signature of the Chiral Magnetic Effect. Within large statistical uncertainties, this difference is consistent with zero in BES-I measurements at 7.7 GeV. Since one of the prerequisites of this phenomenon is the formation of a partonic phase, a statistically significant null result at lower beam energies will be an observation of turn-off of QGP. With the higher event statistics of the BES Phase-II program further effects of the chiral magnetic wave, such as the chiral separation effect and the chiral vortex effect can also be studied.

- ***First-order phase transition***

The relevant measurements include the slope of rapidity dependence of directed flow for protons and net-protons, and tilt angle of the source as measured through azimuthally sensitive femtoscopy. A minimum in dv_1/dy versus center of mass energy has been argued to indicate the softest point in the EOS of the system formed in heavy-ion collisions. A statistically significant measurement has been obtained in BES-I, but the location of the minimum energy point has not been fixed precisely. Current measurements suggest that it lies somewhere between the energy values of 19.6 and 11.5 GeV, corresponding to a μ_B difference of more than 100 MeV. Furthermore, differential measurements of this observable, like as a function of collision centrality at different beam energies and for different baryon and meson species would provide additional data to refine this signature of a first-order phase transition. These additional measurements require increased statistics compared to BES-I. The tilt of the emission source is also proposed to have sensitivity to the softest point in the EOS. This observable is a new measurement unique to BES Phase-II. A measurement of this observable was not possible with the BES-I data to the high statistics demands of the azimuthally sensitive femtoscopy analysis which is necessary to infer coordinate space anisotropies.

- ***CriticalPoint***

A non-monotonic variation of the product of high moments for net- protons, specifically the $\kappa\sigma^2$ with beam energy has been considered in the literature as a signal for a CP. The current measurements indicate that the trend of net-proton $\kappa\sigma^2$ is flat from 200 to 39 GeV. Starting at 27 GeV, the values of $\kappa\sigma^2$ of net-proton show a clear drop. However, the statistical errors on the measurements at 11.5 and 7.7 GeV are too large for the purpose of further gauging the energy dependent variations at the lower energies. A high statistics measurement of the possible rise in the $\kappa\sigma^2$ values at energies below 19.6 GeV would open up an exciting opportunity to study the QCD critical point physics at RHIC.

- ***Chiral Phase Transition***

High statistics dilepton measurements to date provide the most powerful observable to understand in-medium effects and a possible chiral phase transition. While in the low mass region (around and below the ρ meson mass) there is the possibility of investigating symmetry restoration, the intermediate mass region allows a possible temperature measurement of the partonic phase. The

BES program has clearly demonstrated STARs capability for such measurements for energies as low as 19.6 GeV. The results obtained so far are consistent with formation of a partonic phase, with partial restoration of chiral symmetry, and suggest the importance of baryon-dominated interactions in affecting the ρ meson spectra. BES Phase-II will offer a great new opportunity to make a high-statistics measurement of dileptons at energies below 27 GeV to see the effect of the possible turn-off of QGP and the increased baryonic interactions in the system.

Table 7. Event statistics (in millions) needed for Beam Energy Scan Phase-II for various observables

Collision Energy (GeV)	7.7	9.1	11.5	14.5	19.6
μ_B (MeV) in 0-5% central collisions	420	370	315	260	205
Observables					
R_{CP} up to p_T = 5 GeV/c	–		160	125	92
Elliptic Flow (ϕ mesons)	100	150	200	200	400
Chiral Magnetic Effect	50	50	50	50	50
Directed Flow (protons)	50	75	100	100	200
Azimuthal Femtoscopy (protons)	35	40	50	65	80
Net-Proton Kurtosis	80	100	120	200	400
Dileptons	100	160	230	300	400
Required Number of Events	**100**	**160**	**230**	**300**	**400**

Table 7 shows the statistics requires to make a precision measurement of each proposed observable at each proposed energy.

3.2. Bulk correlations

Over the past years, the STAR collaboration has performed a series of correlation measurements directed towards a comprehensive understanding of the QCD phase diagram and the bulk properties of the QGP phase. Here we highlight the most recent STAR results on bulk correlations, which are expected to shed light on the QCD phase diagram as well as on the transport properties of the QGP.

Net-proton number fluctuations and the QCD critical point: One of the main goals of the STAR Beam Energy Scan (BES) program is to search for possible signatures of the QCD critical point (CP) by scanning the temperature (T) and the baryonic chemical potential (μ_B) plane by varying the collision energy. When the system produced in the heavy ion collisions approaches the CP, the correlation length diverges. Higher order cumulants of conserved net-particle multiplicity distributions are sensitive to such correlation lengths as the divergence of correlation length leads to enhanced fluctuations in the net-particle multiplicity distributions.

The ratios of the cumulants of identified net-particle multiplicity distributions, such as net-protons, have been predicted to be ideal observables sensitive to the onset of the QCD phase transition and the location of the CP. A non-monotonic variation of these ratio of cumulants, such as C_4/C_2 ($= k\sigma^2$), as a function of collision energy has been proposed to be an experimental signature of the CP. Taking the ratios of cumulants has advantages as it cancels the volume fluctuations to first order. Further, these ratios of cumulants are related to the ratio of baryon-number susceptibilities at a given T and μB. Near the critical point, QCD-based calculations predict the net-baryon number distributions to be non-Gaussian and susceptibilities to diverge, causing these ratios to have non-monotonic variation as a function of collision energy. However, the finite-size and finite-time

effects in heavy-ion collisions limit the growth of correlation length, and hence it could restrict the values of $k\sigma^2$ from its divergence as a function of collision energy.

Figure 1 shows the collision energy variation of net-proton $k\sigma^2$ for central and peripheral Au + Au collisions within the acceptance of $0.4 < p_T < 2.0$ GeV and $|y| < 0.5$. In central collisions, a non-monotonic variation with beam energy is observed for $k\sigma^2$ with a significance of 3.0 σ. In contrast, monotonic behavior with beam energy is observed for the statistical hadron gas (HRG) model, and for a nuclear transport UrQMD model without a critical point, and experimentally in peripheral collisions.

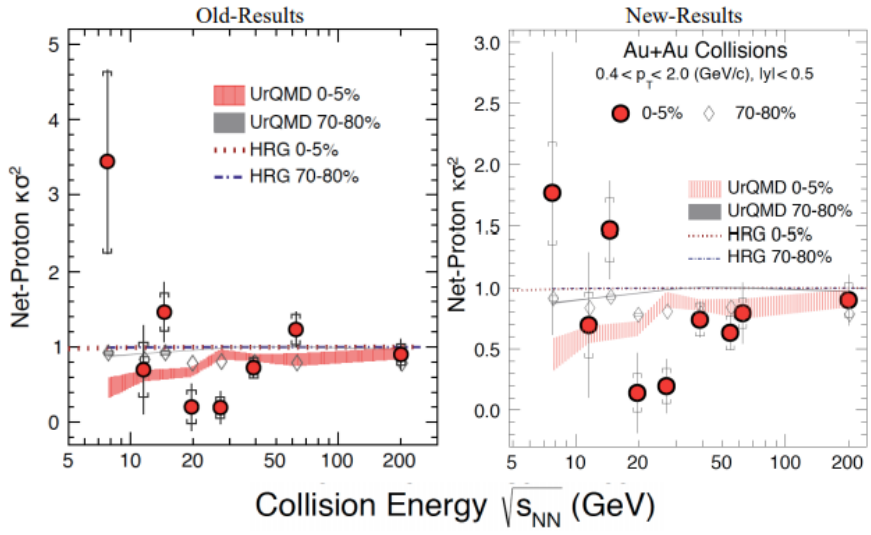

Figure 1. $k\sigma^2$ as a function of collision energy for net-proton distributions measured in central (0–5 %) and peripheral (70–80 %) Au + Au collisions within $0.4 < p_T$ (GeV/c) < 2.0 and $|y| < 0.5$. The error bars and caps show statistical and systematic uncertainties, respectively. The dashed and dash-dotted lines correspond to results from a hadron resonance gas (HRG) model. The shaded bands are the results of a transport model calculation (UrQMD). The model calculations utilize the experimental acceptance and incorporate conservation laws for strong interactions, but do not include the dynamics of phase transition or critical point. The new results are obtained after removing the spoiled events, the largest changes are seen in central Au + Au collisions at 7.7 and 62.4 GeV.

High statistics data from the ongoing BES-II program can provide precision measurements at higher μ_B region in the QCD phase diagram. In addition, due to the iTPC and eTOF upgrades, a differential measurement in $|y| < 1.5$ and $p_T > 0.15$ GeV/c will be explored. The study of acceptance dependence of net-proton $k\sigma^2$ and other cumulants ratios are important to understand critical fluctuation. Furthermore, the forward Event-Plan Detector (EPDs) can also be used to determine the centrality selection in heavy-ion collisions for this measurement.

Global polarization measurements at 27 GeV: In heavy-ion collisions, many theoretical models propose that the large angular momentum in the collisions of two nuclei can be transferred to the microscopic constituent of the created matter. Consequently, the spin of the produced quarks and gluons might be polarized along the direction of the global angular momentum due to spin-orbit coupling. The direction of the global angular momentum is perpendicular to the reaction plane, as defined by the incoming beam and the impact parameter vector. This direction can be determined from directed flow measurements of the spectators. STAR observed significant non-zero polarization of hyperons with increasing strength with decreasing collision energy (from 200 to 7.7 GeV).

We recently report more differential measurements using our newly installed EPDs in Au + Au collisions at 27 GeV as functions of the hyperon's transverse momentum, and pseudo-rapidity. In Figure 2 left panel we observe that the polarization does not show a strong dependence on p_T, albeit large uncertainties. There are several expectations on the p_T dependence on the polarization. If global polarization is generated by the vorticity of the initial state that does not have a strong p_T dependence then the result is compatible with expectations. Alternatively, at lower p_T, due to the smearing effect caused by scattering at later stages of the collisions, we might expect a decrease of the polarization. In addition, one might expect a decrease in the polarization at higher p_T due to the expected larger contribution from jet fragmentation. Figure 2 right panel shows the pseudo-rapidity dependence of the polarization measurement, no η-dependence of the polarization is observed within uncertainties. The vorticity is expected to decrease at larger rapidity, but might also have a local minimum at η = 0 due to complex shear flow structure however, this might be difficult to observe within STAR's acceptance. This preliminary observation of no p_T or η dependence of the polarization is consistent with our previous measurements at 200 GeV. STAR plans to perform the same measurement with an extended pseudo-rapidity coverage using the iTPC detector upgrade and with higher statistics BES-II data set enabling higher a precision result.

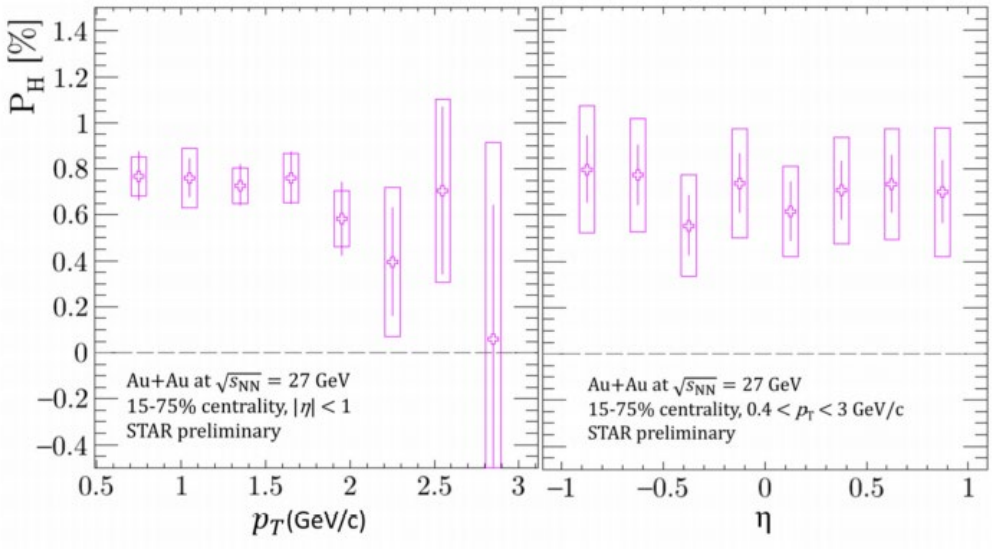

Figure 2. The global polarization measurements as a function of p_T and η in 15–75 % central Au + Au collisions at $\sqrt{s_{NN}}$ = 27 GeV.

Global spin alignment of K^{*0} and φ: Unlike the self-analyzing (anti)Λ, the polarization of vector mesons such as φ (1020) and K^{*0}(892) cannot be directly measured since vector mesons mainly decay through the strong interaction in which parity is conserved. The spin alignment of vector mesons can be given by a 3 × 3 spin density matrix with unit trace. The spin density matrix diagonal elements ρ_{nn}, n = 0,1 and –1, represent the probabilities for the spin component along the quantization axes. When there is no spin alignment this means that all three spin states (ρ_{nn}) have equal probability to be occupied meaning ρ_{nn} = 1/3. Out of the three diagonal elements, only the n = 0 case is independent of the other two. Consequently, it is intriguing to experimentally investigate the ρ_{00} of vector mesons.

Figure 3 shows the centrality dependence of ρ_{00} for both vector meson species for Au + Au collisions at 200 GeV. The φ-meson results are presented for transverse momentum $1.2 < p_T < 5.4$ GeV/c, and ρ_{00} for this species is significantly above 1/3 for mid-central collisions, indicating finite global spin alignment. The K^{*0}-meson results are presented for transverse

momentum $1.0 < p_T < 1.5$ GeV/c, and the magnitude of ρ_{00} for this particle species is observed to be significantly less than 1/3 for mid-central collisions.

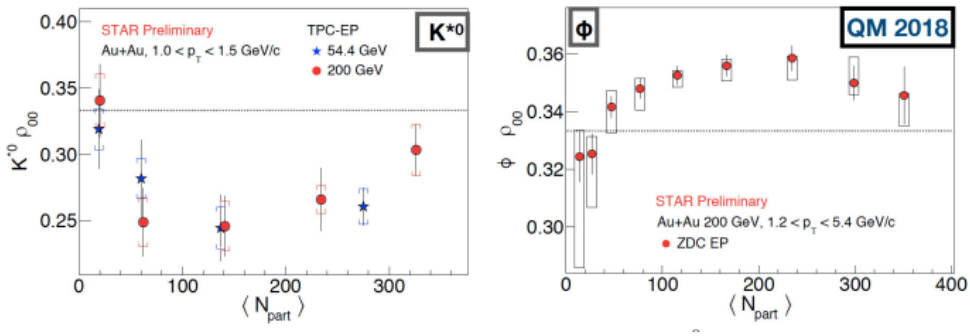

Figure 3. The spin alignment ρ_{00} measurements of vector mesons K^{*0} and φ as a function of N_{part} for the indicated p_T range of the Au + Au collisions at 200 and 54.4 GeV.

The distinction between the global spin alignment for K^{*0} and φ may be assigned to different in-medium interactions due to the difference in the lifetime (φ-meson is 10 times larger than K^{*0}-mesons), and/or a different response to the vector meson field. These global spin alignment results are expected to shed light on the possible vector meson fields. Such investigations are extremely important since vector meson fields are a crucial part of the nuclear force that binds nucleons to atomic nuclei and are also central in describing properties of nuclear structure and nuclear matter.

Small system measurements: The comparisons of theoretical models to the flow harmonics, υ_n, continue to be an essential avenue to evaluate the transport properties of partonic matter produced in large to moderate-sized collision systems. For the small collision systems formed in $p/d/^3$He + Au and p + Pb collisions, collective flow might not develop due to the presence of large gradients in the energy-momentum tensor that could trigger non-hydrodynamic modes. Certainly, the most important question that divided our field is whether an alternative initial-state-driven mechanism dominates over hydrodynamic expansion for these collision systems.

Current measurements for $p/d/^3$He + Au collisions, which supplement earlier measurements at both RHIC and the LHC aim to address the respective influence of collision system size and its subnucleonic fluctuations, and viscous attenuation on the measured υ_n.

Figure 4 shows the $\upsilon_2(p_T)$ and $\upsilon_3(p_T)$ values for $p/d/^3$He + Au collisions at 200 GeV before and after non-flow subtraction, compared for all three subtraction techniques. The presented results show non-flow contributions which are system-dependent, but the non-flow subtracted υ_2 (top panels) and υ_3 (bottom panels) are method-independent within the uncertainties.

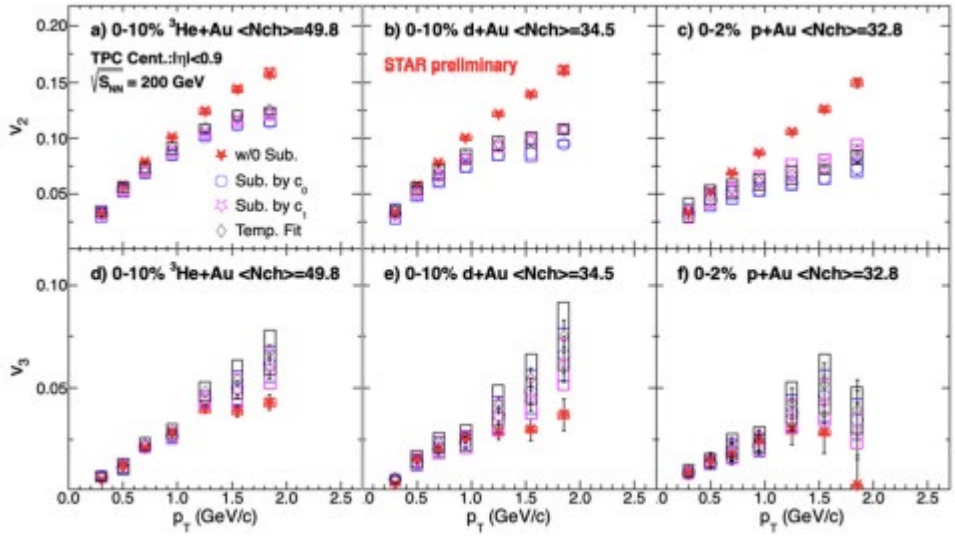

Figure 4. Comparison of the $v_{2,3}(p_T)$ values for $p/d/^3$He + Au collisions at 200 GeV, before and after non-flow subtraction.

These STAR measurements with non-flow subtracted show that for the comparable charged-hadron multiplicity (N_{ch}) events v_2 and v_3, values are independent of collision system. These observations are compatible with the significant influence of the subnucleonic fluctuations-driven eccentricities, $\epsilon_{2,3}$, in a system whose size is primarily determined by N_{ch}. However, they are incompatible with the notion of shape engineering in $p/d/^3$He + Au collisions.

3.3. Net-protons number fluctuations and the QCD critical point

Observations from collisions of heavy ions at relativistic energies have established the formation of a new phase of matter, Quark Gluon Plasma (QGP), a deconfined state of quarks and gluons in a specific region of the temperature versus baryonic chemical potential phase diagram of strong interactions. A program to study the features of the phase diagram, such as a possible critical point, by varying the collision energy ($\sqrt{s_{\mathrm{NN}}}$), is performed at the Relativistic Heavy-Ion Collider (RHIC) facility. Non-monotonic variation with ($\sqrt{s_{\mathrm{NN}}}$)of moments of the net-baryon number distribution, related to the correlation length and the susceptibilities of the system, is suggested as a signature for a critical point. The first evidence of a non-monotonic variation in kurtosis × variance of the net-proton number (proxy for net-baryon number) distribution as a function of $\sqrt{s_{\mathrm{NN}}}$ with 3.0σ significance, for head-on (central) gold-on-gold (Au + Au) collisions measured using the STAR detector at RHIC have been obtained. Non-central Au + Au collisions and models of heavy-ion collisions without a critical point show a monotonic variation as a function of $\sqrt{s_{\mathrm{NN}}}$.

The goal of this work is to search for the possible signatures of the critical point by scanning the temperature (T) versus μ_B in the QCD phase diagram by varying the collision energy $\sqrt{s_{\mathrm{NN}}}$ of the heavy-ion collisions.

Upon approaching a critical point, the correlation length diverges and thus renders, to alarge extent, microscopic details irrelevant. Hence observables like the moments of the conserve dnet-baryon number distribution, which are sensitive to the correlation length, are of interest when searching for a critical point. A non-monotonic variation of these moments as a function of $\sqrt{s_{\mathrm{NN}}}$ has been proposed as an experimental signature of a critical point. However, considering the complexity of the system formed in heavy-ion collisions, signatures of a critical point are detectable only if they can survive the evolution of the system, including the effects of finite size and time. Hence, it was proposed to study higher moments of distributions of conserved quantities (N) due to their stronger

dependence on the correlation length 15. The promising higher moments are the skewness, $S = \langle(N)^3\rangle/\sigma^3$, and kurtosis,$\kappa = [\langle(\delta N)^4\rangle/\sigma^4] - 3$, where $\delta N = N - M$, M is the mean and σ is the standard deviation. The magnitude and the sign of the moments, whichquantify the shape of the multiplicity distributions, are important for understanding the critical point. An additional crucial experimental challenge is to reconstruct, on an event-by-event basis, all of the baryons produced within the acceptance of a detector. However, theoretical calculations have shown that the proton-number fluctuations can also reflect the baryon-number fluctuations at the critical point.

The measurements performed were Au + Au collisions recorded by the STAR detector at RHIC from the years 2010 to 2014. The data covered the range of collision energy $\sqrt{s_{NN}}$ = 7.7, 11.5, 14.5,19.6, 27, 39, 62.4 and 200 GeV and is a part of phase-I of the Beam Energy Scan (BES) program at RHIC. These $\sqrt{s_{NN}}$ values correspond to μ_B values ranging from 420 MeV to 20 MeV at chemicalfreeze-out.

The results presented here correspond to two event classes: central collisions (impact parameters ~0–3 fm, obtained from the top 5 % of the above-mentioned multiplicity distribution) and peripheral collisions (impact parameters ~12–13 fm, obtained from the 70–80 % region of the multiplicity distribution).

The protons (p) and anti-protons ($\bar{p}$) are identified, along with their momentum, by reconstructingtheir tracks in the Time Projection Chamber (TPC) placed within a solenoidal magneticfield of 0.5 Tesla, and by measuring their ionization energy loss (dE/dx) in the sensitive gas-filled volume of the chamber. The analysis included the addition of the TOF detector, where the $p_T$acceptance is increased upto 2 GeV/c. The observation of non-monotonic variation of the kurtosis x variance is much more significant with the increased acceptance.

Figure 5 shows the event-by-event net-proton ($\Delta N_p = N_p - N_{\bar{p}}$) distributions obtained bymeasuring the number of protons (N_p) and anti-protons ($N_{\bar{p}}$) at mid-rapidity ($|y|$<0.5) in the transverse momentum range 0.4 <p_T(GeV/c) < 2.0 for Au + Au collisions at various $\sqrt{s_{\rm NN}}$. To study the shape of the event-by-event net-proton distribution in detail, cumulants (C_n) of variousorders are calculated, where $C_1 = M$, $C_2 = \sigma^2$, $C_3 = S\sigma^3$and $C_4 = \kappa\sigma^4$.

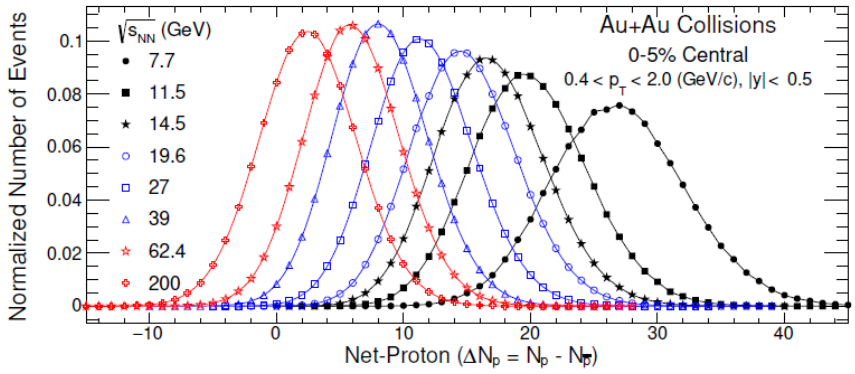

Figure 5. Event-by-event net-proton number distributions for head-on (0–5 % central) Au + Au collisions for nine $\sqrt{s_{\rm NN}}$ values measured by the STAR detector at RHIC. The distributions are normalized to the total number of events at each $\sqrt{s_{\rm NN}}$. The statistical uncertainties are smaller than the symbol sizes and the lines are to guide the eye. The distributions in this figure are not corrected for proton and anti-proton detection efficiency.

Figure 6 shows the variation of net-proton cumulants (C_n) as a function of $\sqrt{s_{\mathrm{NN}}}$ for central and peripheral Au + Au collisions. The cumulants are corrected for the multiplicity variations arising due to finite impact parameter range for the measurements. These corrections suppress the volume fluctuations considerably. The cumulants are also corrected for finite track reconstruction efficiencies of the TPC and TOF detectors.

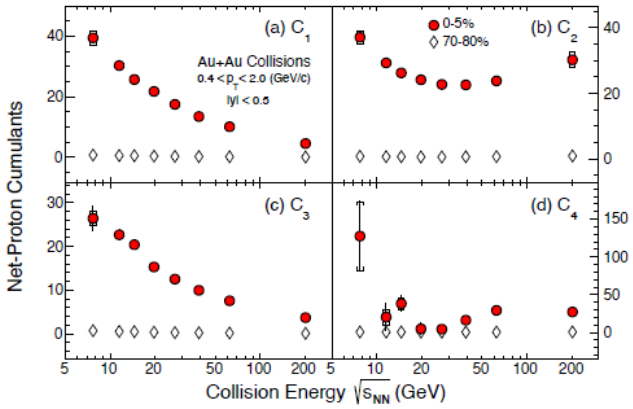

Figure 6. Cumulants (C_n) of the net-proton distributions for central (0–5 %) and peripheral (70–80 %) Au + Au collisions as a function of collision energy. The p_T range for the measurements is from 0.4 to 2 GeV/c and the rapidity (y) range is ± 0.5. The vertical bars represent the statistical uncertainties and the caps correspond to the systematic uncertainties.

The results for the ratios of cumulants $C_3/C_2 = S\sigma$ and $C_4/C_2 = \kappa\sigma^2$ are shown in Figure 7 for central (0–5 %) and peripheral (70–80 %) collisions within $0.4 < p_T$ (GeV/c) < 2.0 and $|y| < 0.5$. The error bars and caps show statistical and systematic uncertainties, respectively. The vertical-dashed (0–5 %) and dash-dotted (70–80 %) lines correspond to results from a hadron resonance gas (HRG) model. The orange (0–5 %) and black (70–80 %) shaded bands are the results from a transport model calculation (UrQMD33). These model calculations utilize the experimental acceptance, and incorporate conservation laws for strong interactions, but do not include a phase transition or a critical point.

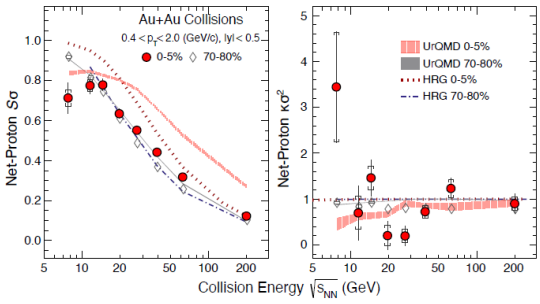

Figure 7. $S\sigma$ (left panel) and $\kappa\sigma^2$(right panel) as a function of collision energy for net-proton distributions measured in Au + Au collisions.

As seen from Figure 7 in central collisions a non-monotonic variation with beam energy is observed for $\kappa\sigma^2$. The $\kappa\sigma^2$ values go below unity (statistical baseline) and then rise to values above unity with decrease in beam energy. The peripheral collisions on the other hand show a monotonic variation with $\sqrt{s_{\mathrm{NN}}}$ and $\kappa\sigma^2$ values are always below unity. It is worth noting that in peripheral collisions, the system formed may not be hot and dense enough to undergo a phase transition or come close to the QCD critical point.

The deviation of the measured $\kappa\sigma^2$ from several baseline calculations with no critical point, and its non-monotonic dependence on $\sqrt{s_{\mathrm{NN}}}$, are qualitatively consistent with expectations from a QCD-based model which includes a critical point. Our measurements can also be compared to the baryon-number susceptibilities computed from QCD to understand various other features of the QCD phase structure as well as to obtain the freeze-out conditions in heavy-ion collisions. Higher event statistics in BES-II will help in establishing the critical point.

Publications:

1. *STAR Collaboration*
"Bulk properties of the medium produced in relativistic heavy-ion collisions from the beam energy scan program", Phys. Rev. C 96, 044904 (2017).

2. *STAR Collaboration*
"Net-proton number fluctuations and the Quantum Chromodynamics critical point", arXiv:2001.02852v1 [nucl-ex] 9 Jan 2020.

3. Stephanov, M.A., On the Sign of kurtosis near the QCD critical point, Phys. Rev. Lett. 107, 052301 (2011).

4. Bzdak, A.,Esumi, S.,Koch, V.,Liao, J.,Stephanov, M. and Xu, N., Mapping the Phases of Quantum Chromodynamics with Beam Energy Scan, arXiv:1906.00936 [nucl-th].

3.4. Spectra of charged particles. Energy dependence and modification

- ***Charged particle spectra***

Huge experimental efforts at the Super Proton Synchrotron (SPS) at CERN, the Relativistic Heavy Ion Collider (RHIC) at BNL, and the Large Hadron Collider (LHC) at CERN are under-taken to produce a new state of the nuclear matter in collisions of heavy ions and to investigate its properties over a wide range of energy and centrality. Various probes were used to deter-mine the features of the phase diagram of the nuclear matter. Experimental results from the RHIC and LHC support the hypothesis that a strongly coupled nuclear medium with partonic degrees of freedom, namely the Quark-Gluon Plasma (QGP), is created in heavy-ion collisions at high energy. Among the properties of the new medium there is opacity characterized by the suppression of particle yields and viscosity which is found to be such small that the matter looks like an ideal liquid rather than a gas of free quarks and gluons.

Measurements of bulk properties of the matter produced in Au + Au collisions at $\sqrt{s_{\mathrm{NN}}}$=7.7, 11.5, 19.6, 27, and 39 GeV using identified hadrons ($\pi^{\pm}$, $\mathrm{K}^{\pm}$, p and $\bar{p}$ from the STAR experiment in the Beam Energy Scan (BES) Program at the Relativistic Heavy Ion Collider (RHIC)) have been performed.

Midrapidity ($|y| < 0.1$) results for multiplicity densities *dN/dy*, average transverse momenta $< p_T >$, and particle ratios are presented. The chemical and kinetic freeze-out dynamics at these energies are discussed and presented as a function of collision centrality and energy. These results constitute the systematic measurements of bulk properties of matter formed in heavy-ion collisions over a broad range of energy (or baryon chemical potential) at RHIC.

The bulk properties of matter in the Beam Energy Scan Program at RHIC have been studied. The BES-I program covers the energy range from 7.7 to 39 GeV, which along with top RHIC energy

corresponds to the baryon chemical potential region of 20–400 MeV. The midrapidity yields of identified hadrons have been presented. They show the expected signatures of a high baryon stopping region at lower energies. At high energies, the pair production mechanism dominates the particle production. At intermediate energies there is clearly a transition between these two regions, which is explored by the BES program. The data have been used to analyze both chemical and kinetic freeze-out parameters. The chemical freeze-out was studied using both GCE and SCE approaches, and the fits were performed using both particle yields and particle ratios. The results show no significant difference between these approaches but indicate in heavy-ion collisions a clear centrality dependence of the baryon chemical potential at lower energies. The centrality dependence of the freeze-out parameters provides an opportunity for the BES program at RHIC to enlarge the (T, μ_B) region of the phase diagram to search for the QCD critical point. The difference between chemical and kinetic freeze-out increases with increasing energy, suggesting increasing hadronic interactions after chemical freeze-out at higher energies.

Despite the tremendous efforts there were found no clear experimental indications on structure of phase diagram of the nuclear matter up to now. The discovery of CP would in a stroke transform the map of the QCD phase diagram based only on reasonable inference from universality, lattice gauge theory and models into one with a solid experimental basis.

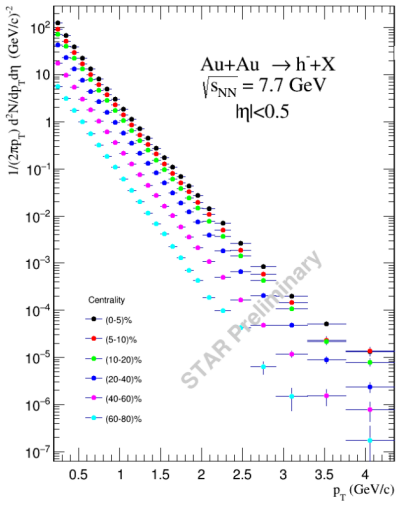

Figure 8. Spectra of charged particles production in BES-II

Publications:

1. M.V. Tokarev (for the STAR Collaboration). Int. J. Mod. Phys. (2015) 1560103.
А.О. Кечечан, М.В. Токарев “High p_T spectra of hadrons in Au + Au collisions at 9.2 GeV”, STAR Collaboration meeting, 14–19 September, 2020.
Stepan Maukhov, Alisher Aitbaev, Alexei Aparin “Au + Au spectra at 27 and 54 GeV”, STAR Collaboration meeting, 2–14 March, 2021

- ***Momentum modification of hadron spectra in Au+Aucollisions at BES energies***

A. Kechechyan, STAR Regional Meeting, Warsaw, Poland, June 27–30, 2017

It has been established that in relativistic heavy-ion collisions a hot, dense medium is rapidly formed, capable of interacting with the high-p_T partons produced in primordial hard scattering and making them lose some energy while traversing the medium. Quantifying this energy loss is an important issue, because it is directly related to the properties of the medium.

The Alternative Method to Estimate Fractional Momentum Loss (FML) was suggested in the Phys. Rev.C 93, 024911 (2016) and used for analysis of RHIC(PHENIX) and LHC (ALICE) data.

STAR BES-I negative charged particle transverse momentum spectra in Au + Au were used for estimation of the fractional momentum loss as a function of collision energy and centrality.

Calculation of the difference of normalized transverse momentum spectra is performed at the same hadron yields. The events are divided into centrality classes: 0–5 %, 5–10%, 10–20 %, 20–40 %, 40–60 %, 60–80 %. The fraction energy loss is defined as follows $\delta p_T/p_T = (p_T^0 - p_T^i)/p_T$,where index "0" corresponds to centrality 60–80 %, and index "*i*"– to the other centralities.

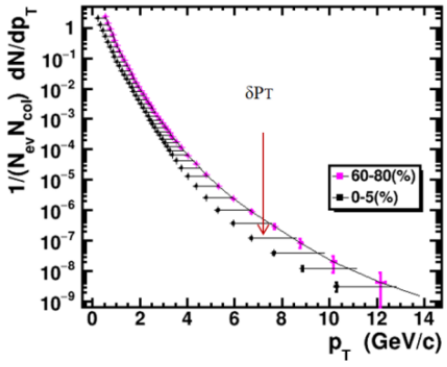

Figure 9. Normalized transverse momentum spectra at 0–5% and 60–80 % centralities.

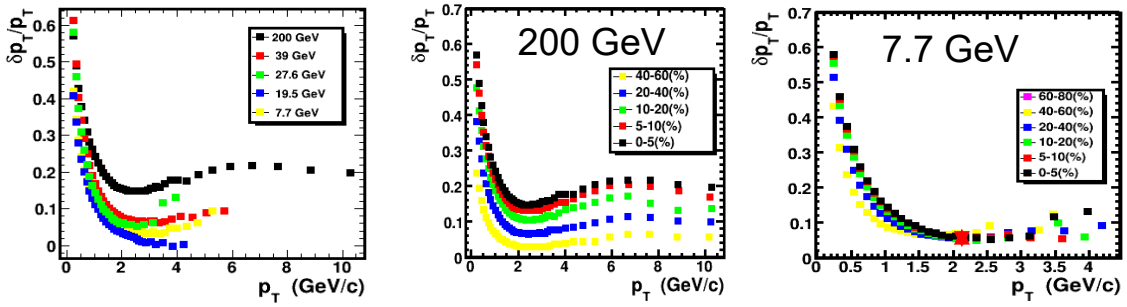

Figure 10. The fractal momentum loss as a function of transverse momentum and centrality at BES-I energies.

Preliminary results of analysis demonstrate that FML decreases with energy, strong centrality dependence of FML is found at 200 GeVand centrality difference of FML decreases with a collision energy.

The experimental STAR BES-I data on changed hadron yields allow us to search for features in transverse momentum distributions as a function of collisions energy and centrality. Modification of the distribution is related to mechanism of constituent energy loss in nuclear medium. The relative transverse momentum is defined by expression

$$\frac{\delta p_T}{p_T} = \frac{p_T^i - p_T^j}{p_T^i + p_T^j},$$

where p_T is a momentum corresponding particle production with the same probability and i = centrality 0–5 %, 5–10 %, 10–20 %, 20–40 %, 40–60 % and j = centrality 60–80 %. As seen from Figure 11 the strong dependence of $\delta p_T/p_T$ on collision energy $\sqrt{s_{NN}}$ with p_T is observed.

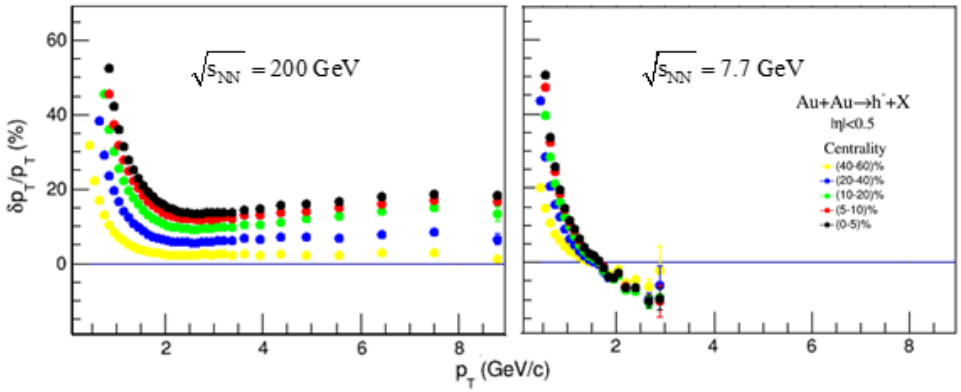

Figure 11. Modification of the transverse hadron yields in Au + Au collision as a function of energy and centrality.

Localization of the cross-point at energy 7 GeV and minimum at 200 GeV and the study of its dependence on centrality could give information in searching for critical point.

4. The Study of Event Structure, Collective Effects and High p_T

4.1. Binding energy of the hypertriton and antihypertriton

Nature Physics, 16 (2020) 409–412.

Nuclear collisions at ultrarelativistic energies, such as those studied at RHIC, create a hot and dense phase of matter containing approximately equal numbers of quarks and antiquarks. In this phase, called the quark-gluon plasma (QGP), quarks are free to move throughout the volume of the nuclear collision region. The QGP exhibits fluid properties with an exceptionally low ratio of viscosity to entropy density, and a far higher vorticity than any other system produced in a laboratory or observed in nature. The QGP persists for only a few times 10^{-23} seconds, then cools and transitions into a lower temperature phase comprised of mesons, baryons and antibaryons, including the occasional anti-nucleus or anti-hypernucleus. Thus, these collisions offer an ideal laboratory to explore fundamental physics involving nuclei, hypernuclei, and their antimatter partners.

The CPT theorem holds that all processes must exactly conserve the combined operation of C (charge conjugation, which interchanges a particle with its antiparticle), P (parity, which reverses the direction of all spatial axes), and T (time reversal). One implication is that every particle should have a mass and lifetime identical to those of its antiparticle, but opposite electric charge and magnetic moment. No CPT violation has ever been observed up to now. Qualitatively different tests of CPT symmetry are a continuing priority for fundamental physics, as are revisitations of past tests with improved accuracy. While CPT invariance has been verified to a precision of 10^{-19} in the strange quark sector for kaons, we present here the first test of CPT in a nucleus having strangeness content.

The hyper-nucleus ${}^{3}_{\Lambda}\mathrm{H}$ is reconstructed through its mesonic decay channels ${}^{3}_{\Lambda}\mathrm{H} \rightarrow {}^{3}\mathrm{He} + \pi^{-}$ (2-body decay) and ${}^{3}_{\Lambda}\mathrm{H} \rightarrow d + p + \pi-$ (3-body decay). Figure 12 depicts a typical event in which a ${}^{3}_{\Lambda}\overline{\mathrm{H}}$ candidate decays to $\bar{d}+ \bar{p} + \pi+$ in the STAR HFT and TPC. The ${}^{3}_{\Lambda}\overline{\mathrm{H}}$ candidate is produced at the primary vertex of a gold-gold collision and remains in flight for a distance on the order of centimeters, as shown by the dashed green curve starting at the center of the right-hand side of the figure, before decaying as depicted by the bold colored curves.

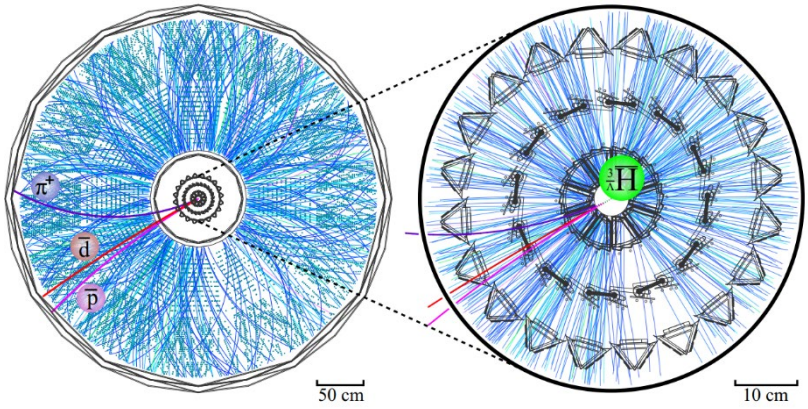

Figure 12. A typical event in which there is a candidate for the production and 3-body decay of ${}^{3}_{\Lambda}\overline{\mathrm{H}}$ in the STAR HFT and TPC detectors.

The left side in Figure 12shows a less magnified view of the STAR detector with the beam axis normal to the page, including a projected view of the large number of tracks detected by the TPC in a typical gold-gold collision. The right side shows an end-on view of the four cylindrical layers of the HFT located at the center of the TPC. The bold red, pink, and violet curves represent the trajectories of the $\bar{d}$, $\bar{p}$ and π^{+} decay daughters, respectively. The reconstructed decay daughters can be traced back to the decay vertex, at where the ${}^{3}_{\Lambda}\overline{\mathrm{H}}$ decays after flying for a distance on the order of centimeters, as shown by the dashed green curve starting at the center of the right side.

This binding energy is presented in Figure 13 along with earlier measurements from nuclear emulsion and helium bubble chamber experiments. The current STAR result differs from zero with a significance of 2.6σ. The masses used for Λ, π^{-}, p, d and ^{3}He in the early measurements of B_{Λ} were different from contemporary standard CODATA and PDG values. Thus, the early B_{Λ} values have been recalculated using the most precise mass values known today, and the recalibrated results are shown by short horizontal magenta lines in Figure 13. Even after recalibration, the central value of the current STAR measurement is larger than the measurement from 1973 which is widely used. Until this discrepancy is well understood, an average of the current measurement with early results cannot be reliably carried out.

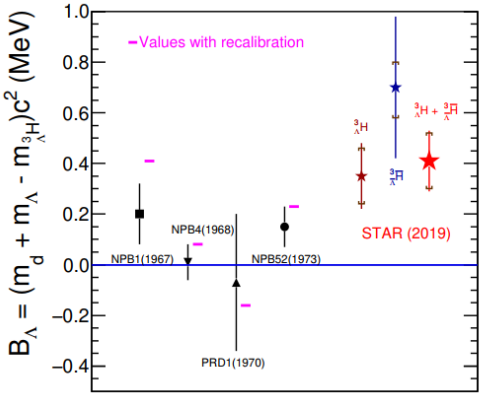

Figure 13. Comparison of the STAR results with earlier measurements of B_{Λ} for ${}^{3}_{\Lambda}\mathrm{H}$ and ${}^{3}_{\Lambda}\overline{\mathrm{H}}$. The black points and their error bars (which are the reported statistical uncertainties) represent B_{Λ} for ${}^{3}_{\Lambda}\mathrm{H}$ based on earlier data. The short horizontal magenta lines represent the best estimates of for ${}^{3}_{\Lambda}\mathrm{H}$ based on the same early data but using modern hadron and nucleus masses. The current STAR measurement plotted here is based on a combination of ${}^{3}_{\Lambda}\mathrm{H}$ and ${}^{3}_{\Lambda}\overline{\mathrm{H}}$ assuming CPT invariance. Error

bars show statistical uncertainties and caps show systematic errors. The green lines in the right panel represent theoretical calculations of B_Λ.

Thus, the first test of CPT invariance in the sector of hyper-nuclear matter where (anti)strange quarks play a role in (anti)nuclear binding. The relative mass difference between the hypertriton and antihypertriton is [1.1 ± 1.0 (stat.) ± 0.5 (syst.)] × 10^{-4}, consistent with no violation of CPT symmetry. Prior comparisons of nuclear binding for nuclei and anti-nuclei involved only up and down quarks, and this measurement both includes a strange quark and improves the uncertainty for mass number A = 3 by roughly an order of magnitude. A new measurement of the Λ hyperon binding energy in the hypertriton: B_Λ = 0.41 ± 0.12 (stat.) ± 0.11 (syst.) MeV was determined. The value differs from zero with a significance of 2.6σ, and it is larger than the prior measurement from 1973 which is widely used. Models in which the hypertriton is treated as a weakly-bound Λ-deuteron system predict smaller BΛ values. These results constrain the hyperon-nucleon interaction, providing improved data to understand the role of hyperons in neutron stars, and thus have wide-ranging implications spanning nuclear physics, particle physics, and astrophysics.

Publications:

1. The STAR Collaboration
"Measurement of the mass difference and the binding energy of the hypertriton and antihypertriton", Nature Physics, 16 (2020) 409–412.

4.2. Global polarization of Λ hyperon

Nature 548, 62 (2017)

Phys. Rev. C 98, 014910 (2018)

Global polarization can arise from spin coupling to both the fireball vorticity and the spectator magnetic field. Vortical coupling aligns emitted particle spin with the total system angular momentum, which can be partially transferred to the mid-rapidity fireball. Particle spins may also (anti-) align to the short-lived magnetic field (in the same direction as the total angular momentum) via intrinsic magnetic moment coupling. The vortical coupling would be even with respect to baryon number, while the magnetic coupling would be odd. STAR has seen a positive (6σ) even signal and a small (1.5σ) odd signal for the Λ– $\overline{\Lambda}$ system in the BES-I data.

The vorticity and magnetic field present during the evolution of a heavy ion collision are crucial inputs to the Chiral Vortical Effect (CVE) and Chiral Magnetic Effect (CME), respectively. These two effects are among the RHIC program's most exciting and visible topics today. To test the hypothesis of a magnetically induced splitting between the Λ and $\overline{\Lambda}$ global polarization, we propose to focus on a single energy and obtain high statistics there. Collisions at 19.6 GeV and lower energy will be obtained in the BES-II, so we focus on $\sqrt{s_{\mathrm{NN}}}$ > 19.6 GeV. The high statistics at one energy will also provide more differential study of possible p_T and rapidity dependence of the global polarization itself. This, in turn, would be important in clarifying potential difference in Λ and $\overline{\Lambda}$ global polarization due to stopping and final-state absorption. An approximate factor 15 increase in statistics is therefore needed to realize a 3σ splitting in the hyperon polarization (assuming the central value stays fixed) driving our request for 1B minbias events.

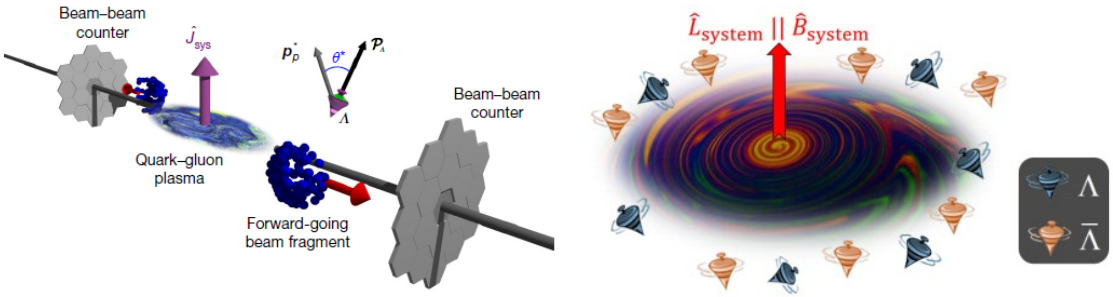

Figure 14. A sketch of Au + Au collision in the STAR detector system. Rotation nuclear matter.

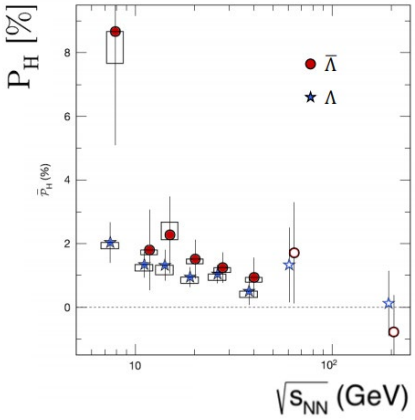

Figure 15. The hyperon average polarization in Au + Au collisions. The average polarization for Λ (blue stars) and $\bar{\Lambda}$ (red circles) from 20–50 % central collisions are plotted as a function of collision energy. Error bars represent statistical uncertainties only, while boxes represent systematic uncertainties. The results of the present study, indicated by filled symbols, are shown together with those reported earlier for 62.4 GeV and 200 GeV collisions, indicated by open symbols and for which only statistical errors are plotted.

Due to the parity-violating nature of their weak decay, Lambdas reveal the direction of their spin by preferentially emitting the daughter proton along that direction. The average spin direction of a population of Lambdas is the polarization. Lambdas at midrapidity were topologically reconstructed in the STAR TPC, and the Beam-Beam Counters (BBC) at forward and backward rapidity were used to estimate the direction of the total angular momentum of the collision. We discovered that the polarization direction of the Lambdas was correlated at the level of several percent with the direction of the system angular momentum in non-central collisions at $\sqrt{s_{NN}}$ = 7.7–39 GeV.

It has been well-established that the hot system created at midrapidity in the system may be considered a fluid, and hydrodynamic calculations relate the polarization of emitted particles is directly related to the vorticity – the curl of the flow field – of the fluid. Using this relation, we estimate that the curl of the fluid created at RHIC is about 9×10^{21} s^{-1}, 14 orders of magnitude higher than any fluid ever observed. Previous results have established the system at RHIC to be the hottest and the least viscous (relative to entropy density) fluid ever created. Our new result adds another record – collisions at RHIC produce the most vortical fluid.

This first view of the rotational substructure of the fluid at RHIC represents an entirely new direction in hot QCD research. It has generated considerable theoretical activity in the field and may have important connections with the Chiral Magnetic and Chiral Vortical Effects (CME and CVE). With increased statistics, there may even be the opportunity to probe the magnetic field

produced in heavy ion collisions by measuring the difference in polarization of Lambda and anti-Lambda hyperons. Such studies are planned for the future.

Nucleus-nucleus collisions at the Relativistic Heavy Ion Collider (RHIC) and at the Large Hadron Collider produce a state of partonic matter, the quark-gluon plasma (QGP). Various experimental observations together with sophisticated theoretical calculations indicate that the QGP behaves as an early perfect liquid, i.e., a fluid with the lowest ratio of shear viscosity to entropy density (η/s).

One of the most important observables in heavy-ion experiments is the azimuthal anisotropic flow that is usually quantified by the Fourier coefficients of the azimuthal distribution of the final-state particles relative to the collision symmetry planes. The first-order coefficient, called the directed flow, is argued to be sensitive to the equation of state of the matter and could serve as a possible signature of the QGP phase transition. The second-order coefficient, elliptic flow, offers strong evidence for the fluid like behavior of the created matter.

Several theoretical models suggest that the large angular momentum carried by two colliding nuclei can be transferred to the created system. As a consequence, the spin of particles composing the system might be globally polarized along the direction of the system angular momentum, due to spin-orbit coupling. Such a global polarization can be measured experimentally with hyperons via parity-violating weak decays, in which the daughter baryon is preferentially emitted in the direction of the hyperon spin. If the parent hyperon is an antiparticle, then the daughter baryon tends to be emitted in the opposite direction to the parent spin.

The angular distribution of daughter baryons in the hyperon decays is given by

$$dN/d\cos\theta^* \propto 1 + \alpha_H P_H \cos\theta^*,$$

where α_H is the hyperon decay constant, P_H is the hyperon polarization, and θ^* is the angle between the momentum of daughter baryon and the polarization vector in the hyperon rest frame. Since the angular momentum of the system is perpendicular to the reaction plane (a plane defined by the impact parameter vector and the beam direction), the polarization of hyperons can be measured via the azimuthal distribution of daughter baryons with respect to the reaction plane in the hyperon rest frame, similarly to anisotropic flow measurements.

The STAR Collaboration performed the first global polarization measurements of Lambda hyperons in Au + Au collisions at $\sqrt{s_{\mathrm{NN}}}$ = 62.4 and 200 GeV in 2007.These results were consistent with zero within large statistical uncertainties. More recently, the STAR Collaboration has reported a nonzero signal for the global polarization in Au + Au collisions at lower energies ($\sqrt{s_{\mathrm{NN}}}$ = 7.7–39 GeV), with a possible difference between Lambda and anti-Lambda polarizations that may indicate the effect of the spin alignment by the initial magnetic field. These results can be qualitatively described by hydrodynamic and transport models. The global polarization seems to decrease with increasing collision energy, and those models predict a finite signal (~0.2 %) at the top RHIC energy, $\sqrt{s_{\mathrm{NN}}}$ = 200 GeV. It is thus important to measure the global polarization signal at $\sqrt{s_{\mathrm{NN}}}$ = 200 GeV with all available statistics in order to enhance understanding of the role of vorticity in heavy-ion collisions.

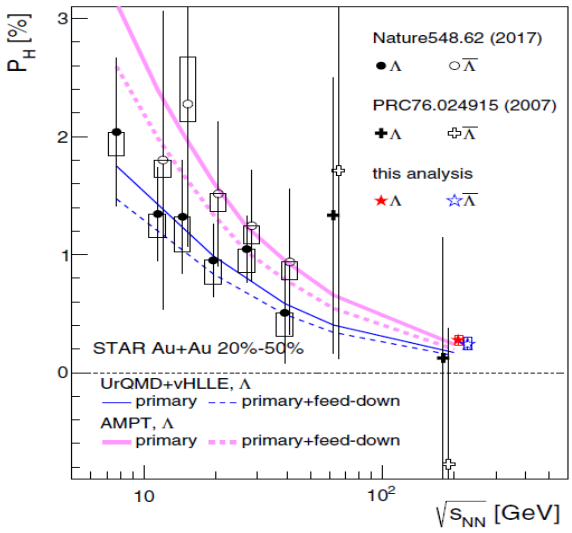

Figure 16. Global polarization of Lambda and anti-Lambda as a function of the collision energy $\sqrt{s_{NN}}$ for 20–50 % centrality Au + Au collisions. Thin lines show calculations from a 3 +1D cascade + viscous hydrodynamic model (UrQMD + vHLLE) and bold lines show the AMPT model calculations. In the case of each model, primary Lambda with and without the feed-down effect are indicated by dashed and solid lines, respectively. Open boxes and vertical lines show systematic and statistical uncertainties, respectively. Note that the data points at 200 GeV and for anti-Lambda are slightly horizontally shifted for visibility.

The global polarization of Lambda and anti-Lambda hyperons in Au + Au collisions at $\sqrt{s_{NN}}$ = 200 GeV using the data recorded by the STAR experiment in the years 2010, 2011, and 2014 have been obtained. The total data set is about 150 times larger than the data set analyzed in the previous search by STAR for hyperon polarization in Au + Au collisions at $\sqrt{s_{NN}}$ = 200GeV. We present the results as functions of the collision centrality, the hyperon's transverse momentum, and pseudorapidity. We also present comparisons with available theoretical calculations. Furthermore, we present the dependence of the polarization on the event-by-event charge asymmetry to study a possible relation between the polarization and axial current induced by the initial magnetic field.

Figure 16 presents the global polarization of Lambda and anti-Lambda as a function of the collision energy for the 20–50 % centrality bin in Au + Au collisions. The results from this analysis are shown together with the results from lower collision energies $\sqrt{s_{NN}}$ = 7.7–62.4 GeV. The 2007 result for $\sqrt{s_{NN}}$= 200 GeVhas a large uncertainty and is consistent with zero. Our new results for $\sqrt{s_{NN}}$ = 200 GeV with significantly improved statistical precision reveal nonzero values of the polarization signal, 0.277 ± 0.040(stat) ± 0.039 – 0.049 (sys) [%] and 0.240 ± 0.045(stat) ± 0.061–0.045 (sys) [%] for Lambda and anti-Lambda, respectively, and are found to follow the overall trend of the collision energy dependence. While the energy dependence of the global polarization was not obvious from the lower energy results, together with the new200 GeV results, the polarization is found to decrease at higher collision energy.

Monte Carlo simulation of Au + Au collisions over a range of $\sqrt{s_{NN}}$ = 5, 7.7, 11.5, 20, 30 GeV has been performed. Reconstructed Lambda hyperons have been used to determine the global Lambda polarization.

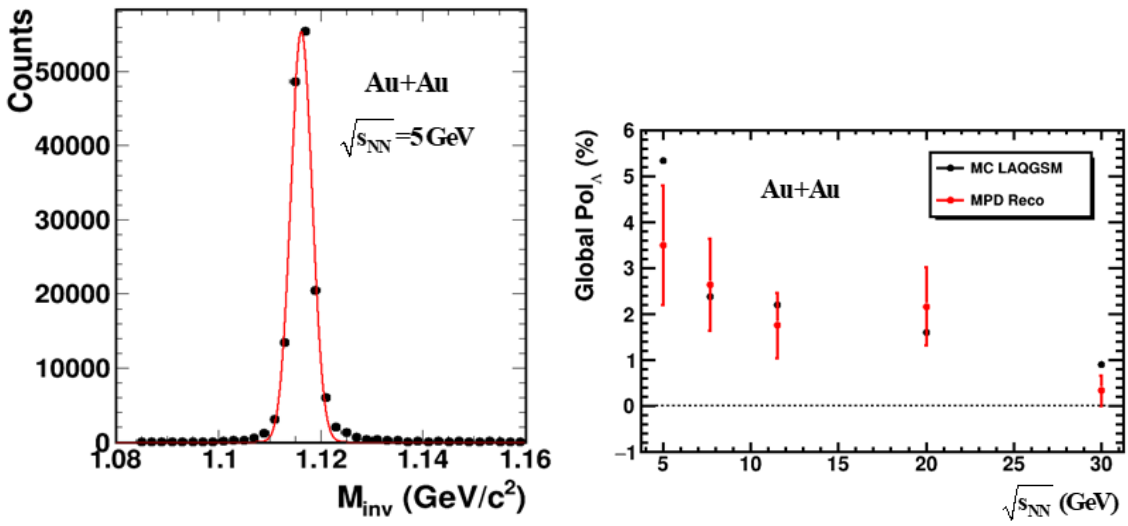

(a) (b)

Figure 17. Event distribution on invariant mass ($p + \pi^-$) (a). Global polarization of reconstructed Lambda hyperon versus collision energy $\sqrt{s_{NN}}$ (b).

Publications:

1.The STAR Collaboration
"Global Λ hyperon polarization in nuclear collisions", Nature 548, 62 (2017).

2. The STAR Collaboration
"Global polarization of Λ hyperons in Au + Au collisions at $\sqrt{s_{NN}}$ = 200 GeV",
Phys. Rev. C 98, 014910 (2018).

4.3. Fractality and self-similarity in AA interactions

It is generally considered that symmetry is an important tool for study of such phenomenon as the nuclear medium. Different possible phases of the matter, like liquid, solid, superfluid are related to a realization of global symmetries. Symmetry of constituent interactions and dimension of a space are crucial ingredients for description of critical phenomena. It is understood that all physical systems should reveal a discontinuity in some characteristics describing their behavior nearby a phase boundary or a critical point. Therefore, the concepts of "scaling" and "universality" have been widely developed to explain the critical phenomena. Scaling implies that systems near CP exhibit self-similarity and are invariant with respect to scale transformations. The universality of their behavior lies in the fact that vastly different systems behave in a similar way (they are described by the same power law) near the respective CP. The critical exponents in the power laws are determined by the interaction symmetry and space dimension only. The notions of scaling and universality have also been applied for the study of particle production far from the boundary of a phase transition or a CP. In high energy collisions, the scaling regularities were traditionally subject of intense investigations.

One of the methods allowing systematic analysis of experimental data on inclusive cross sections over a wide range of the collision energies, multiplicity densities, transverse momenta, and angles of various particles is based on the z-scaling approach found in high energy proton-(anti)proton collisions. The concept of this scaling is based on the principles of self-similarity, locality and fractality reflecting general features of particle interactions. The function $\psi(z)$and the self-similar variable z are calculated via measurable quantities (masses and momenta of the colliding and inclusive particles, total inelastic and differential cross section, and particle multiplicity density).

The model parameters of the scaling – c, δ and ε, have physical interpretation as the specific heat of the produced matter, the fractal dimension of structure of the colliding hadrons (or nuclei) and the fractal dimension of the fragmentation process, respectively.

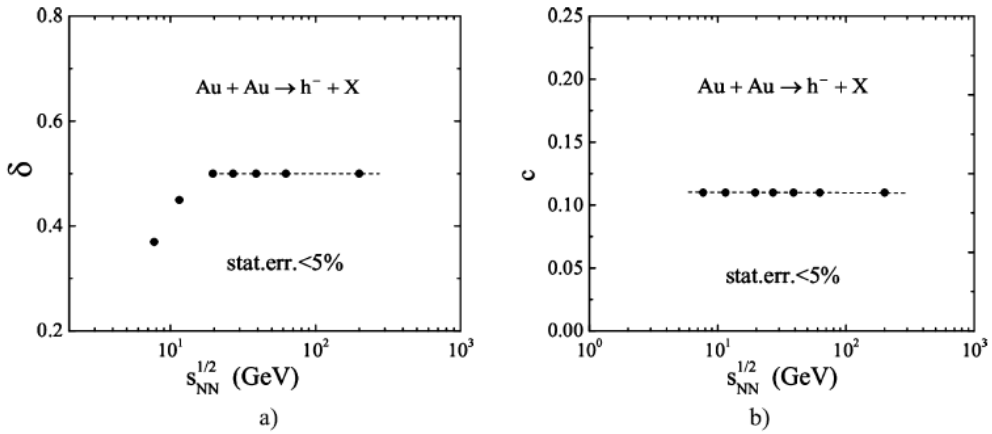

Figure 18. The structural dimension (a) and heat capacity (b) for negative hadron production in Au + Au collisions in dependence on the energy $\sqrt{s_{\mathrm{NN}}}$ for all centralities and |η| <0.5.

There are three model parameters in the z-scaling approach – the nucleus fractal dimension δ_A, the fragmentation fractal dimension ε_{AA}, and the "specific heat" c_{AA}. They are determined from the requirement of scaling behavior of the function ψ(z)which depends on the self-similarity variable z. Figure 18 shows the dependence of the structural dimension δ and the "specific heat" c on energy $\sqrt{s_{\mathrm{NN}}}$ for negative particle production in Au + Au collisions. The fractal dimension of the nucleus is expressed in terms of the nucleon fractal dimension δ and the atomic number A as follows, $\delta_A = A\delta$. The parameter δ_A characterizes structure of the colliding nucleus and reflects its structural self-similarity. For structureless objects and objects with invisible structure, the structural dimensions are zero. One can expect therefore, that both dimensions δ_A and δ should tend to zero below some threshold energy. This corresponds to a smearing of the constituent structure of the colliding hadrons and nuclei at sufficiently low energies. One can see from Figure 18(a) that values of the structural fractal dimension are found to be constant, δ = 0.5, for $\sqrt{s_{\mathrm{NN}}} \geq 19.6$ GeV. The same is valid for the nucleus fractal dimension $\delta_{Au} = A\delta$. A decrease of δ (δ_{Au}) at lower energies $\sqrt{s_{NN}} = 7.7$and 11.5 GeV is observed (see Figure 18(a)). The parameter c interpreted as "specific heat" of the produced medium in Au + Au collisions is shown in Figure 18 (b). The scaling regularity in Au +Au collisions is consistent with the constant value of $c_{AuAu} = 0.11$. This value is smaller than $c_{pp} = 0.25$ for p+p interaction. We estimate the errors for determination of the model parameters at the level ≤ 5 %. The estimation is based on statistical uncertainties of the nuclear data only. The same values of both parameters as shown in Figure 18 are compatible with the z-scaling for all centralities. We expect a change of δ, δ_A and c with $\sqrt{s_{NN}}$ and enhancement of their correlations in the cumulative region at high p_T as possible indication of the vicinity of a phase transition or a region where a CP can be located.

The fractal dimension ε_{AA} characterizing the fragmentation of objects produced in constituent collisions in the nuclear medium is suggested to be a function of multiplicity density. The fragmentation dimensions are expected to tend to zero at very low energy. For $\sqrt{s_{NN}} \geq 19.6$ GeV, the value $\varepsilon_{pp} = 0.2$ is found to be approximately constant.

The parameter $\varepsilon_0$depends on the collision energy. It was found logarithmic increase of $\varepsilon_0$with $\sqrt{s_{NN}}$. This behavior reflects growing tendency of the suppression of hadron yields in the central collisions of heavy nuclei when the collision energy increases.

The value of multiplicity density in the central collisions is about 6 times larger than for the peripheral ones. The growth of multiplicity density with centrality results in a considerable increase of ε_{AA} and thus in larger energy losses by the production of the inclusive particle.

The effect becomes more significant at higher energy, as both the multiplicity density and the parameter $\varepsilon_0$increase with $\sqrt{s_{NN}}$.

The most central events are expected to be preferable to search for signatures of a CP and a phase transition due to the high energy density of the produced nuclear matter.

For more precise determination of the model parameters, the multiplicity dependent spectra over a wide range of transverse momentum and collision energy are needed. We consider that new data on multiplicity and p_T dependencies of particle yields at different energies over a wide kinematic range could give us additional constraints on the parameters. Specifically, this could help in discrimination between different scenarios with different sets of parameters studied in nuclear collisions at lower energies.

A microscopic scenario of constituent interactions in high energy collisions of hadrons and nuclei is studied. The concept is based on the *z*-scaling of inclusive spectra observed in a wide range of collision energies, multiplicity densities, momenta, and angles of detected particles. We bring arguments that, due to the fractality and self-similarity of the hadron interactions assumed in the *z*-scaling scheme, there exists a conservation law of a new quantity named “fractal cumulativity”. The conserved quantity is proportional to the corresponding fractal dimensions and is a simple function of the respective momentum fractions. Based on statistical ideas and entropy considerations we demonstrate that the fractal dimensions possess quantum character. The fractality of hadron structure and fragmentation processes manifests itself most prominently near the kinematic limit of the reaction. The entropy of the constituent configurations in this region bears information on fractal characteristics of the hadron interactions at small distances. In the vicinity of the kinematic limit (i.e. near the fractal limit), the entropy can be expressed in a specific form which allows to draw some physical conclusions. We have argued that the z-scaling can be a tool to search for and study of new symmetries, conservation laws and quantum properties of hadron structure and fragmentation processes especially at small distances. The measurements of particle spectra with high transverse momenta at the energies of the future accelerators FAIR (GSI) and NICA (JINR) will be extremely suitable for studying the regime of large fractal cumulativities and could contribute to a verification of the quantum nature of fractality in the interactions of hadrons and nuclei.

Multiparticle production in interactions of leptons, hadrons, and nuclei of high energies includes many processes. In the PYTHIA Monte Carlo event generator, widely used in high energy physics, the mechanism of particle production corresponds to the following scenario. Hadron–nucleus collisions are described in terms of quarks and gluons. The hard interaction is considered in the context of perturbative quantum chromodynamics (QCD). A nonperturbative part is model-dependent and connected with the choice of parton-distribution function and fragmentation function, as well as with scales of factorization, renormalization, and fragmentation. As a rule, these scales are considered equal. After hard scattering, each parton emits daughter partons and forms a shower in the final state. The mechanism of parton-shower evolution is suggested to be self-similar. The radiation cutoff in virtuality leads to the fact that partons cease to decay at different levels and form an incomplete fractal structure. The fractal nature of parton showers may be distorted by secondary interactions and by the hadronization process. In this case, a question

arises as to the degree of fractality violation and the possibility of reconstructing the data on initial-process characteristics.

Fractal processes are characterized by dimension D_F, number of levels N_{lev} and base P of fractal formation.

The fractal analysis of mixed data set, containing fractals and background events with the multiplicity, was carried out. The set understudy included incomplete fractals with independent partition and complete fractals with dependent and combined partitions. As background events, the random sets of points were considered, the multiplicity distribution of which coincided with similar distributions for the fractals under study. In this work a procedure for analyzing incomplete fractals by the SePaC method is proposed which is based on the consideration of only three levels. Procedures for choosing the method parameters for incomplete and complete fractals coincide. It is found that the SePaC method reconstructs all incomplete fractals and fully suppresses background events. The reconstruction of incomplete fractals using the Box Counting method and the suppression of background events depend on the base of fractal formation (the greater the base, the fewer the impurities in the extracted events). The accuracy of the reconstruction of fractal dimension is investigated using the SePaC and BC methods. It is shown that, with the use of the SePaC method for fractals with combined partition, a correction is needed in determining dimension. In this work, a procedure for such correction is developed and applied which takes into account the difference in values of reconstructed dimensions based on hypotheses of independent and dependent partitions. It is shown that, for the SePaC method, dimensions of fractals with independent and dependent partition are reconstructed exactly, while errors in the determination for fractals with combined partition are no more than10 %. The relevant distributions of events over for the test and reconstructed fractals match well (the maximum deviation in bins does not exceed 2 %). For the BC method, the dimension is reconstructed with an error while the relevant distributions over are shifted to the region of greater values and do not retain a shape. Thus, this work shows the advantage of the SePaC method in the extraction of fractals from the mixed events and in the accuracy of reconstructing distributions over dimension in comparison with the Box Count method.

Publications:

1. M.V. Tokarev, I. Zborovsky,
Self-similarity of hadron production: *z*-scaling
Theoretical and Mathematical Physics, ISSN:0040-5779, eISSN:1573-9333, Изд:Springer New York, 184, 3, 1350-1360, 2016

2. T.G. Dedovich, M.V. Tokarev,
“Incomplete fractal showers and restoration of dimension”,
EPJ Web of Conferences 204, 06003 (2019)

3.M.V. Tokarev, A.O. Kechechyan, I. Zborovský
“Self-Similarity of Negative Particle Production in Au + Au Collisions at STAR”, Physics of Particles and Nuclei Letters, 2019, Vol. 16, No. 5, pp. 510–515.

4. M.V. Tokarev, A.O. Kechechyan, I. Zborovský
“Validation of *z*-scaling for negative particle production in Au + Au collisions from BES-I at STAR”, Published in Nuclear Physics A 993 (2020) 121646.

5. I. Zborovsky
“Fractality in hadron interactions: a conservation law and quantization of fractal dimensions”, EPJ Web of Conf. 204, 06002 (2019).

6. M.V. Tokarev, I.Zborovsky
Self-Similarity, Fractality and Entropy Principle in Collisions of Hadrons and Nuclei at Tevatron, RHIC and LHC,
Proceedings of 40th International Conference on High Energy physics – ICHEP2020, July 28 – August 6, 2020, Prague, Czech Republic, Proceedings of Science, 2020. PoS (ICHEP2020) 575.

7. M.V. Tokarev, I.Zborovsky, A.O.Kechechyan, T.G. Dedovich
z-Scaling in $p + p$, anti-$p + p$ and Au + Au Collisions at RHIC, Tevatron and LHC
ISSN 1063-7796, Physics of Particles and Nuclei, 2020, Vol. 51, No. 2, pp. 141–171. © Pleiades Publishing, Ltd., 2020.

8.M.V. Tokarev, I.Zborovsky
“Self-Similarity, Fractality and Entropy Principle in Collisions of Hadrons and Nuclei at Tevatron, RHIC and LHC”, JINR Preprint E2-2020-24,
Phys. Part. Nucl. Lett., 2021, v.18, № 3 (accepted for publication)

4.4. Monte Carlo study of fractal structure of events

Multiparticle production in interactions of leptons, hadrons, and nuclei of high energies includes many processes. In the PYTHIA Monte Carlo event generator, widely used in high energy physics, the mechanism of particle production corresponds to the following scenario. Hadron–nucleus collisions are described in terms of quarks and gluons. The hard interaction is considered in the context of perturbative quantum chromodynamics (QCD). A nonperturbative part is model-dependent and connected with the choice of parton distribution function and fragmentation function, as well as with scales of factorization, renormalization, and fragmentation. As a rule, these scales are considered equal. After hard scattering, each parton emits daughter partons and forms a shower in the final state. The mechanism of parton shower evolution is suggested to be self-similar. The radiation cutoff in virtuality leads to the fact that partons cease to decay at different levels and form an incomplete fractal structure. The fractal nature of parton showers may be distorted by secondary interactions and by the hadronization process. In this case, a question arises as to the degree of fractality violation and the possibility of reconstructing the data on initial-process characteristics.

Fractal processes are characterized by dimension D_F, number of levels N_{lev} and base P of fractal formation. The fractal analysis of mixed dataset, containing fractals and background events with the multiplicity, was carried out. The set understudy included incomplete fractals with independent partition and complete fractals with dependent and combined partitions.

Let us consider fractals with independent partition. The most well-known representative of this type is thetriadic Cantor set. The process of this fractal formation is presented in Figure 19a. Let the initial set be the segment [–5,5]. We divide it conditionally into three parts. At the first level of the fractal, the first and third parts remain. At the subsequent levels, the partition process is repeated for each remaining part. The initial set is divided conditionally into $n = P^{lev}$ parts, where *lev* is the level and P is the base of fractal formation. For a triadic Cantor set, P is equal to three. Each partis divided independently; therefore, we call this fractal type fractals with independent

partition. Figure 19b presents the formation of fractals with dependent partition. The initial set (segment [– 5,5]) is divided conditionally into four parts. At the first level of the fractal, the first, third, and fourth parts remain. At the subsequent levels of fractal formation, the partition process is repeated, taking into account that the third and fourth parts are the unified segment (dependent partition). Base P of the fractal under study equals four.

A process of formation of the fractal with combined partition is shown in Figure 19 c. The initial set is divided conditionally into $n = 5^{lev}$parts (the base of fractal is $P = 5$). In each event of partition, the second, third, and fourth parts remain. Despite the fact that the remaining parts are a unified segment, the second partis divided independently in the partition process, while the third and fourth parts are considered a unified object (they are divided dependently). We call this process of fractal formation a combined one.

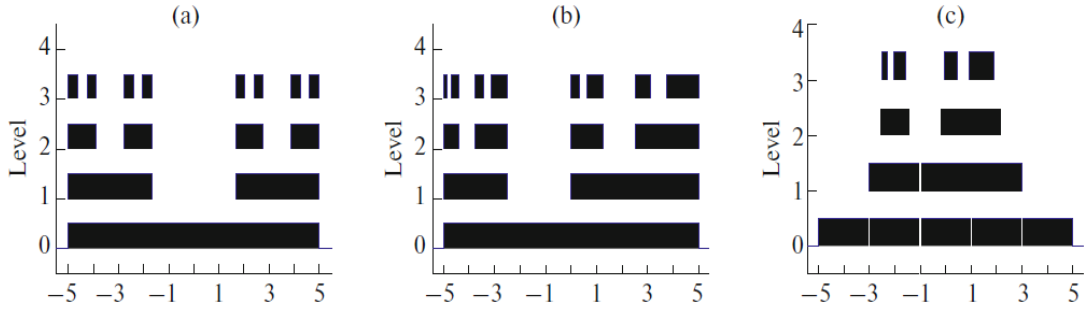

Figure 19. Formation of fractals with independent (a), dependent (b), and (c) combined partition.

As background events, the random sets of points were considered, the multiplicity distribution of which coincided with similar distributions for the fractals under study. A procedure for analyzing incomplete fractals by the SePaC method was proposed which is based on the consideration of only three levels. Procedures for choosing the method parameters for incomplete and complete fractals coincide. It was found that the SePaC method reconstructs all incomplete fractals and fully suppresses background events.

The test distribution of fractals over dimension D_F as well as the distribution obtained using the hypothesis of independent partition with correction, are presented in Figure 20 (a). It is found that distributions agree well. The total bin wise deviation from the test distribution is $\Delta = 0.23$, while the maximum deviation in bins is $\delta_{max} = 0.05$.

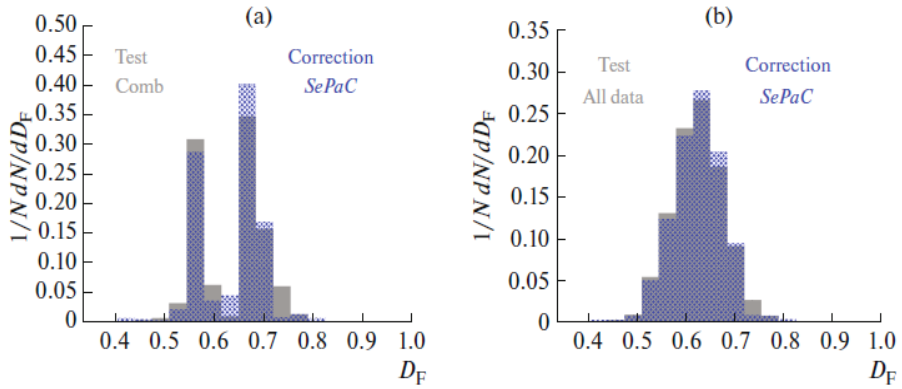

Figure 20. Analysis of fractals by the SePaC method with the D_F correction. Distributions of fractals (a) with combined partition and (b) of the initial set over the test and reconstructed dimension DF.

The described method of dimension reconstruction for fractals with combined partition was verified for another dataset as well. The tested set included all types of combined fractals with the bases $P = 3 – 8$ andthe multiplicity $N \geq 64$. The distributions over with a different number of bins were considered. It was found that the number of peaks and boundaries of reconstructed distributions coincide with those of the initial distribution if the width of bins is no less than 0.03. Figure 20 (b) shows the test and reconstructed distributions of the initial fractal set over D_F. We recall that the dimension was determined as follows: at first the basic SePaC method (allowing the DF of fractals with independent and dependent partition to be reconstructed most exactly) was used; then the dimension of fractals with combined partition was determined by the hypothesis of independent partition with allowance for correction. From the figure it can be seen that boundaries and shapes of distributions coincide well. The total bin wise deviation from that of the test distribution(Δ=0.08,) and the maximum deviation in bins ($\delta_{max} = 0.02$) are insignificant.

The reconstruction of incomplete fractals using the Box Counting method and the suppression of background events depend on the base of fractal formation (the greater the base, the fewer the impurities in the extracted events). The accuracy of the reconstruction of fractal dimension is investigated using the SePaC and BC methods. It is shown that, with the use of the SePaC method for fractals with combined partition, a correction is needed in determining dimension. In this work, a procedure for such correction is developed and applied which takes into account the difference in values of reconstructed dimensions based on hypotheses of independent and dependent partitions. It is shown that, for the SePaC method, dimensions of fractals with independent and dependent partition are reconstructed exactly, while errors in the determination for fractals with combined partition are no more than 10 %. The relevant distributions of events over for the test and reconstructed fractals match well (the maximum deviation in bins does not exceed 2 %). For the BC method, the dimension is reconstructed with an error while the relevant distributions over are shifted to the region of greater values and do not retain a shape. Thus, this work shows the advantage of the SePaC method in the extraction of fractals from the mixed events and in the accuracy of reconstructing distributions over dimension in comparison with the Box Count method.

Publications:

1. T.G. Dedovich, M.V. Tokarev,
“Incomplete fractal showers and restoration of dimension”,
EPJ Web of Conferences 204, 06003 (2019)

2.T. Dedovich and M. Tokarev,
“Analysis of fractals with combined partition,” Phys. Part. Nucl. Lett. 13, 169–177 (2016)

3. T. Dedovich and M. Tokarev,
“A two-step procedure of fractal analysis,” Phys. Part. Nucl. Lett. 13, 178–189(2016)

4. T. Dedovich and M. Tokarev,
“Fractal reconstruction
in the presence of background,” Phys. Part. Nucl. Lett.14, 856–873 (2017)

5. T.G. Dedovich, M.V.Tokarev,
”Reconstruction of the Dimension of Complete and Incomplete Fractals“, Physics of Particles and Nuclei Letters, 16, 3, 240-250, 2019

6. T.G. Dedovich, M.V.Tokarev

"Criteria of fractal reconstruction and suppression of background events by SePaC method", Physics of Particles and Nuclei Letters, 2021, Vol. 18, No. 1, pp. 93–106.

4.5. Cumulative processes in AA collisions

The high-density nuclear matter can be produced in cumulative processes. Production of any inclusive particle with a momentum far beyond the nucleon-nucleon kinematic region can be accompanied by cumulation of a nucleus. It is assumed that transition of the nuclear matter from the hadron to quark and gluon degrees of freedom near the critical point should reveal large fluctuations, correlations and discontinuity of some experimental quantities characterizing the system. Therefore, particle production in the cumulative regions is of special interest for search for signatures of phase transition and critical point. High sensitivity of elementary constituent interactions to properties of the compressed nuclear matter is expected to be in this region. Study of the cumulative effect is of great interest to search for signatures of phase transitions and a critical point in highly compressed nuclear matter.

The first results on cumulative hadron production in heavy-ion collisions at collider mode are the data on transverse momentum spectra obtained by the STAR collaboration in Au + Au collisions in central rapidity range at $\sqrt{s_{\mathrm{NN}}}$ = 7.7and 11.5 GeV at the RHIC. A special interest represents the study of particle production taking into account the dependence of the momentum fraction on the centrality of nuclear collisions. The fractionis named as order of cumulativity or the cumulative number. The region A_1x_1 and/or A_2x_2 corresponds to the cumulative processes, indication of which is detection of a cumulative particle. The cumulative particles are particles produced in the kinematic region forbidden for free nucleon nucleon interactions. The energy of the constituent interactions with production of a cumulative particle is larger than it can be reached in the interactions on free nucleons. The cumulative particles originate from processes characterized by the order of cumulativity larger than unity. These particles are only produced in reactions with participation of nuclei.

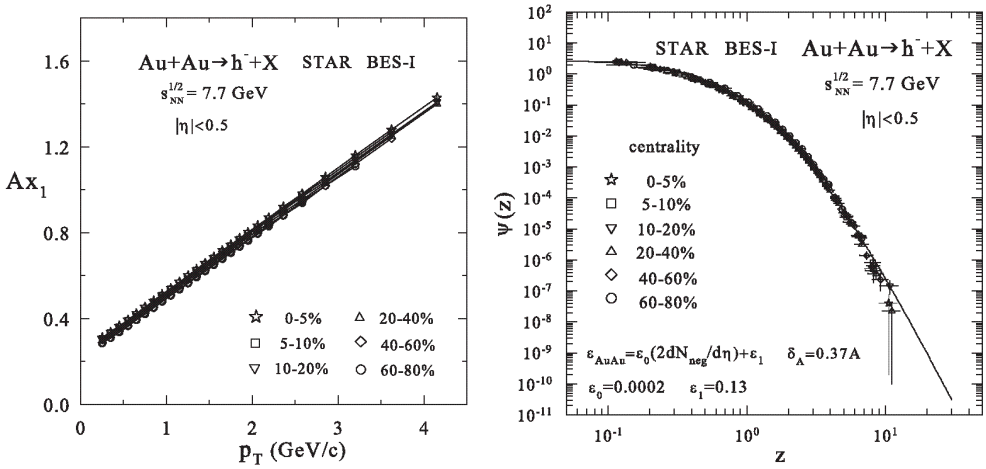

Figure 21. The scaling function ψ(z) and momentum fraction Ax_1 for negative hadrons produced in Au + Au collisions at the energy $\sqrt{s_{NN}}$= 7.7GeV for different centralities. The solid line is a reference curve for $p + p$ collisions.

We expect that, when going to the cumulative region, the fractal dimensions, and the "specific heat" may be sensitive to the magnitude of the cumulation. A variation in these quantities is proposed as a signature of new effects and, in particular, of a phase transition. Determining the dependence of fractal dimensions on the process cumulativity order, one may examine the structure of fluctons themselves and the properties of fragmentation of particles produced in their collisions. An account of the centrality dependence of the cumulative particles yields may enhance

the sensitivity of these characteristics to the order of cumulativity. It is assumed that the relation may be violated in the cumulative region. The fractal dimension is expected to grow with the cumulativity order in this region: it should be greater for fluctons (the local cumulations of the nuclear matter in the nucleus) than for the ordinary nucleons in nuclei.

The performed analysis extends applicability of the self-similarity principle to the description of hadron production in nucleus-nucleus collisions. The presented results indicate on self-similarity of fractal structure of the colliding nuclei and support the hypothesis of fractality in fragmentation processes with production of inclusive particles in the system. A violation of such symmetry could be an indication on a change of fractal structure of hadron constituents and their interactions due to unusual properties of the nuclear medium created in collisions at high transverse momentum and large multiplicity density. A discontinuity of the model parameters – the structural and fragmentation fractal dimensions and specific heat" is considered from the point of view of searching for signatures of a phase transition and acritical point in nuclear matter. Based on the obtained results we conclude that new confirmation of the scaling properties of hadron production in heavy ion collisions was found.

Publications:

1. M. Tokarev, A. Kechechyan

"High-p_T spectra of h-hadrons in Au + Au collision at $\sqrt{s_{\mathrm{NN}}}$ = 9.2 GeV" STAR Collaboration Meeting, 14–25 September, 2020,
Indian Institute of Science Education and Research (IISER) Tirupati, India

4.6. Collective effects for heavy flavor

- ***Anisotropic flow and NCQ scaling***

A key piece of evidence for this new state of matter is the strong collective, anisotropic flow of produced light flavor particles, suggesting possibly hydrodynamic behavior of the strongly interacting matter during the collision.

The number counting quark scaling has been found for light flavors.

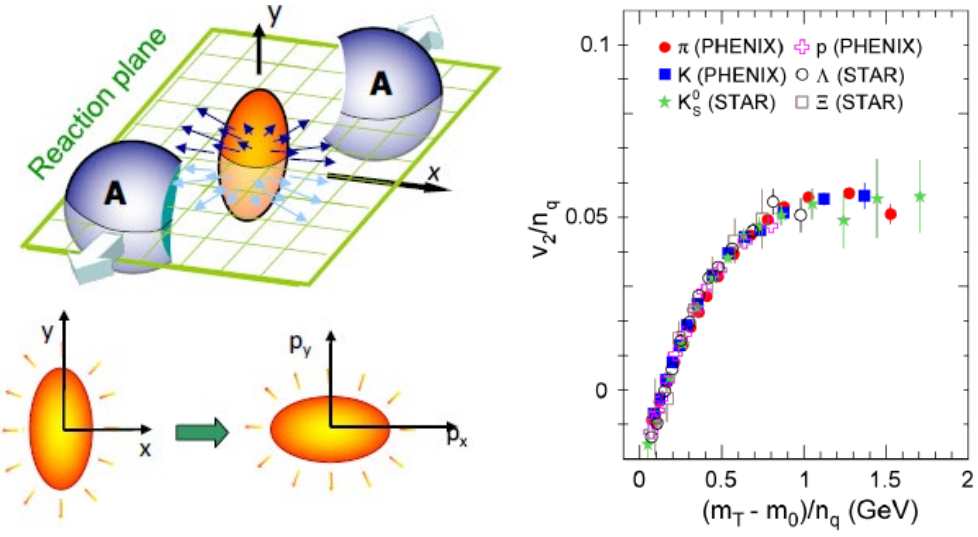

Figure 22. Elliptic flow v_2 vs transverse mass at 200 GeV for light flavors

It was also observed that NCQ scaling is broken at lower energies, where larger v_2 for baryons than antibaryons were observed. Therefore, NCQ scaling for strange and multi-strange hadrons was tested down to $\sqrt{s_{NN}}$= 27 GeV. The energy scan of v_2 for different at higher $\sqrt{s_{NN}}$ is also important for search for signature of phase transition and critical point. Elliptic flow is related with collective effects of interacting constituents in nuclear matter.

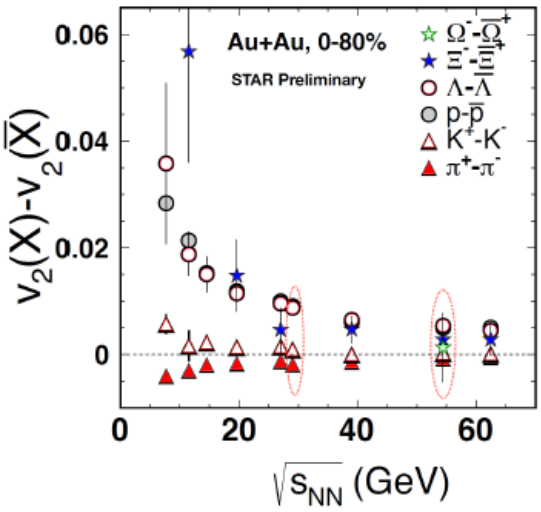

Figure 23.The difference in v_2 between particles and their corresponding antiparticles as a function of $\sqrt{s_{NN}}$ for 0 % – 80 % central Au + Au collisions. The dashed lines in the plot are fits with a power-law function. The error bars depict the combined statistical and systematic errors.

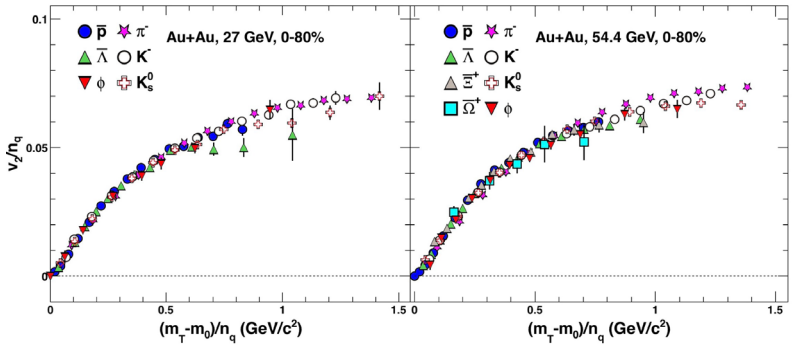

Figure 24. Elliptic flow v_2 vs transverse mass at $\sqrt{s_{NN}}$=27 and 54.4 GeV for light flavors

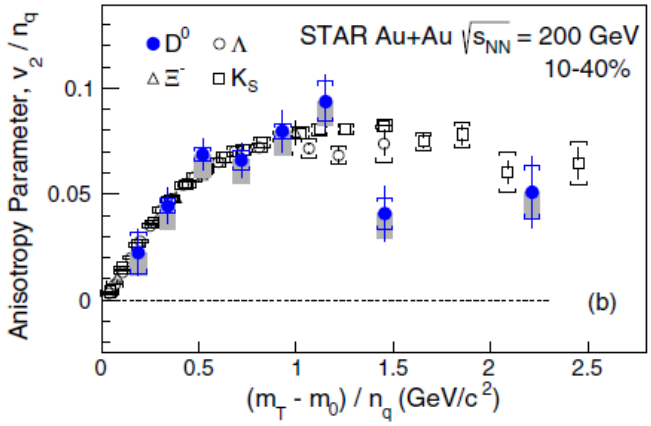

Figure 25.v_2 as a function of p_T and (b) v_2/n_q as a function of $(m_T - m_0/n_q$ for D^0 in 10–40 % centrality Au + Au collisions compared with K^0_S, Λ, and Ξ^-. The vertical bars and brackets represent statistical and systematic uncertainties, respectively, and the gray bands represent the estimated nonflow contribution.

Elliptic flow v_2 of D^0 mesons in Au + Au collisions at 200 GeV has been measured with the STAR detector using the heavy flavor tracker, a newly installed high-resolutions silicon detector. The measured $D^0 v_2$ follows the mass ordering at low p_T observed earlier. The v_2/n_q of D^0 is consistent with that of other hadrons at $(m_T - m_0)/n_q < 1$ GeV/c^2 in 10 % – 40 % centrality collisions. A 3D viscous hydrodynamic model describes the $D^0 v_2$ for $p_T < 4$ GeV = c. Our results suggest that charm quarks exhibit the same strong collective behavior as the light hadrons and may be close to thermal equilibrium in Au + Au collisions at 200 GeV.

Charm quarks acquire similar elliptic flow as light flavor quarks a data suggest strong interaction of charm quarks with QGP.

Publications:

1. STAR Collaboration
"Measurement of D0 Azimuthal Anisotropy at Midrapidity in Au + Au Collisions
at energy 200 GeV", PRL 118, 212301 (2017)

2. STAR Collaboration
"Observation of an Energy-Dependent Difference in Elliptic Flow between Particles and Antiparticles in Relativistic Heavy Ion Collisions"
Phys. Rev.Lett. 110(2013)142301

- ***Nuclear modification factor for heavy flavor***

Over the last few decades, experimental results from RHIC and LHC using light flavor probes have demonstrated that a strongly coupled quark-gluon plasma (sQGP) is created in these heavy-ion collisions. The most significant evidence comes from the strong collective flow and the large high transverse momentum (p_T) suppression in central collisions for various observed hadrons including multistrange-quark hadrons φ and Ω.

Heavy quarks (*c, b*) are created predominantly through initial hard scatterings due to their large masses. The modification to their production in transverse momentum due to energy loss and radial flow and in azimuth due to anisotropic flows is sensitive to heavy quark dynamics in the partonic sQGP phase. Transverse mass spectra can be used to study the collectivity of produced hadrons in heavy-ion collisions. Figure 26shows the D^0 invariant yield at mid-rapidity ($|y| < 1$) as a function of transverse kinetic energy ($m_T - m_0$) for different centrality classes, where m_T= sqrt ($p_T^2 + m_0^2$) and m_0 is the D^0meson mass at rest.

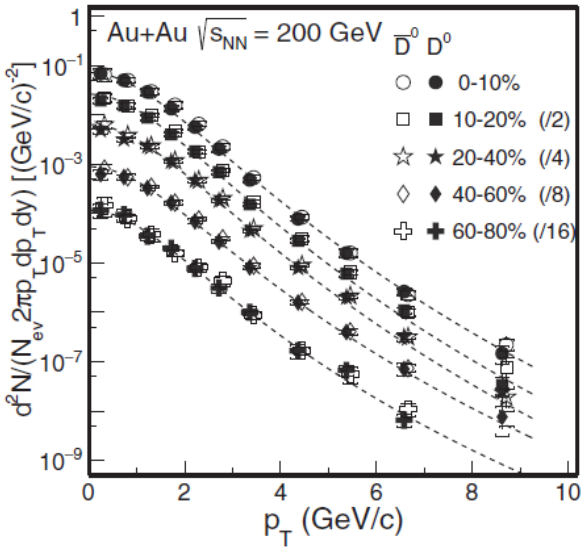

Figure 26. Yields of D^0 mesons produced in Au + Au collisions at $\sqrt{s_{NN}}$=200 GeV versus transverse momentum for different centrality

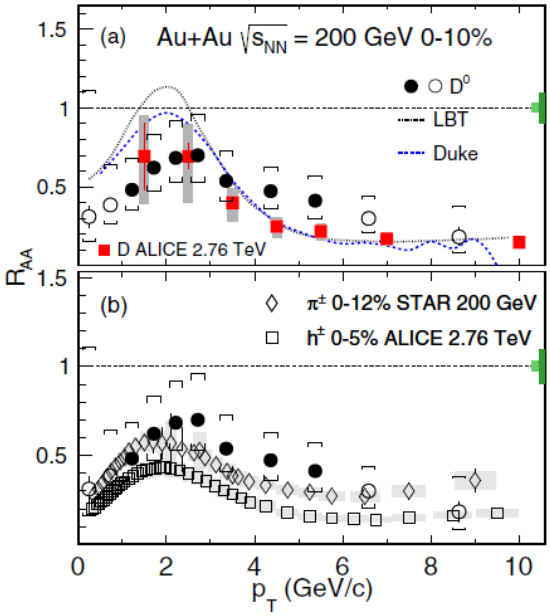

Figure 27. Nuclear modification factor for D^0 mesons produced in central Au + Au collisions at $\sqrt{s_{NN}}$=200 GeV versus transverse momentum

The nuclear modification factors RCP of D0 mesons is significantly suppressed at high p_T and the suppression level is comparable to that of light hadrons at $p_T > 5$ GeV/c. This indicates that charm quarks lose significant energy when traversing through the hot QCD medium.

It was also found that D mesons show similar suppression as light flavor hadrons at high p_T in central Au + Au collisions and suppression is similar of that at LHC energy.

Publications:

1. STAR Collaboration
"Centrality and transverse momentum dependence of D^0-meson production at mid-rapidity in Au + Au collisions at $\sqrt{s_{NN}}$= 200 GeV", Phys.Rev.C99 (2019) 034908

5. Spin physics Results in STAR Experiment at RHIC

A main goal of the spin physics program at the Relativistic Heavy Ion Collider (RHIC) at Brookhaven National Laboratory is to investigate processes of particle production in collisions of polarized protons, to understand the spin origin of the proton in terms of quarks and gluons as fundamental degrees of freedom of Quantum Chromodynamics. The ability to collide polarized beams at RHIC provides unique information on polarization phenomena over a wide range of collision energy, momentum and rapidity of the various probes produced (pions, photons, W bosons and jets). The STAR experiment at RHIC provides measurements of single and double-spin asymmetry in longitudinally and transversely polarized $p + p$ collisions at $\sqrt{s} = 200$ and 510 GeV to deepen our understanding of the proton spin structure and dynamics of parton interactions. Polarized processes with W^{-}boson production allow us to study the spin-flavor structure of the proton. The new results – the double longitudinal asymmetry, A_{LL}, of pion and jet production at $\sqrt{s} =$ 200 and 510 GeV, the single longitudinal, A_L, and transverse, A_N, asymmetry of W production at $\sqrt{s} = 510$ GeV, are recently obtained by STAR. Measurements on the transverse spin transfer of Λ and anti-Λ in $p + p$ collisions providing insights into transversely polarized fragmentation function and nucleon transversity distribution, and the nuclear modification of transverse spin asymmetry, A_N, from polarized $p +$ Au collisions are widely discussed. The proposed Forward Calorimeter System (FCS) and Forward Tracking System (FTS) upgrades at STAR would significantly improve the capabilities of existing detectors for measurements of observables such as asymmetries of pion, jet, Drell-Yan pair production at forward rapidity.

The double longitudinal asymmetry A_{LL} of the meson and jets production in collisions of polarized protons at the energy of $\sqrt{s} = 200$ GeV has been measured. The asymmetry was used to extract the spin-dependent gluon distribution. A compelling evidence on positive sign of the integral gluon contribution ΔG in the proton spin was obtained. The growth of the single spin asymmetry A_N of pion production in experiments with transversally polarized protons was found. The first measurements of the single longitudinal asymmetry A_L of $W^{\pm}$ boson production in proton-proton collisions at energy $\sqrt{s} = 510$ GeV allow us to extract spin-dependent distribution of sea u- and d-quarks ($\Delta\bar{u}$, $\Delta\bar{d}$).

5.1. Polarization of sea quarks

The STAR experiment at RHIC has provided significant contributions to our understanding of the spin structure and dynamics of the proton. The production of $W^{\pm}$ bosons in longitudinally polarized p-p collisions at$\sqrt{s}$= 510 GeV provides a direct probe of the spin-flavor structure of the proton through the measurement of the parity-violating single-spin asymmetry, A_L. $W^{\pm}$ bosons are produced in anti-$u + d$ (anti-$d + u$) collisions and can be detected through their leptonic decays, where only the respective charged lepton is measured. The STAR experiment is well equipped to measure $W \rightarrow e + \nu$. The main STAR detector sub-systems used in this measurement are the Time Projection Chamber and Electromagnetic Calorimeters. The published 2011/2012 STAR A_L results based on 86 pb^{-1} provided significant impact in constraining the helicity distributions of anti-u and anti-d quarks. In 2013, STAR collected an additional, larger data sample of 250 pb^{-1}. Results from the 2013 dataset for the measurement of $W^{\pm}$ A_L as well as for $W^{\pm}$ A_{LL} and ZA_L give the impact on the sea-quark helicity distribution functions.

Studying the processes with production of W bosons provides information on the spin-dependent flavor structure of the proton spin.

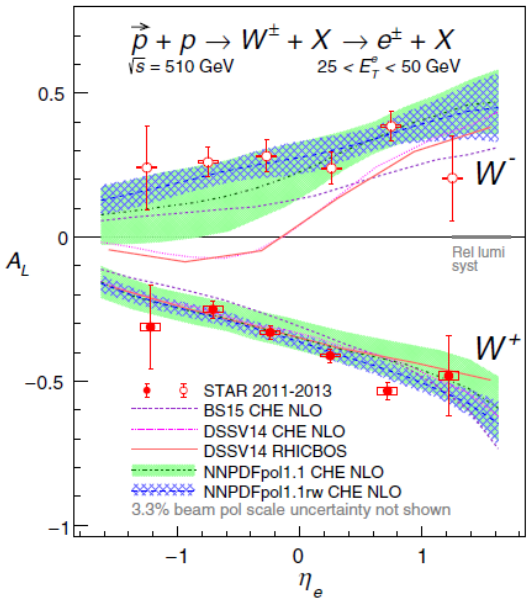

Figure 28.Longitudinal single-spin asymmetries, A_L, for W production as a function of the positron or electron pseudorapidity, η_e, for the combined STAR 2011 + 2012 and 2013 data samples for $25 < E_{eT} < 50$ GeV (points) in comparison to theory expectations (curves and bands) described in the text.

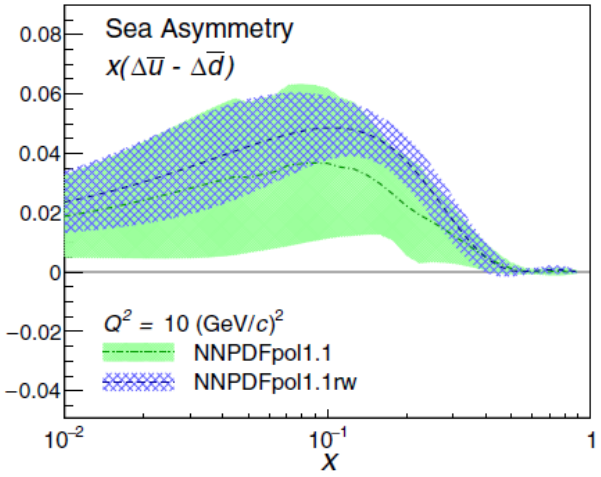

Figure 29.The difference of the light sea-quark polarizations as a function of x at a scale of $Q2 = 10$ (GeV^2). The green band shows the NNPDFpol1.1 results and the blue hatched band shows the corresponding distribution after the STAR 2013 W data are included by reweighting.

Single spin asymmetry of W production in collision with one polarized proton. Clear sea quark polarization asymmetry seen based on new STAR data $\Delta\bar{u} > \Delta\bar{d}$.

5.2. Asymmetry of jet production and gluon polarization

The proton consists of quarks and antiquarks, bound by gluons. The gluons provide about half of the momentum of the proton, and their interactions provide most of the mass. Nonetheless, we know very little about the role that gluons play in determining the fundamental proton quantum numbers, such as its spin. The spin program at the Relativistic Heavy Ion Collider(RHIC) has made significant progress toward addressing the question of how much, if at all, gluon spins contribute to the spin of the proton.

The first measurement of the inclusive jet and the dijet longitudinal double-spin asymmetries, A_{LL}, at midrapidity in polarized pp collisions at a center-of-mass energy 510 GeV. The inclusive jet A_{LL}

measurement is sensitive to the gluon helicity distribution down to a gluon momentum fraction of $x \approx 0.015$, while the dijet measurements, separated into four jet-pair topologies, provide constraints on the$x$ dependence of the gluon polarization. Both results are consistent with previous measurements made at 200 GeV in the overlapping kinematic region, $x > 0.05$, and show good agreement with predictions from recent next-to-leading order global analyses.

The results are sensitive to the gluon polarization over the momentum fraction range from $x \approx 0.015$ to $x \approx 0.2$. The inclusive jet results will provide important new constraints on the magnitude of the gluon polarization and the dijet results will provide important new constraints on the shape of $\Delta g(x)$ when they are included in future global analyses of the polarized PDFs, especially in the region $x < 0.05$that has been unconstrained by input data in previous global analyses.

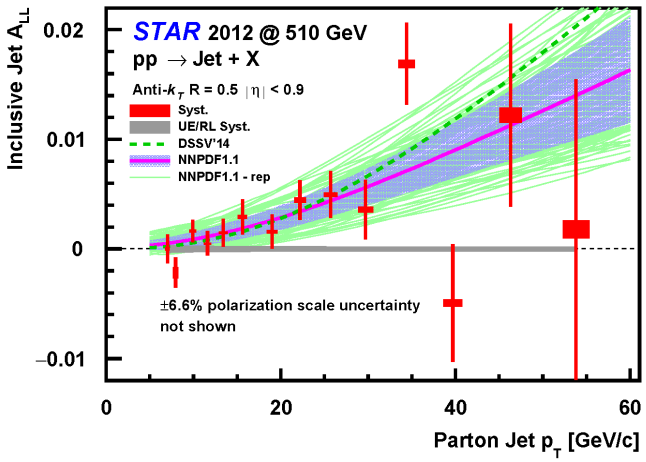

Figure 30. Asymmetry A_{LL} as a function of parton jet p_T for inclusive jets with |η|<0.9 in 510 GeV pp collisions. The bars show statistical errors, while the size of the boxes show the point-to-point systematic uncertainties on A_{LL} (vertical) and p_T (horizontal). The gray band on the horizontal axis represents the combined relative luminosity and underlying event uncertainties, which are common to all the points. The results are compared to predictions from DSSV14and NNPDFpol1.1 including the solid blue uncertainty band for the latter. The green curves are predictions from the 100 equally probable NNPDFpol1.1replicas.

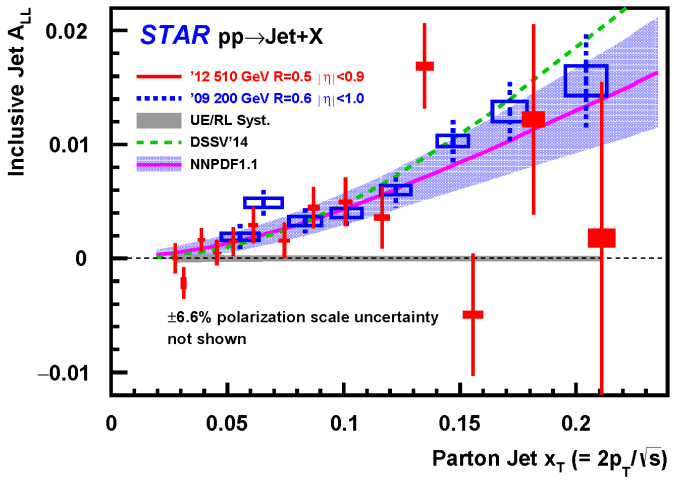

Figure 31. Asymmetry A_{LL} as a function of x_T for inclusive jets in 510 GeV pp collisions (red solid lines), compared to previous measurements of A_{LL} at 200 GeV (blue dotted lines).

5.3. Transverse spin distributions. Collins and Silvers asymmetries

The partonic structure of the nucleon at leading twist in a collinear picture can be described by three parton distribution functions (PDFs): the unpolarized parton distribution, $f(x;Q^2)$; the parton helicity distribution, $\Delta f(x,Q2)$ and the transversity distribution, $h1(x,Q^2)$.

The first measurements of transverse single-spin asymmetries from inclusive jet and jet + π production in the central pseudo-rapidity range from $p\uparrow + p$ at500 GeV. The data were collected in 2011 with the STAR detector. As in previous measurements at200 GeV, the inclusive jet asymmetry is consistent with zero at the available precision. The first-ever measurements of the "Collins-like" asymmetry, sensitive to linearly polarized gluons in a polarized proton, are found to be small and provide the first constraints on model calculations. For the first time, we observe a nonzero Collins asymmetry in polarized-proton collisions. The data probe values of Q^2 significantly higher than existing measurements from SIDIS. The asymmetries exhibit a dependence on pion z and are consistent in magnitude for the two charged-pion species. For π^+, asymmetries are found to be positive, while those for $\pi-$ are found to be negative. The present data are compared to Collins asymmetry predictions based upon SIDIS and e^+e^- data. The comparisons are consistent with the expectation for TMD factorization in proton-proton collisions and universality of the Collins fragmentation function. The data show a slight preference for models assuming no suppression from TMD evolution. Further insight into these theoretical questions can be gained from a global analysis, including di-hadron asymmetries and Collins asymmetries from STAR.

Transverse Momentum Dependent PDFs (TMD): TMDs allow us to go beyond the one-dimensional picture of the proton.

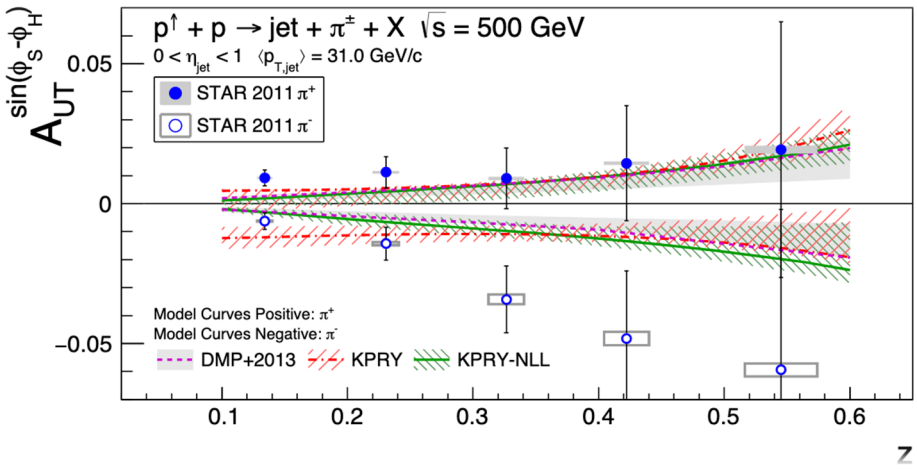

Figure 32. Collins asymmetries as a function of pion z for jets reconstructed with $22.7 < p_T < 55.0$ GeV/c and $0 < \eta < 1$.

Results for Collins-like asymmetries are presented in terms of particle-jet p_T and pion z (Figure 33). Because the subprocess fraction changes as a function of particle-jet p_T, it is informative to examine how the asymmetries depend on p_T. The Collins-like asymmetry is expected to arise from gluon linear polarization; thus, the best sensitivity should reside at lower values of jet p_T. The left-hand panel of Figure 33 shows the asymmetry as a function of particle-jet p_T for different ranges of jet η and ion z. The right-hand panel of Figure 33 presents the Collins like asymmetry dependence on pion z in bins of jet η and jet p_T . Across the board, the asymmetries are consistently small. Systematic uncertainties are well constrained with the dominant uncertainties arising from statistics. The largest systematics arise from the parton-jet matching probabilities at low-p_T and leak-through at mid-to-high values of p_T.

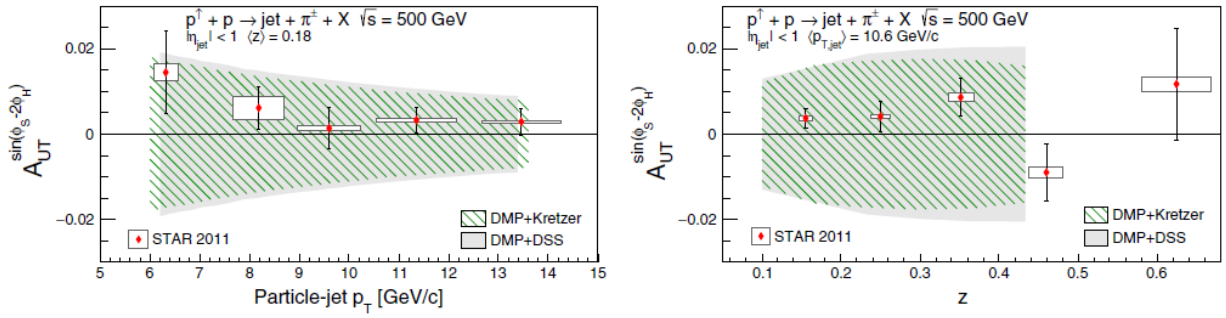

Figure 33. Collins-like asymmetries as a function of particle-jet p_T for pions reconstructed with $0.1 < z < 0.3$ (left) and as a function of pion z for jets reconstructed with $6.0 < p_T < 13.8$ GeV = c (right).

The transverse single spin asymmetry of weak boson production in transversely polarized proton-proton collisions at $\sqrt{s}$ = 500GeV with a recorded luminosity of 25pb^{-1} were measured by the STAR experiment at RHIC. Asymmetry A_N is defined as

$$A_N = \frac{d\sigma^{\uparrow} - d\sigma^{\downarrow}}{d\sigma^{\uparrow} + d\sigma^{\downarrow}},$$

where $d\sigma^{\uparrow}(d\sigma^{\downarrow})$ is the differential cross section as a function of azimuthal angle when the spin direction of the proton beam pointing up (down).

The measured observable is sensitive to the Sivers function, one of the transverse-momentum-dependent (TMD) parton distribution functions, which is predicted to have the opposite sign in proton-proton collisions from that observed in deep inelastic lepton-proton scattering (SIDIS). The Sivers function describes the correlation between the intrinsic transverse momentum of a parton and the spin of the parent proton. These data provide the first experimental investigation of the nonuniversality of the Sivers function, fundamental to our understanding of QCD.

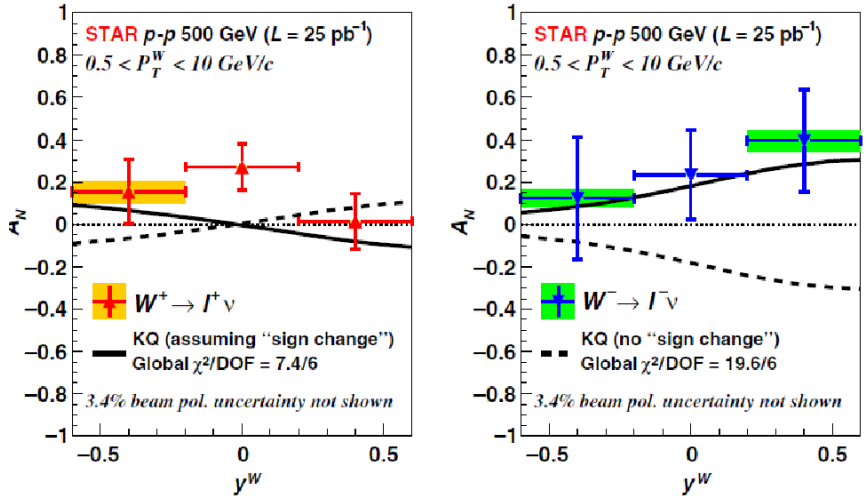

Figure 34. Asymmetry A_N of W^+ and W^- production in $p\uparrow + p$ collisions at $\sqrt{s}$=200 GeV as a function of boson rapidity.

Figure 34 shows a combined fit on W^+ and W^- asymmetry A_N as a function of rapidity y_W to the theoretical prediction in the model without TMD evolution assuming a sign change in the Sivers function (the solid line) and without sign change (the dashed line).

The current data favor theoretical models that include a change of sign for the Sivers function relative to observations inSIDIS measurements, if TMD evolution effects are small. The results presented here can help to constrain theoretical models including the TMD evolution.

5.4. Asymmetry in polarized proton collisions with nuclei (Al, Au) at 200 GeV

The measurements and the interpretation of Transverse Single Spin Asymmetries (TSSA) for forward pion production in high energy *pp* collisions have a rich history. The π^0 single spin asymmetry A_N that is defined below is measured and compared for collisions between the polarized proton and another proton (*pp*), an aluminum nucleus (*p*Al) or a gold nucleus(*p*Au). These data from the Solenoid Tracker At RHIC (STAR) experiment at the Relativistic Heavy Ion Collider (RHIC) were collected during the 2015 RHIC run, involving collisions between nucleons at center-of-massenergy200 GeV per nucleon pair. The photon pair from the decay of the π^0 was detected with the STAR Forward Electromagnetic Calorimeter (FMS).

Referring to a right-handed coordinate system, an initial state polarized proton is referred to as spin "up" it has a positive spin projection along the y axis while proton momentum is along the the*z* axis. This polarize proton collides with an unpolarized proton or nucleus travelling along the *z* axis. A forward pion has a positive longitudinal component of momentum, given by a positive fraction $X_F = 2\,p_z/\sqrt{s}$ of the polarized proton momentum. The angle φ is the pion azimuthal angle about the *z* axis measured from the *x* axis. The three component of pion momentum are specified with coordinates X_F, p_T and φ. The dependence of the pion differential cross section on transverse spin, expressed as the pion momentum dependent asymmetry $a_N(X_F, p_T, \varphi)$ and the TSSA A_N, is defined for the process $p\uparrow + p$(or A) $\rightarrow \pi^0 + X$:

$$a_N(x_F, p_T, \phi) = \frac{\sigma^{\uparrow}(x_F,p_T,\phi) - \sigma^{\downarrow}(x_F,p_T,\phi)}{\sigma^{\uparrow}(x_F,p_T,\phi) + \sigma^{\downarrow}(x_F,p_T,\phi)} = A_N(x_F, p_T)\,cos(\phi).$$

The single spin asymmetry for π^0 production has been measured in *pp*, *p*Al and *p*Au collisions. The kinematic dependence of A_N on X_F and p_T is similar for the three collision types. In each case, up to $X_F \approx$ 0:5 the asymmetry increases with p_T at fixed X_F. The suppression of A_N in collisions with nuclear beams is modest, with A_N ratio between *p*Au and pp on the order of 80 %. This corresponds to a power law nuclear A dependence $A_N(A) \propto A^P$ with powers, depending on the kinematic interval considered, in the range of $-0.05 < P < 0.05$. There is no evidence of further suppression of A_N in the low p_T region where gluon saturation effects may be most relevant.

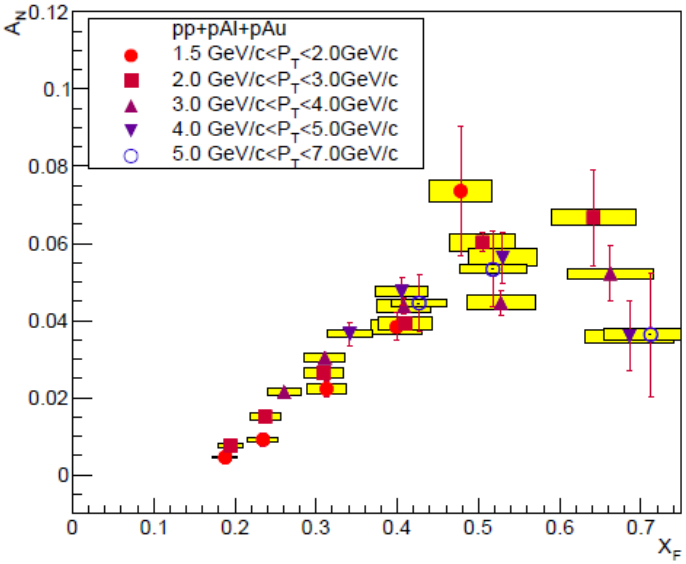

Figure 35. The X_F dependence of the π^0 A_N is shown with data from the combined *pp*, *p*Al and *p*Au data points combined, collecting points within X_F intervals and the indicated p_T range. Data points are shown separately for five intervals of transverse momentum indicated by different

symbols and plotted horizontally at the average X_F for each combined point. Vertical error bars represent statistical errors and the systematic horizontal and vertical errors are shown with filled boxes.

5.5. Fractal structure and self-similarity in process with polarized protons

- ***Self-similarity of proton spin and asymmetry of jet production***

M.V.Tokarev,I.Zborovsky, Physics of Particles and Nuclei Letters, V.12, №2, 2015, pp.313–323

M. Tokarev, I.Zborovský
"Self-similarity of the proton spin", Workshop "Physics programme for the first stage of the NICA SPD experiment", JINR, Dubna, LHEP, 5-6 October 2020

Spin is one of the most fundamental properties of elementary particles. The proton spin structure is studied for a long time in processes with polarized leptons and protons. The goal is to understand complete picture of the proton spin in terms of quark and gluon degrees of freedom.

The concept of z-scaling was extended for description of processes with polarized protons. The double longitudinal spin asymmetry, A_{LL}, of inclusive jets produced in proton-proton collisions at $\sqrt{s}$ = 200 GeV (Phys. Rev. Lett. 115, (2015) 092002) measured by the STAR Collaboration at RHIC is shown in Figure 36. The asymmetry was analyzed in the framework of z-scaling approach. A hypothesis of self-similarity and fractality of the proton spin structure are suggested and developed. The possibilities to extract information on spin-dependent fractal dimensions of proton and jet fragmentation process from the asymmetry are justified. The spin-dependent fractal dimension of proton is estimated. Authors consider that the quantity is a new fundamental property of every particle as a mass, charge, spin.

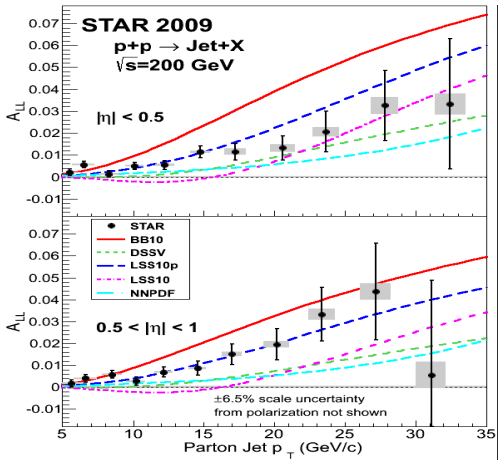

Figure 36.Double longitudinal spin asymmetry of jet production in polarized p-p collisions at $\sqrt{s}$ = 200 GeV, measured by the STAR collaboration.

Figure 37shows the cross section of inclusive jet production in $\vec{p}+\vec{p} \rightarrow jet+X$ reaction in z-presentation and the ratio of the spin-independent and the spin dependent scaling functions and the corresponding fractal dimensions. The functions coincide each other with high accuracy in all considered region of z. The coincidence is the indication on self-similarity of polarization processes seen in the data z-presentation.

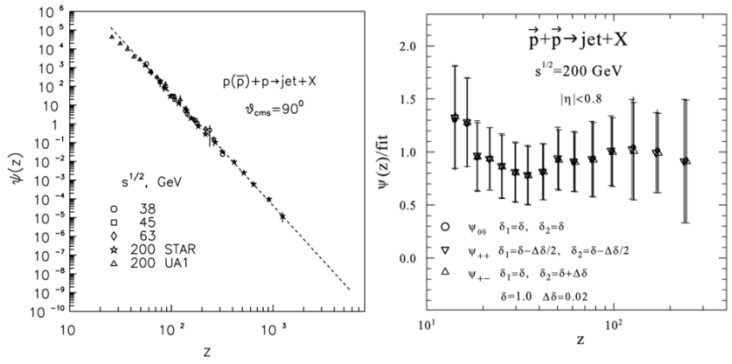

Figure 37. The ratios of the scaled spin-dependent and spin-independent functions for inclusive jet production in polarized *p-p* collisions at$\sqrt{s}$ = 200 GeV.

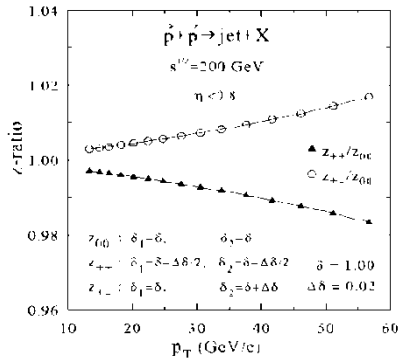

Figure 38.The ratios of the spin-dependent self-similarity parameters for inclusive jet production in polarized p-p collisions at $\sqrt{s}$ = 200 GeV.

The respective ratios of the spin-dependent self-similarity parameters (z_{++}/z_{00}, z_{+-}/z_{00}) as functions of the transverse momentum are shown in Figure 38. The effect of spin-spin interactions on the ratios does not exceed 4 %. The ratio decreases as function of p_T for the interactions of protons with the same (positive or negative) helicities and increases with p_T for the opposite orientation of proton helicities. The larger values of z_{+-} mean that spin structure of proton can be probed with higher resolution (i.e. at smaller scales) in the collisions of protons with opposite helicities relative to the interactions where the protons have the same helicities.Similarly as for unpolarized processes, an abrupt change of the spin-dependent fractal dimensions should indicate on a spin phase transition. To test such hypothesis, the measurements of spin asymmetries and cross sections need very good accuracy. The measurements of non-zero asymmetry, A_{LL}, give us strong motivation to study fractal properties of proton spin in the reactions with inclusive jet production. We believe that considered scaling property for polarization processes reflects the self-similarity of the spin structure of the colliding objects and interaction mechanism of their constituents.

- ***Fractal structure of hadrons in processes with polarized protons***

M.V. Tokarev, I. Zborovsky, A.A. Aparin, Phys. Part. Nucl .Lett., Vol.12, № 1, 2015, 48–58.

M. Tokarev, I. Zborovský
"Self-similarity of the proton spin", Workshop "Physics programme for the first stage of the NICA SPD experiment", JINR, Dubna, LHEP, 5–6 October 2020.

The concept of *z*-scaling previously developed for analysis of inclusive reactions in proton-proton collisions was applied for description of processes with polarized protons.

The *z*-scaling approach shows itself as an effective tool for sophisticated data analysis in searching for new phenomena, verification of theoretical models, etc. Extension of the method for analysis of polarization phenomena and verification of self-similarity of spin-dependent inclusive cross sections for particle production in $p + p$ collisions is an interesting problem which could give new insight into the origin of proton spin at small scales. The spin-dependent fractal dimensions are new parameters of the *z*-scaling theory. They are new characteristics of polarization properties of proton structure, constituent interactions and hadronization process. The double longitudinal spin asymmetry A_{LL} of π^0-meson production and the coefficient of the polarization transfer D_{LL} of Λ-hyperon production in proton-proton collisions measured by STAR collaboration at RHIC were analyzed in the framework of *z*-scaling. The spin-dependent fractal dimensions of proton and fragmentation process with polarized Λ hyperon were estimated. A study of the spin-dependent constituent energy loss as a function of transverse momentum of the inclusive hadron and collision energy was suggested.

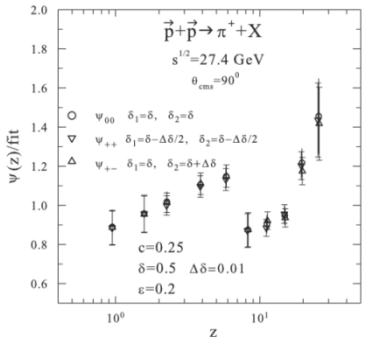

Figure 39. The ratios of the scaled spin-dependent and spin-independent functions for inclusive jet production in polarized p-p collisions at$\sqrt{s}$ = 200 GeV.

The scaled spin-dependent Ψ_{++}, Ψ_{+-} and spin-independent Ψ_{00} functions of pion production in proton-proton collisions at $\sqrt{s}$ = 27.4, 200 GeV and ϑ_{cms}= 90° in z -presentation.

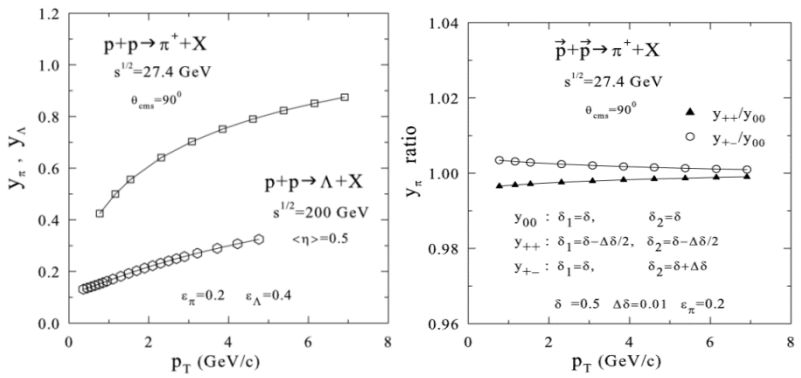

Figure 40. The momentum fraction y_a and the scaled ratio of the momentum fractions for pion production in unpolarized and polarized p-p collisions at$\sqrt{s}$ = 27.4 GeV.

6. Proposed Program – Hot QCD in Run-21, 23, and 25

6.1. Run-21 – completion of the BES-II Program

The highest priority for Run-21 is the completion of the proposed BES-II program. At this time, the only system that remains to be taken is the 7.7 GeV collider data set. This energy is extremely important for several reasons. First, theoretical calculations suggest that the highest baryon density is achieved in collisions at this energy; second, several of the BES-I experimental signatures which have been put forth to be sensitive to the presence of deconfined matter either lose significance or are no longer present at this energy; third, the BES-I data showed enhanced fluctuations at this energy; finally, this energy provides the best acceptance overlap with the fixed-target program.

Although the 7.7 GeV collider data set is extremely important from the point of view of the science, it is also technically the most challenging data set. The technical challenge of achieving a viable collision rate at this energy was the motivation to develop the Low Energy RHIC electron Cooling (LEReC) and is the reason that this energy has been left to the final year of the program.

The specific physics goals (and required statistics) include: measurement of the elliptic flow of the phi meson for which the constituent quark scaling was suggested to break down in the lowest energy BES-I data (80 M events required); measurement of the correlators associated with the charge separation induced by the chiral magnetic effect which were seen to collapse at the lowest BES-I energies (50 M events required); differential measurements of the directed flow of protons which was seen to show evidence of a softening of the equation of state in the lowest BES-I data (20 M events required); Azimuthal femtoscopy measurements of protons to study the tilt angle of the source (35 M events required); measurement of the net-proton kurtosis which showed significant enhanced fluctuations at 7.7 GeV in the BES-I data (70 M events required); measurements of the di-lepton invariant mass distributions to determine in the excess in the low mass region is proportional to the total baryon density (100 M events required); and the global lambda polarization to determine the magnetic field significance (50 M events required). These analyses are being pursued at all of the BES-II collider energies; for several of the physics measurements, the 7.7 GeV energy is expected to be either the most significant or the most challenging.

The 7.7 GeV collider system provides the essential bridge between the collider and fixed-target energy scans. Although in later sections we detail a request to acquire fixed-target data at higher overlap energies, there is the largest region of common coverage at this energy. This will provide critical cross checks between the different modes.

Although the 7.7 GeV collider system is the most technically challenging system of the suite of BES-II and FXT energies, one can use the performances which have already been achieved during the BES-II program to help develop projections for the 7.7 GeV collider energy. In 2010, STAR achieved a good event rate of 7 Hz; a factor of three improvement would result in a 21 Hz rate. Scaling the performance at 9.2 GeV by γ^3 would predict a good event rate of 19.3 Hz. We project the good event rate to fall between 16 and 24 Hz. We project the range of hours of data taking per day to fall between 12 and 15. These numbers suggest a range in the expected number of weeks to reach the goals from 11 to 20 weeks. We should note that CAD has provided projections which suggest that it will take 28 weeks to reach the goals. Our projections are more optimistic. Although we recognize that it is likely that running the 7.7 system will require all the available beam time in 2021, the optimistic range of our predictions suggests that we should prepare for success and we have therefore considered and prioritized other programs which could be run in 2021 if time were to be available.

6.2. Au + Au collisions in FXT mode at $\sqrt{s_{NN}}$ = 3.0 GeV (300 million goal)

QCD matter at high baryon chemical potential region contains a wealth of unexplored physics and is one the central focus of current and future heavy-ion collision programs in few GeV energy range around the world. RHIC has been able to deliver beams with the energy as low as 3.85 GeV per nucleon. Utilizing the gold fixed target (FXT) installed in the STAR experiment, we were able to record collision events at the center-of-mass-energy as low as $\sqrt{s_{\mathrm{NN}}} = 3.0$ GeV, which corresponds to baryon chemical potential of $\mu_B \sim 720$ MeV in central collisions. The STAR detector configuration (including the iTPC and eTOF) has full midrapidity coverage ($|y < 0.5|$)

at this energy and enables us to carry a systematic investigation of the dynamics of the QCD matter created in these collisions at $\sqrt{s_{\mathrm{NN}}}$ from 3.0 up to 200 GeV.

At such a high μ_B region and moderate temperatures, baryon dynamics become important or even dominant in understanding the QCD matter properties. Strange quarks, due to their heavier masses, play an important role in study the high net-baryon density QCD matter. The combination of increased sensitivity of strange quarks with the existing high baryon density in low energy heavy-ion collisions offers a unique condition to create various light hypernuclei, which enables us to study *e.g.* the hyperon-nucleon (*Y–N*) interactions, which have potential implications for the inner structure of compact stars in nuclear astrophysics.

STAR has collected ~ 250 million FXT Au + Au events at $\sqrt{s_{\mathrm{NN}}} = 3.0$ GeV in 2018 before iTPC and eTOF were installed. We propose to collect a minimum of 300 million events with the extended phase-space coverage enabled by iTPC and eTOF for the following measurements:

- high moments of proton multiplicity distributions covering the same midrapidity acceptance $|y < 0.5|$, $0.4 < p_T < 2.0$ GeV/c, comparable to that with the BES-I and BES-II measurements in collider mode.
- precision φ meson production at midrapidity to test the validity of Canonical Ensemble (CE) for strangeness production at high baryon density region.
- systematic measurements of lifetime, binding energy, production yield, collective flow of light hypernuclei ($^{3}_{\Lambda}$H, $^{4}_{\Lambda}$H, $^{5}_{\Lambda}$H etc.).
- measurement of low- and intermediate-mass dileptons to extract fireball lifetime, its average temperature and to access the microscopic properties of matter. This would be the first measurement of electromagnetic radiation at this energy which will guide the future high μ_B facilities at FAIR and NICA.

With additional beam time allowed, we would like to further collect up to 2 billion Au + Au FXT events at $\sqrt{s_{\mathrm{NN}}} = 3.0$ GeV which will be elaborated in the next section.

One feature we would like to point out is that the single beam energy for FXT collisions at $\sqrt{s_{\mathrm{NN}}} = 3.0$ GeV is 3.85 GeV per nucleon, the same beam energy to be used for colliding to collect the major 7.7 GeV collision dataset in Run-21. This leads to a negligible transition time for operation between $\sqrt{s_{\mathrm{NN}}} = 7.7$ GeV collider mode and $\sqrt{s_{\mathrm{NN}}} = 3.0$ GeV FXT mode.

High moments of proton multiplicity distributions: A non-monotonic behavior of net-proton high moments $\kappa\sigma^2$ as a function of collision energy has been suggested to be an evidence of the existence of QCD critical point. Figure 41 (left panel) shows the final STAR measurement from the BES-I data as a function of energy exhibiting a suggestive non-monotonic behavior. A complete picture of the non-monotonic behavior requires measurements at collision energies below the lowest collider mode energy (7.7 GeV) by utilizing the FXT mode collisions. STAR detector configuration has the best midrapidity coverage for fixed target collisions at the lowest collision energy $\sqrt{s_{\mathrm{NN}}} = 3.0$ GeV. Figure 41 middle and right panels show the proton acceptance with TPC and barrel TOF in Run-18 FXT data at 3.0 GeV and Run-10 collider data at 7.7 GeV, respectively. In the 2018 FXT data, to ensure > 95 % purity of the proton sample, one needs to utilize the barrel TOF for high momentum particle identification. With this requirement, the proton acceptance in Run-18 covers full negative rapidity region ($-0.5 < y < 0, 0.4 < p_T < 2.0$ GeV/c), while missing a considerable acceptance in the positive rapidity region. A new run, with eTOF and iTPC, would allow for phase space coverage comparable to the one in collider mode (indicated by the box in the middle panel). The estimated acceptance boundary for protons is indicated by

the red line shown in Figure 41 middle panel. We can therefore cover the full midrapidity $y < 0.5$ region from $0.4 < p_T < 2.0$ GeV/c which will be the same as these measurements conducted in collider mode data, shown in the right panel. This would allow to perform a systematic scan of the net-proton high moments analysis within the same mid-rapidity acceptance across the collision energy from 3.0 up to 200 GeV. In the meantime, the increased rapidity coverage will also enable us to investigate the rapidity-window (Δy) dependence of these fluctuations, which will offer us deep understanding on the physics origin through the development of these fluctuations vs. Δy.

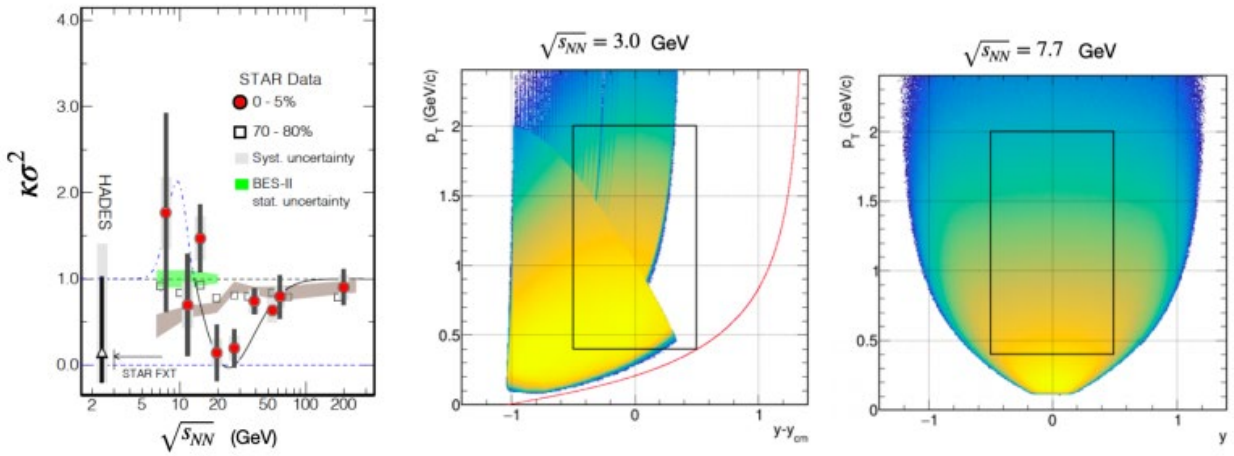

Figure 41. (Left) The net-proton $\kappa\sigma^2$ in most central (0–5 %) and peripheral (70–80 %) Au + Au collisions as a function of collision energy. (Middle/Right) Proton acceptance plot p_T vs. y in the center-of-mass frame at $\sqrt{s_{\mathrm{NN}}} = 3.0$ GeV (FXT data from Run-18) and 7.7 GeV (collider data from Run-10), respectively. The red curve in the middle panel indicates the acceptance boundary with iTPC and eTOF.

φ meson production: Yields of strange hadron produced in relativistic heavy-ion collisions from RHIC BES-I energies up to the LHC energy ($\sqrt{s_{\mathrm{NN}}} = 7.7$–5500 GeV) can be well described by thermal model with Grand Canonical Ensemble (GCE) in which strange quark number is conserved on average. It has been argued that at low energy heavy-ion collisions when the fireball created in these collisions becomes small enough the GCE for strange quarks will break down. Strangeness needs to be conserved on the event-by-event basis, therefore only Canonical Ensemble (CE) is applicable to strange hadron production. Strange hadrons with finite strangeness number (e.g. K, Λ etc.) will suffer from a suppression due to the strangeness number conservation, often characterized by a canonical radius (r_c) for strange quark profile in comparison to the regular radius (r) for light quarks. The φ meson is the lightest bound state of s and $\bar{s}$ quarks with zero net-strangeness number. Its production yield, on the contrary, will not suffer from the canonical suppression. Therefore, CE models predict the φ/K^- ratio will show an enhancement in very low energy heavy-ion collisions while GCE models calculate the φ/K^- ratio will gradually drop to zero at the φ production threshold in $p + p$ collisions. ($\sqrt{s_{\mathrm{NN}}} = 2.89$ GeV).

Experimentally, the measured φ/K^- values stay around 0.15 at $\sqrt{s_{\mathrm{NN}}} > 5$ GeV up to the LHC energy. At collision energies below the φ production threshold in $p + p$ collisions, measurements from HADES and FOPI suggest an enhancement compared to those at high energies, consistent with the CE description for strange quarks at such low energies within appreciable uncertainties. High precision measurement of the φ/K^- at such low energies will be of great interest to systematic investigate the φ meson and strangeness production mechanism in heavy-ion collisions.

We have performed such a measurement using the FXT data at $\sqrt{s_{\mathrm{NN}}}$ = 3 GeV taken in 2018. Figure 42 middle panel shows the reconstructed K^+K^- invariant mass distributions in 0–60 %

centrality. The shaded histogram shows the K^+K^- pair distributions from the mixed-event technique while normalized at the mass region above the φ meson signal. The red data points show the mixed-event background subtracted distributions and the φ meson signal obtained in this data is about 60σ. The right panel shows the φ meson acceptance coverage in center-of-mass frame. Due to the small production yield of kaons, one needs to rely on clean particle identification using TOF detector to obtain a control background in the φ meson reconstruction. The black curve indicates the single track acceptance boundary from TPC and barrel TOF in 2018 year run. One can see the φ meson p_T acceptance at midrapidity is limited at 0.6–0.8 GeV/c. This covers roughly only 40 % of the φ meson yield in the full p_T region, leading to a considerable amount of systematic uncertainty due to the p_T extrapolation. The blue curve in the same panel indicates the anticipated single track boundary with iTPC and eTOF. The p_T lower limit can be extended down to 0.2 GeV/c, yielding a p_T coverage of 90 % of total dN/dy at midrapidity. This will greatly reduce the systematic uncertainty in the total φ meson yield measurement.

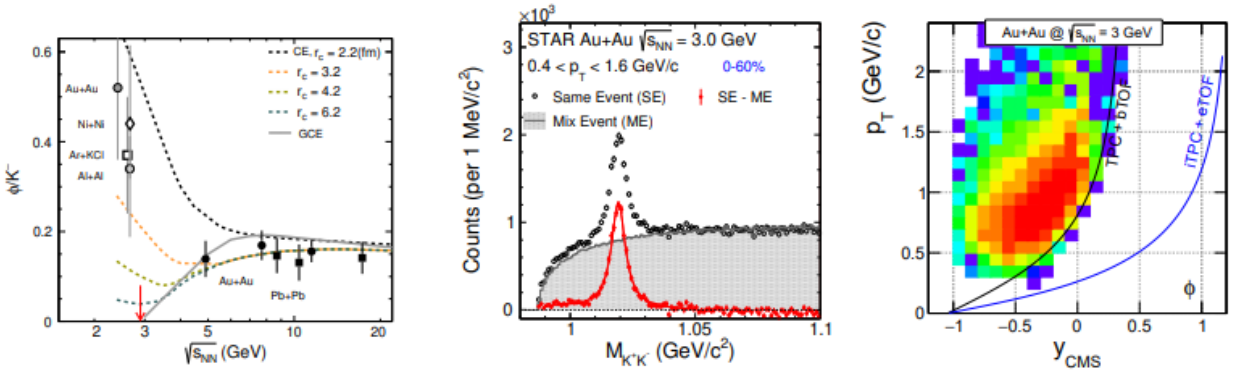

Figure 42. (Left) φ/K^- ratio as a function of collision energy from several heavy-ion experiments in comparison to thermal model calculations assuming strangeness following GCE and CE with different canonical radius. (Middle) Invariant mass distributions of K^+ K^- pairs and the φ meson signal in Run-18 FXT data at $\sqrt{s_{\mathrm{NN}}}$ = 3.0 GeV. (Right) Reconstructed φ meson candidate phase space distributions using Run-18 FXT data taken at $\sqrt{s_{\mathrm{NN}}}$ = 3.0 GeV. The black line shows the boundary of combining the TPC and barrel TOF detector for kaon identification. The blue line indicates the anticipated boundary extended by iTPC and eTOF for kaon identification in the proposed Run-21 FXT run at $\sqrt{s_{\mathrm{NN}}}$ = 3.0 GeV.

We therefore request to take the FXT data at $\sqrt{s_{\mathrm{NN}}}$ = 3 GeV with iTPC and eTOF detectors in RHIC Run-21. A roughly similar amount of statistics (300 million) will allow us to perform the measurement of φ/K^- ratio with high precision both statistically and systematically.

Hypernuclei production: Hypernuclei are those nuclei with one or more nucleons re- placed with hyperons (typically Λs). The study of hypernuclei lifetime, binding energy and their production mechanism offer insights to the understanding of hyperon-nucleon (*Y–N*) interactions. The *Y–N* interactions could have significant implications to our understanding of the internal structure of compact stars in nuclear astrophysics.

Heavy-ion collisions have shown great potential in studying the light hypernuclei properties and their production mechanism. There have been unprecedented measurements from RHIC and LHC on both the lifetime and binding energy (anti-)hypertriton ($^3_\Lambda$H and $\overline{^3_\Lambda\mathrm{H}}$). At low energy heavy-ion collisions, due to the high baryon density and high strangeness population, statistical hadronization thermal model predicts a significant enhancement of various light hypernuclei production yield, shown in Figure 43 left panel. The STAR FXT energy region from $\sqrt{s_{\mathrm{NN}}}$ = 3.0 –7.7 GeV sits

nicely in the maximum mid-rapidity production yield of various hypernuclei while STAR detector layout has the best midrapidity acceptance coverage at 3.0 GeV. Figure 43 right panel shows the reconstructed ${}^{4}_{\Lambda}\mathrm{H}$ and ${}^{5}_{\Lambda}\mathrm{He}$ signal from the Run-18 FXT dataset at $\sqrt{s_{\mathrm{NN}}} = 3.0$ GeV. These are so far the most unprecedented statistics on these light nuclei that will allow us to systematically investigate their lifetimes, binding energies as well as their production yield and collective flow behavior in heavy-ion collisions.

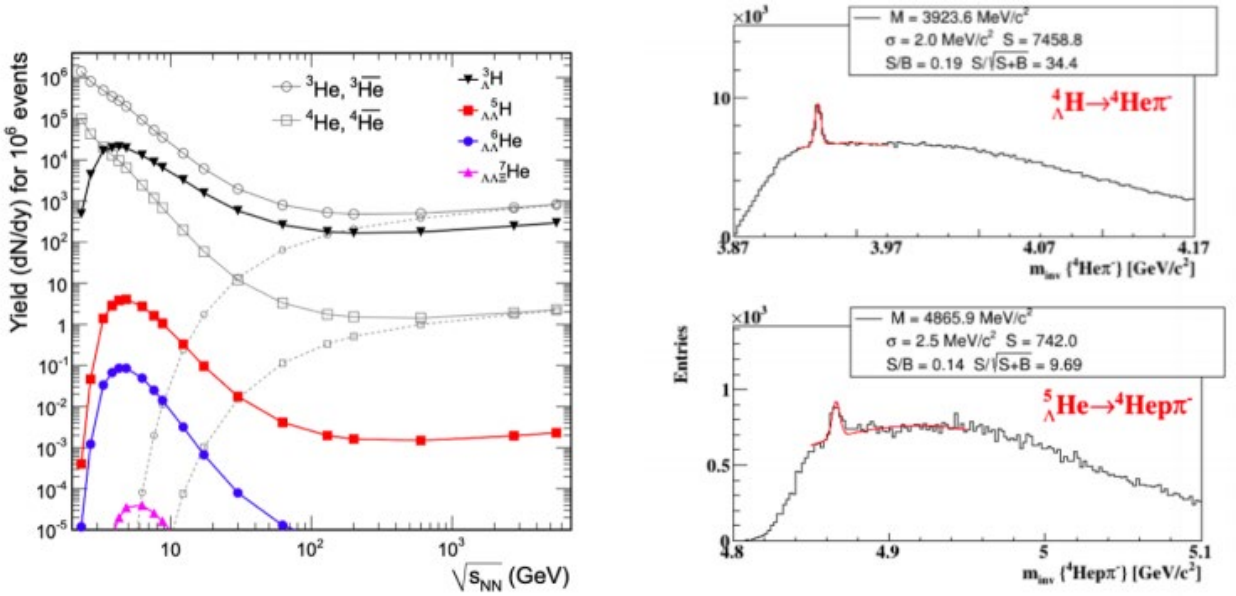

Figure 43. (Left) Thermal model predictions of various light nuclei and hypernuclei production yield at midrapidity in central heavy-ion collisions as a function of collision energy. (Right) Invariant mass distribution of ${}^{4}\mathrm{He}\pi^{-}$ (top) ${}^{4}\mathrm{He}p\pi^{-}$ (bottom) from 2018 FXT data at $\sqrt{s_{\mathrm{NN}}} = 3.0$ GeV. The ${}^{4}_{\Lambda}\mathrm{H}$ and ${}^{5}_{\Lambda}\mathrm{He}$ hypernuclei signal is clearly visible on top of background.

6.3. *Au + Au collisions in FXT mode at $\sqrt{s_{\mathrm{NN}}}$ = 9.2, 11.5, and 13.7 GeV*

The BES-II program aims to study the nature of QCD matter by varying the temperature and baryon chemical potential. High baryon chemical potentials are achieved by 'stopping' the baryons which made up the two colliding nuclei. To better understand the development of the baryon chemical potential and its profile through the interaction region, it is necessary to study the rapidity density distribution of the protons across a broad range in rapidity. It is important that the rapidity range covered includes the peak of the participant distribution which have been accelerated during the collision process. For all collider energies available at RHIC (7.7 GeV and above), the peak of the rapidity distribution of the stopped protons is outside or at the edge of the acceptance of the STAR TPC (which only extends 0.6 units beyond mid-rapidity with particle identification via dE/dx, this is extended to 1.0 units of rapidity using eTOF particle ID); for $\sqrt{s_{\mathrm{NN}}}$ = 9.2, 11.5, and 13.7 GeV, the shifted 0.9, 1.0, and 1.1 units away from mid-rapidity respectively. However, in fixed-target mode the STAR detector is excellent for studies of stopping as the acceptance extends 1.7 units from target rapidity (see Figure 44) toward mid-rapidity; for $\sqrt{s_{\mathrm{NN}}}$ = 9.2, 11.5, and 13.7 GeV, y_{CM} = 2.28, 2.50, and 2.68 respectively. Combining collider and fixed-target measurements at each energy will provide full coverage from target rapidity to center-of-mass rapidity. The stopping of the incident protons is the key to changing the baryon chemical potential in the interaction region and the changing baryon chemical potential is the key to mapping out the phase diagram of QCD matter.

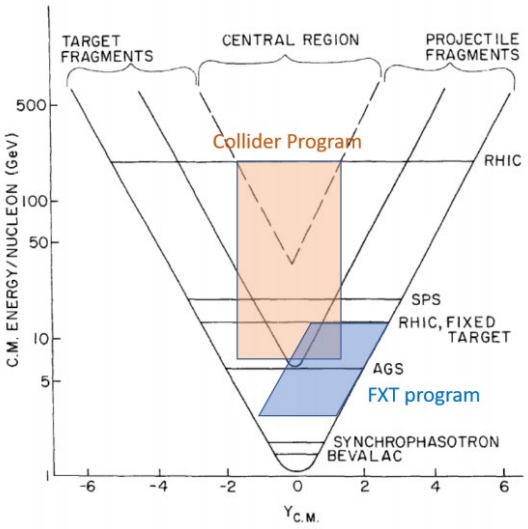

Figure 44. This figure has been modified from a figure in the introduction of the Conceptual Design Report for the RHIC facility. The black lines indicate different regions in the rapidity – center of mass energy space. The 'V' shaped region in the top center of the figure which is labeled at the central region have been predicted and demonstrate to be a low baryon chemical potential region characterized by a continuous phase transition between the QG and the hadron gas. The outer 'V' shaped region is dominated by the target fragments. Colored regions are overlaid to indicate the coverage of the STAR detector for collider (Orange) and FXT (Blue) modes. For the three higher energies currently being proposed, the FXT acceptance covers the region dominated by target fragments while the collider acceptance covers the equilibrated central region.

Complete rapidity density distribution for identified particles will provide important constraints for models. It has been noted by Shen that the high rapidity tails of the dN/dy distributions are very important and that high rapidity data are rare. In the energy range from $\sqrt{s_{\mathrm{NN}}}$ = 5.0 to 200 GeV, the only available proton rapidity density distribution measurements are from NA49 at 8.77 and 17.3 GeV and from BRAHMS at 62.4 and 200 GeV. Shen used these data to constrain his 3-D models of the collisions to better understand the elliptic flow measurements in heavy-ion collisions. In the BES-II energy range, around 10 GeV, these models can set strong constraints on the dependence of Quark-Gluon Plasma shear viscosity on temperature and net baryon chemical, however, in order to do so, it is necessary to have knowledge of the rapidity distributions of net-protons and produced particles.

It has been proposed that the trend of the rapidity shift of the stopped protons with collision energy will provide a signature of the softening of the equation of state at the phase transition. Specifically, the model which has a two-phase equation of state shows that he increases in the rapidity shift with collision energy stalls in the $\sqrt{s_{\mathrm{NN}}}$ = 8 to 12 GeV range.

We proposed to extend the studies to proton stopping through the BES-II energy regime. Specifically we propose to add three more energies to the high end of the FXT energy range. These energies are chosen to provide three more overlap energies with the collider program. Single beam energies of 44.5, 70, and 100 GeV will provide interactions at $\sqrt{s_{\mathrm{NN}}}$ = 9.2, 11.5, and 13.7 GeV (the top energy is not quite an overlap energy with the 14.6 GeV collider system). Combining the midrapidity coverage from the collider mode and the target rapidity coverage from the fixed-target mode will provide full rapidity coverage for inclusive observables. Since the focus for program will be inclusive observables, 50 M events will be sufficient at each energy. We propose that at each of these three energies, twelve hours be spent on beam development and twelve hours be spent taking data.

6.4. Run-21 – further opportunities

- ***Small System Run: O + O at $\sqrt{s_{NN}}$ = 200 GeV***

Collective long-range azimuthal correlations in A + A collisions have been successfully described as a hydrodynamic response by a fluid-like system to geometric shape fluctuations in the initial state. In recent years, observation of similar collective phenomena in small-system collisions, such as p + p and p + A collisions, have attracted wide interest in the community. The interpretation of a fluid-like state formed there has been challenged, as the small size and short lifetime might prevent the system from quickly thermalizing and evolving hydrodynamically. Instead, collectivity arising either from initial momentum correlations motivated by gluon saturation models or via a few scatterings among partons (without hydrodynamization) has been proposed as alternative sources that may be dominant in small systems. Lots of experimental and theoretical efforts have been devoted to the study of collectivity in small-system collisions, with the goal of understanding the time-scale for the emergence of collectivity and the mechanism for early-time hydrodynamization in large collision systems.

One key feature that distinguishes initial momentum correlation models (ISM) from final-state interaction models (FSM, including hydrodynamics or a few scatterings) is the connection to the initial-state geometry. In FSM, the collectivity is a geometrical response to initial shape fluctuations, i.e., v_n is approximately proportional to the n^{th}-order initial-state eccentricity ε_n. In ISM, such a geometrical response is expected to be absent. It was proposed that a geometry scan of various colliding systems with different spatial eccentricities can help distinguish between contributions of these two scenarios.

Such a small system scan program has been recently carried out at RHIC for a few asymmetric small systems including p + Au, d + Au and ^{3}He + Au, where studies of elliptic flow (v_2) and triangular flow (v_3) have been performed. In a Glauber model that only considers the fluctuations of nucleon positions, ε_2 in d + Au and ^{3}He + Au is expected to be larger than in p + Au, while ε_3 in p + Au and d + Au are expected to be smaller than in ^{3}He + Au. However, once the fluctuations at subnucleonic scales are included, the ε_3 are expected to be similar among all three systems. Figure 45 compares the STAR v_2 and v_3 results with three hydrodynamic models predictions with different assumptions about the initial state. Calculations that include both initial momentum anisotropy and hydrodynamic response to subnucleonic fluctuations indeed describe the STAR v_3 data in all three systems, but one of the models overestimates the v_2 data. On the other hand, the hydrodynamic model based on fluctuations only at nucleonic level fails to describe the v_3 data. This implies that the initial state in these asymmetric small collision systems are not well constrained, in particular in p + Au and d + Au system (there is reasonable consensus that the flow results in ^{3}He + Au is dominated by FSM). The relative importance of FSM vs. ISM for the v_n data in small systems is an area of intense debate.

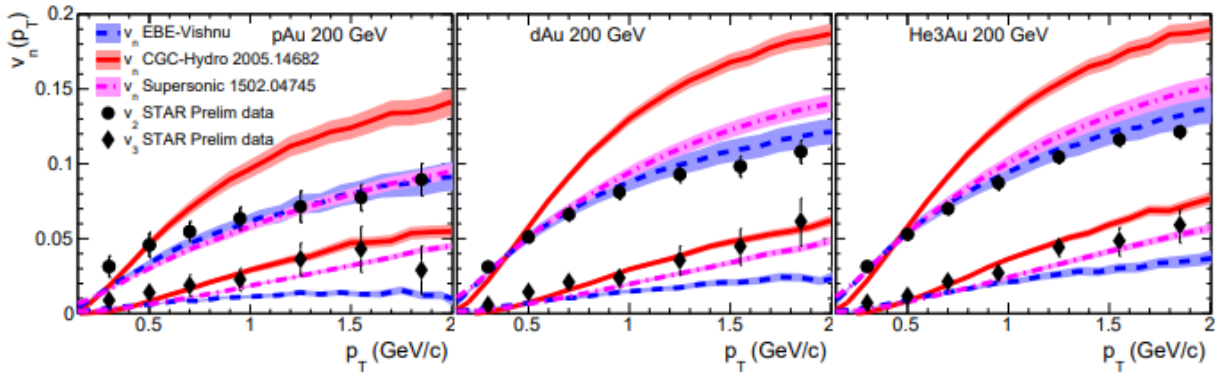

Figure 45. Comparison of v_2 and v_3 in p + Au, d + Au and ^{3}He + Au collisions at $\sqrt{s_{\mathrm{NN}}}$ = 200 between STAR data and various model calculations.

Physics case for a small A + A scan: So far, both RHIC and the LHC carried out collisions for either relatively large systems (Pb + Pb, Au + Au, Xe + Xe, Cu + Cu, …), which are well described by hydrodynamic models, or small asymmetric systems (p + Pb, p + Au, d + Au, and ^{3}He + Au), whose initial state are poorly constrained as discussed above. To quantitatively understand the initial momentum anisotropy and the role of subnucleonic fluctuations, collisions of small but symmetric systems, such as O + O, Al + Al and Ar + Ar will be necessary. They will also fill the gap between p + p and Cu + Cu systems, which is a crucial unexplored frontier, where a transition from ISM to FSM dominated collectivity may be observable. The list of key open questions related to collectivity in small systems includes:

- How much do initial-state correlations vs. geometry-driven final-state interactions contribute to the observed collectivity? Can we unambiguously establish experimental evidence of initial-state correlations?
- For final-state scenarios, to what extent does the collectivity arise from a hydrodynamic fluid-like QGP, as opposed to an off-equilibrium system with only a few scatterings per parton?
- What is the role of subnucleonic fluctuations in determining the initial-state geometry?
- Can we observe jet quenching in small systems?

In principle, a scan of colliding ion species at RHIC by systematically varying the system size and geometry between p + p and Cu + Cu collisions, will provide an unique lever-arm to dial contributions from various mechanisms and impose strong constraints on both ISM and FSM. Since the last RHIC p/d/He + Au scan, the STAR experiment has completed several detector upgrades that extend p_{T} and particle identification to $|\eta| < 1.5$, and provide centrality and event plane determination in $2.1 < |\eta| < 5.1$. This extended detector capability will allow a full exploration of collectivity using all the observables and methods developed for large systems at RHIC/LHC. We will have better control of the non-flow systematics, leading to a better understanding of the multi-particle nature of the collectivity and the longitudinal correlations to constrain the full 3D initial conditions. As an illustration, model studies of v_2 and v_3 in a series of small systems including symmetric (C + C, O + O, Al + Al, Ar + Ar) and asymmetric (p + Au, d + Au, ^{4}He + Au) collisions using the AMPT model are shown in Figure 46. AMPT belongs to the category of final-state interaction models, where v_n is largely driven by the geometry of initial nucleon distributions. The v_2 values from asymmetric systems follow different trends from symmetric systems: the v_2 in d/^{4}He + Au increases with N_{ch}, while it is relatively constant in p + Au. The v_3 values show a similar N_{ch} dependence as symmetric systems, except for d + Au which deviates from the common trend at large N_{ch}. This study demonstrates that, in a scenario driven by final-state interactions, a clear difference is expected between d/^{4}He + Au and A + A for v_2,

while a relatively similar behavior should be observed for v_3. Contributions from other sources, especially ISM, are expected to follow a drastically different behavior; as the system size increases, the ISM contribution will gradually become subdominant. In this proposal, we shall focus on a short O + O run, which should already help us to address many of the points raised above.

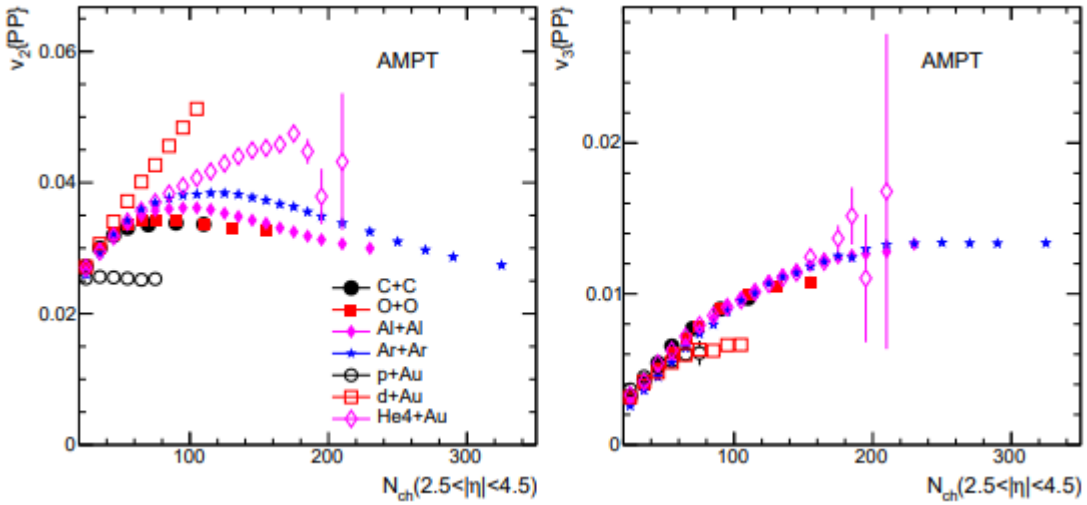

Figure 46. (Left) AMPT predictions for v_2 and (Right) v_3 as a function of N_{ch} in four symmetric and three asymmetric small collision systems.

Arguments for a short O + O run in 2021: In this BUR, we propose a O + O run at $\sqrt{s_{\mathrm{NN}}}$ = 200 GeV towards the end of the BES-II in 2021. The choice of O + O collisions as the starting point is motivated by the following reasons: 1) O + O has an N_{part} coverage comparable to p + Au and d + Au but with a much flatter distribution (see Figure 47), which allows much better control of initial geometry and centrality bias, 2) Oxygen is a reasonably sized system for which the both the nucleonic and subnucleonic DOF are important, which together with p/d + Au data can be used disentangle these contributions, 3) a strong synergy with the proposed higher-energy O + O run at the LHC around 2023–2024 to enable a direct comparison of the same small-system collision species at drastically different energies. More details, including hydrodynamic model predictions, are presented and discussed below.

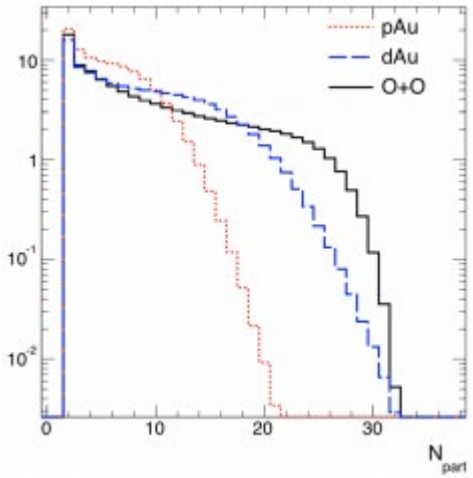

	pAu	dAu	^{16}O + ^{16}O
$\langle N_{\mathrm{part}} \rangle$	5.8	8.8	9.5

Figure 47. The N_{part} distribution in O + O collisions compared with p + Au and d + Au collisions at $\sqrt{s_{\mathrm{NN}}}$ = 200 GeV estimated from Glauber model. The table to the right shows the average N_{part} values in the three systems.

- ***Au+Au Collisions at $\sqrt{s_{NN}}$ = 17.1 GeV***

Net-proton kurtosis and light nuclei yield ratio from RHIC BES-I: One of the main goals of the RHIC Beam Energy Scan (BES) program is the search for the QCD critical point (CP), which is a distinct singular feature of the QCD phase diagram. The experimental confirmation of the existence of the CP would become a landmark in the exploration of the phase structure of hot dense nuclear matter. The characteristic feature of the CP is the divergence of the correlation length and density fluctuations. These critical phenomena can be probed by measuring event-by-event fluctuations of conserved quantities, such as baryon, electric charge, and strangeness numbers. The effect of the CP could show as a non-monotonic energy dependence of higher order moments of these conserved quantities in close proximity of the critical point during a beam energy scan.

In the years 2010–2017 RHIC finished the BES-I after taking data in Au + Au collisions at $\sqrt{s_{NN}}$ = 7.7, 11.5, 14.5, 19.6, 27, 39, 54.4, 62.4, and 200 GeV. With these experimental data STAR measured the higher order fluctuations of net-proton, net-charge, and net-kaon multiplicity distributions. One striking observation was the behavior of the fourth-order cumulants, or kurtosis, of the net-proton fluctuation $\kappa\sigma^2$ in most central (0–5 %) Au + Au collisions as a function of beam energy. As shown on the left of Figure 48, the fourth order net-proton fluctuation is close to unity above 39 GeV but deviates significantly below unity at 19.6 and 27 GeV, then approaches or turns above unity at lower energies. This behavior may suggest that the created system skims close by the CP, and receive positive and/or negative contributions from critical fluctuations. The right of Figure 48 shows the characteristic signature of the critical point for energy dependence of the fourth order fluctuations when the system passes through the critical region. Along this argument, a peak structure above unity for net-proton kurtosis measurement at lower energies could be the signature of the CP. However, it is worth to point out that a first order phase transition could also cause a large increase of net-proton kurtosis. When entering into the spinodal region (mixed phase), the double peak structure of σ field may cause the increase of the fourth order cumulants (C_4).

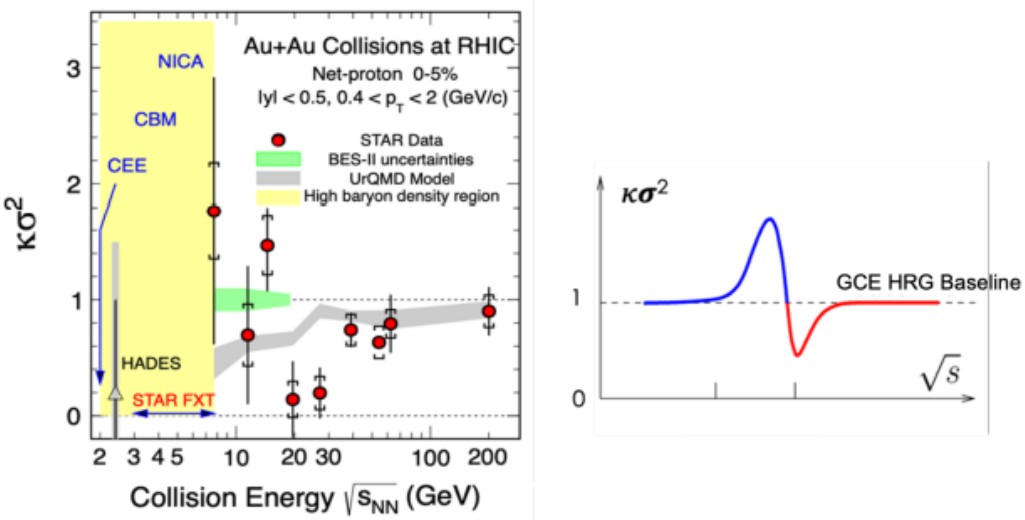

Figure 48. (Left) The fourth order net-proton fluctuations $\kappa\sigma^2$ in most central (0–5 %) Au + Au collisions as a function of collision energy from STAR BES-I measurements. (Right) The characteristic signature predicted by the theoretical model for energy dependence of the fourth order fluctuations when the system passes through the critical region.

In addition, STAR has measured light nuclei (deuteron and triton) production in Au + Au collisions at RHIC BES energies. The ratio of these yields are predicted to be sensitive to the neutron relative

density fluctuations at kinetic freeze-out, which is expected to increase near the critical point and/or a first order phase transition. The neutron density fluctuation is defined as $\Delta n = \langle(\delta n)^2\rangle/\langle n\rangle^2$, which can be approximated from:

$$\Delta n = \frac{1}{g}\frac{N_t \times N_p}{N_d^2} - 1,$$

where N_p, N_d and N_t are the proton, deuteron and triton yields, respectively and g is a constant factor of 0.29. In the left panel of Figure 49, we show the yield ratio $N_t \times N_p/N_d^2$ in central Au + Au collisions as a function of collision energy. These light nuclei yield ratios are obtained by using the feed-down corrected proton yields, deuteron yield, and preliminary triton results. The ratio as a function of energy exhibits a non-monotonic energy dependence with a peak around 19.6 GeV. The blue band showing a flat energy dependence represents the calculation of the light nuclei yield ratio in Au + Au collisions (b < 3 fm) from a transport JAM model. Furthermore, the yield ratio shown in Figure 49 seems to show a drop between 14.5 and 19.6 GeV. The experimental observation of non-monotonic energy dependence in yield ratio may suggest a double peak structure of the neutron density fluctuation, indicating that the system goes through the critical region and the first order spinodal region, as displayed in Figure 49 right.

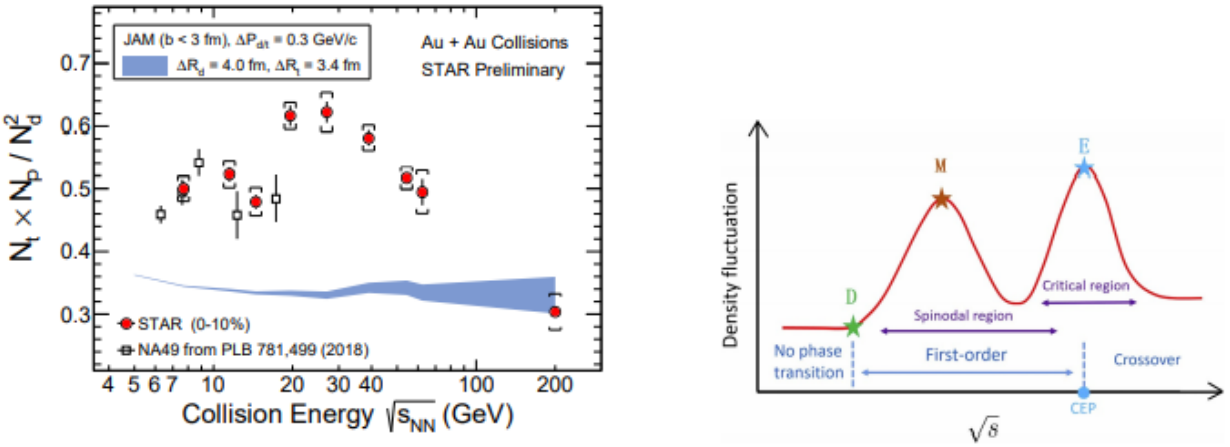

Figure 49. (Left) Collision energy dependence of the light nuclei yield ratio ($N_t \times N_p/N_d^2$) in central Au + Au collisions. The open square data based on NA49 results in central Pb + Pb collisions at $\sqrt{s_{\mathrm{NN}}}$ = 6.3 (0–7 %), 7.6 (0–7 %), 8.8 (0–7 %), 12.3 (0–7 %), and 17.3 (0–12 %) GeV. (Right) Illustration of the density fluctuation as a function of collision energy in the critical region and the spinodal region .

At the end of Run-21, we propose to take one more energy point for Au + Au collisions at 17.1 GeV based on the two observations discussed above and presented in Figure 48 and Figure 49:

1. Net-p kurtosis and light nuclei yield ratio, which are both sensitive to the critical fluctuation, show dip and peak structures around 19.6 GeV. These may suggest that the system passed through the critical region around 19.6 GeV.
2. We observe sudden changes between 19.6 and 14.5 GeV in the energy dependence of net-p kurtosis and light nuclei ratio measurements in the BES-I data measured by the STAR experiment. The neutron density fluctuations at low energies below 14.5 GeV are consistent with the results from NA49 experiment.

These two observations indicate that the critical point may be close to 19.6 GeV. Since there are sudden changes in both observables between 19.6 (chemical freeze-out μ_B = 205 MeV) and

14.5 GeV (μ_B = 266 MeV), it is important to conduct a finer beam energy scan between these two energies. Therefore, we request a run with Au + Au collisions at $\sqrt{s_{\rm NN}}$ = 17.1 GeV (μ_B = 235 MeV), which divides the range into approximately equal μ_B gaps.

If nature puts the critical point in the QCD phase diagram between 14.5 and 19.6 GeV (with μ_B around 200–270 MeV), RHIC has the best chance to discover it.

- ***Au + Au Collisions in FXT Mode at $\sqrt{s_{NN}}$ = 3.0 GeV (2 Billion Goal)***

In the previous section, we have discussed the great physics interests for low energy heavy-ion collisions utilizing the FXT setup at the STAR experiment. We have made our arguments for taking a minimum of 300 million Au + Au FXT events at $\sqrt{s_{\rm NN}}$ = 3.0 GeV. With further available beam time, we would like to request to collect up to 2 billion events with the same setup for the following physics measurements.

Proton correlations higher than 4-th order are useful to study the possible contributions of protons from hadronic phase or QGP phase. The requested 2 billion events statistics will enable us to perform the analyses of proton moments and cumulants up to 5-th and 6-th orders. Measurements of 5-th and 6-th order moments and cumulants have been proposed to be sensitive to the search for the phase boundary in the high baryon density region. A much larger data sample (2 billion events) will enable us to further investigate the centrality dependence of φ meson production. The Run-18 data analysis in 40–60 % centrality bin yields ~13 % relative uncertainty in the φ production yield. A two-billion dataset will reduce the statistical uncertainty to be < 5 %. This will allow us to study the system size dependence of φ meson production to quantitatively understand the canonical suppression for strangeness. The large statistics will also offer the opportunity to further measure φ meson directed and elliptic flow behavior in these collisions.

While there have been tens of hypernuclei measured so far, there are only very few double-Λ hypernuclei candidates reported from emulsion experiments. Their properties are directly related to the ΛΛ interaction. Low energy heavy-ion collisions can be a unique environment to copiously produce these light double-Λ hypernuclei. For instance, according to the thermal model prediction, the ${}^{5}_{\Lambda\Lambda}\mathrm{H}$ production yield increases by more than 3 orders of magnitude at the low energies compared to that at top RHIC and LHC energies.

We performed a Monte Carlo simulation study for the decay chain ${}^{5}_{\Lambda\Lambda}\mathrm{H} \rightarrow {}^{5}_{\Lambda}\mathrm{He} + \pi^-$, and ${}^{5}_{\Lambda}\mathrm{He} \rightarrow {}^{4}\mathrm{He} + p + \pi^-$ within the STAR detector acceptance. Assuming the production yield based on the thermal model prediction, with 2 billion Au + Au FXT data at $\sqrt{s_{\rm NN}}$ = 3.0 GeV and with the iTPC and eTOF detector, we will have a chance to observe ~27 signal counts. This will be an unprecedented sample that allows us to study double-Λ hypernuclei properties and their production mechanism, providing new insights towards the understanding of the ΛΛ interaction.

6.5. Exploring the microstructure of the QGP (Run-23 and Run-25 Au+Au)

The completion of the RHIC's scientific mission involves the two central goals:

- mapping out the phase diagram of the QCD,
- probing the inner workings of the QGP by resolving its properties at short length scales.

The complementarity of the RHIC and LHC facilities to study the latter is scientifically as essential as having more than one experiment independently study the microstructure of the QGP. With several years of operating the recently installed iTPC upgrade and the soon-to-be installation and operation of STAR's forward detectors, the STAR collaboration will be in an excellent position to take advantage of its vastly improved detection capabilities. Combine this with the prospect of a

substantial increase in beam luminosities and RHIC will be uniquely positioned to fully engage in a detailed exploration of the QGP's microstructure. Through careful discussions in its physics working groups, the STAR collaboration has identified a number of topics that together make a compelling case to take data during Runs 23-25 alongside sPHENIX, and successfully complete RHIC's scientific mission. In this section, we present a selection of those topics that will take full advantage of both STAR and RHIC's unique capabilities and address the following important questions about the inner workings of the QGP.

- What is the precise temperature dependence of the shear η/s, and bulk ζ/s viscosity?
- What is the nature of the 3-dimensional initial state at RHIC energies? How does a twist of the event shape break longitudinal boost invariance and decorrelate the direction of an event plane?
- How is global vorticity transferred to the spin angular momentum of particles on such short time scales? And, how can the global polarization of hyperons be reconciled with the spin alignment of vector mesons?
- What is the precise nature of the transition near $\mu_B = 0$, and where does the sign- change of the susceptibility ratio χ_6^B/χ_2^B take place?
- What is the electrical conductivity, and what are the chiral properties of the medium?
- What can we learn about confinement and thermalization in a QGP from charmonium measurements?

What are the underlying mechanisms of jet quenching at RHIC energies? What do jet probes tell us about the microscopic structure of the QGP as a function of resolution scale?

The event statistics projections that are used in this section will rely on the CAD's recently update 2023E and 2025E Au + Au luminosities and are listed in Table 8. For each year we presume 24 weeks of RHIC operations, and based on past run operations an overall average of 85 % × 60 % (STAR × RHIC) uptime, respectively. The minimum-bias rates assume a conservative 1.5 kHz DAQ rates which will allow sufficient bandwidth for specialized triggers which are listed as integral luminosities. In order to achieve the projected luminosities, the collaboration will look into optimizing the interaction rates at STAR by allocating low and high luminosities periods within fills. Such periods, in which low interaction rates are sampled in the early part of a fill and high interaction rates typically in the later part, will allow us to collect clean, low pile-up, minimum bias events, while at the same time not burn beam luminosities that could affect interaction rates for sPHENIX. Clean minimum bias events will improve tracking efficiencies which in turn are expected to benefit many of the proposed correlation analyses. Optimization of the available bandwidth for high-p_T triggers would allow us to push for lower p_T thresholds, thus further reducing biases. The impact of such an optimization will lead to some reduction in the projected rates, while still enabling a significant improvement in the precision and kinematic reach of current STAR measurements, and making important measurements that are yet more differential possible.

Table 8. STAR minimum bias event statistics and high-p_T luminosity projections for the 2023 and 2025 Au + Au runs. For comparison the 2014/2016 event statistics and luminosities are listed as well.

year	minimum bias [$\times 10^9$ events]	high-p_T int. luminosity [nb^{-1}] all vz	|vz|<70cm	|vz|<30cm
2014 2016	2	26.5	19.1	15.7
2023	10	43	38	32
2025	10	58	52	43

At RHIC it is possible to build detectors that can span from mid-rapidity to beam rapidity – with the two recent upgrades STAR is able to achieve this unique capability. STAR's BES-II upgrade sub-systems comprised of the inner Time Projection Chamber (iTPC, $1.0 < \eta < 1.5$) , endcap Time Of Flight (eTOF, $1 < \eta < 1.5$) and Event Plane Detector (EPDs, $2.1 < \eta < 5.1$), that are all commissioned and fully operational since the beginning of 2019. The STAR collaboration is constructing a forward rapidity ($2.5 < \eta < 4$) upgrade that will include charged particle tracking and electromagnetic/hadronic calorimetry. For charge particle tracking the aim is to construct a combination of silicon detectors and small strip thin gap chamber detectors. The combination of these two tracking detectors will be referred to as the forward tracking system (FTS). The FTS will be capable of discriminating the hadron charge sign. It should be able to measure transverse momentum of charged particles in the range of $0.2 < p_T < 2$ GeV/c with 20–30 % momentum resolution. In what follows, we will refer to the combination of the existing TPC ($\eta < 1$) and the iTPC upgrade as iTPC ($\eta < 1.5$) for simplicity.

The impetus for running STAR during the year of 2023–2025 in terms of bulk correlation measurements in Au + Au 200 GeV collisions comes from gains via: extended acceptance and enhanced statistics. In the first subsections, we briefly describe how these two opportunities can be exploited to perform correlations measurements that are unique to the physics goals of the RHIC heavy-ion program.

Next, thanks to a reduced material budget between the beam and the iTPC, STAR will be uniquely positioned to perform dielectron measurements with which we propose to probe degrees of freedom of the medium and its transport properties. For that we will use the high precision dilepton excess yield, i.e. l^+l^- invariant mass distribution after subtraction of dilepton sources produced after freeze-out, and contributions from the initial collisions such as Drell-Yan and correlated charm-anticharm pairs. Furthermore, we propose to study the virtuality, Wigner function and final-state magnetic field in the QGP. For the latter photon-photon collisions in ultra-peripheral, peripheral, and midcentral reactions and p + A (all centralities) in both channels e^+e^-, $\mu^+\mu^-$ will be measured with high accuracy.

One of the key sets of measurements is of interests – pseudorapidity dependence of global hyperon polarization.

Pseudorapidity dependence of global hyperon polarization: The global polarization of hyperons produced in Au + Au collisions has been observed by STAR. The origin of such a phenomenon has hitherto been not fully understood. Several outstanding questions remain. How exactly is the global vorticity dynamically transferred to the fluid-like medium on the rapid time scales of collisions? Then, how does the local thermal vorticity of the fluid gets transferred to the spin angular momentum of the produced particles during the process of hadronization and decay? In order to address these questions one may consider measurement of the polarization of different particles that are produced in different spatial parts of the system, or at different times. A concrete proposal is to: 1) measure the Λ(anti-Λ) polarization as a function of pseudorapidity and 2) measure it for different particles such as Ω and Ξ. Both are limited by the current acceptance and statistics available. With the addition of the iTPC and FTS, and with high statistics data from Run-23 it will be possible to perform such measurements with a reasonable significance. iTPC (+ TPC) has excellent PID capability to measure all these hyperons. Although the FTS has no PID capability we can do combinatorial reconstruction of Λ(anti-Λ) candidates via displaced vertices. A similar analysis was performed and published by STAR using the previous FTPC. In

order to make a conservative projection we assume similar momentum resolution of 10−20% for single charged tracks, similar overall tracking efficiency, charge state identification capability for the FTS and FTPC (see the forward upgrade section for exact numbers). We also assume the FTS, with it's novel-tracking framework, will be able to measure a minimum separation of 20 cm between the all pairs of one positive and one negative track (a possible decay vertex) from the main vertex of the event. This will give rise to about 5 % efficiency of Λ(anti-Λ) reconstruction with about (15–20) % background contribution from $K_S^0 \rightarrow \pi^+ + \pi^-$. With this we can make projections for a polarization measurement in Au + Au 200 GeV (40–80) % assuming 10 Billion minimum-bias events. The two different error bars correspond to lower and upper limits considering cur- rent uncertainties on the efficiency of charged track reconstruction and the final efficiency of Λ reconstruction. Currently theoretical models predict contradictory trends for the pseudorapidity dependence of Λ polarization. If the initial local orbital angular momentum driven by collision geometry plays a dominant role it will lead to increases of polarization with pseudorapidity. On the other hand if the local thermal vorticity and hydrodynamic evolution play a dominant role it will predict decreasing trend or weak dependence with pseudorapidity. Such tensions can be easily resolved with the future proposed measurement during Run-23.

7. Cold QCD Physics with $p\uparrow + p\uparrow$ and $p\uparrow$ + A Collisions at 510 and 200 GeV

The exploration of the fundamental structure of strongly interacting matter has always thrived on the complementarity of lepton scattering and purely hadronic probes. As the community eagerly anticipates the future Electron Ion Collider, an outstanding scientific opportunity remains to complete "must-do" measurements in $p + p$ and $p + A$ physics during the final years of RHIC. These measurements will be essential if we are fully to realize the scientific promise of the EIC, by providing a comprehensive set of measurements in hadronic collisions that, when combined with future data from the EIC, will establish the validity and limits of factorization and universality. Much of the Run-22 and Run-24 physics program outlined here is, on the one hand, unique to proton-proton and proton-nucleus collisions and offers discovery potential on its own. On the hand, these studies will lay the groundwork for the EIC, both scientifically and in terms of refining the experimental requirements of the physics program, and thus are the natural next steps on the path to the EIC. When combined with data from the EIC these STAR results will provide a broad foundation to a deeper understanding of fundamental QCD.

The separation between the intrinsic properties of hadrons and interaction-dependent dynamics, formalized by the concept of factorization, is a cornerstone of QCD and largely responsible for the predictive power of the theory in many contexts. While this concept and the associated notion of universality of the quantities that describe hadron structure have been successfully tested for unpolarized and, to a lesser extent, longitudinally polarized parton densities, its experimental validation remains an unfinished task for much of what the EIC is designed to study – the three-dimensional structure of the proton and the physics of dense partonic systems in heavy nuclei. To establish the validity and limits of factorization and universality, it is essential to have data from *both* lepton-ion and proton-ion collisions, with experimental accuracy that makes quantitative comparisons meaningful.

Beginning in Run-22, STAR will be in a unique position to provide this essential $p + p$ and $p + A$ data. A full suite of forward detectors will be installed, providing excellent charged-particle tracking at high pseudorapidity ($2.5 < \eta < 4$) for the first time, coupled with bothelectromagnetic and hadronic calorimetry. This will enable STAR to explore the interestingregimes of high-x

(largely valence quark) and low-x (primarily gluon) partonic physics withunparalleled precision. In addition, mid-rapidity detector upgrades motivated primarily by the BES-II program – the iTPC, eTOF, and EPD systems – will substantially extend STAR'salready excellent kinematic reach and particle identification capabilities beyond those that existed during previous $p + p$ and p + A runs.

For the case of $p + p$ spin physics, it's important to recognize the complementary roles that will be played by Run-22 at 510 GeV and Run-24 at 200 GeV. The combination of 510 GeV $p + p$ collisions and the STAR Forward Upgrade will provide access to forward jet physics at perturbative scales, thereby enabling measurements at the highest and lowest x values. In parallel, mid-rapidity measurements at 510 and, especially, 200 GeV will interpolate between the high and low x values, with significant overlaps to probe evolution effects and provide cross-checks. Together, the two runs will allow STAR to measure fundamental proton properties, such as the Sivers and transversity distributions, over nearly the entire range $0.005 < x < 0.5$.

Run-24 will also provide outstanding opportunities to probe fundamental questions regarding QCD in cold nuclear matter. The STAR Forward Upgrade will enable an extensive suite of measurements probing the quark-gluon structure of heavy nuclei and the regime of low-x non-linear gluon dynamics, as predicted by saturation models. STAR will also explore how a nucleus, serving as a color filter, modifies the propagation, attenuation, and gluons.

For these reasons, STAR requests at least 16 weeks of polarized $p + p$ data-taking at $\sqrt{s} = 510$ GeV in Run-22. All data taking will involve proton beams polarized transversely relative to their momentum direction in order to focus on those observables where factorization, univerality, and/or evolution remain open questions, with spins aligned either vertically or radially at the STAR IR (still to be determined through more detailed simulation studies). Based on the latest guidance from CAD, and mindful of 'lessons learned' in previous $p + p$ runs at full energy, we will ask for luminosity-leveling of the collision rate to maximize the efficiency of our main tracking detectors. Assuming we will have running conditions similar to those achieved in Run-17, we expect to sample at least 400 pb^{-1} for our rare / non-prescaled triggers.

STAR also requests at least 11 weeks of polarized $p + p$ data-taking at $\sqrt{s} = 200$ GeV and 11 weeks of polarized p + Au data-taking at $\sqrt{s_{\mathrm{NN}}} = 200$ GeV during Run-24. Similar to Run-22, all of the running will involve transversely polarized protons, with the choice between vertical or radial polarization to be determined during the coming year. Based on recent (08–21–20) CAD guidance, we expect to sample at least 235 pb^{-1} of $p + p$ collisions and 1.3 pb^{-1} of p + Au collisions. These totals represent 4.5 times the luminosity that STAR sampled during transversely polarized $p + p$ collisions in Run-15, and 3 times the luminosity that STAR sampled during transversely polarized p + Au collisions in Run-15.

7.1. Run-22 request for p↑ +p↑ collisions at 510 GeV

- ***Inclusive transverse spin asymmetries at forward rapidities***

The experimental study of spin phenomena in nuclear and particle physics has a long history of producing important, and often surprising, results. Attempts to understand such data have pushed the field forward, forcing the development of both new theoretical frameworks and new experimental techniques. Recent and ongoing detector upgrades at STAR, at mid- and forward-rapidity, coupled with the versatility of RHIC, will allow us to gain new insights into long-standing puzzles, and to probe more deeply the complexities of emergent behavior in QCD.

Results from PHENIX and STAR have shown that large transverse single-spin asymmetries (TSSA) for inclusive hadron production, first seen in $p + p$ collisions at fixed-target energies

and modest p_T, extend to the highest RHIC center-of-mass energies, $\sqrt{s} = 510$ GeV, and surprisingly large p_T. Figure 50 summarizes the world data for the inclusive pion asymmetries A_N as a function of Feynman-x. The asymmetries are seen to be nearly independent of $\sqrt{s}$ over the very wide range of roughly 5 to 500 GeV.

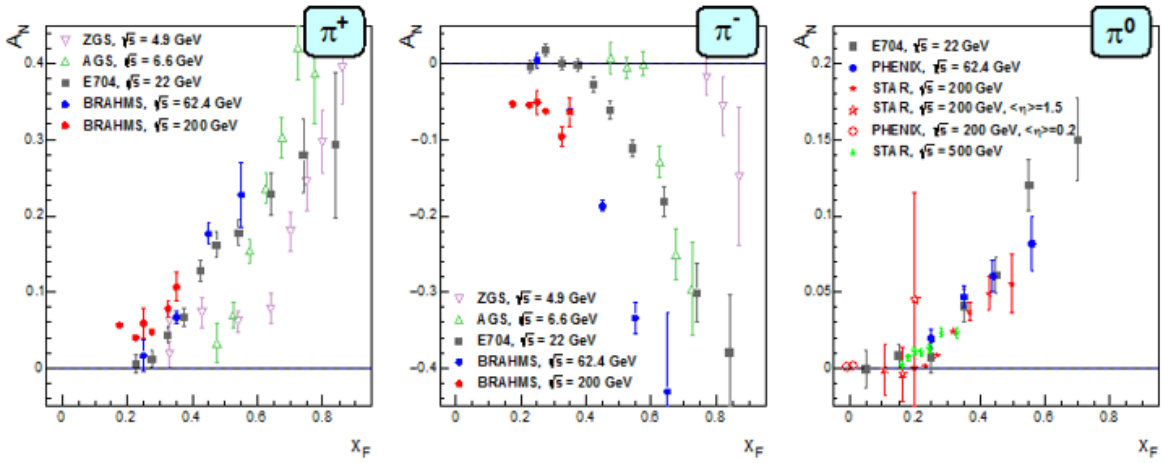

Figure 50. Transverse single-spin asymmetry A_N measurements for charged and neutral pions at different center-of-mass energies as a function of Feynman-x.

To understand the observed TSSAs, one needs to go beyond the conventional leading-twist (twist-2) collinear parton picture for the hard-scattering processes. Two theoretical formalisms have been developed to try to explain these sizable asymmetries in the QCD framework: transverse-momentum-dependent (TMD) parton distribution and fragmentation functions, such as the Sivers and Collins functions; and transverse-momentum-integrated (collinear) quark-gluon-quark correlations, which are twist-3 distributions in the initial state proton or in the fragmentation process. For many of the experimentally accessible spin asymmetries, several of these functions can contribute, and need to be disentangled in order to understand the experimental data in detail, in particular the observed p_T dependence. These functions manifest their spin dependence either in the initial state – for example, the Sivers distribution and its twist-3 analog, the Efremov-Teryaev-Qiu-Sterman (ETQS) function – or in the final state via the fragmentation of polarized quarks, such as in the Collins function and related twist three function $\widehat{H}_{FU}(z, z_z)$.

Incorporating the fragmentation term within the collinear twist-3 approach demonstrated the ability of this formalism to describe the large values of A_N for π_0 production observed at RHIC. In this work, the relevant (non-pole) 3-parton collinear fragmentation function $\widehat{H}_{FU}(z, z_z)$ was fit to the RHIC data. The so-called soft-gluon pole term, involving the ETQS function $T_{q,F}(x_1, x_2)$, was also included by fixing $T_{q,F}$ through its well-known relation to the TMD Sivers function $f_{1T}^{\perp}$. The authors obtained a very good description of the data due to the inclusion of the non-pole fragmentation function and based on this work they were able to make predictions for π^+ and π^- production asymmetries A_N at the forward rapidities covered by the STAR upgrades, $2.5 < \eta < 4$. The results are shown in Figure 51 for $\sqrt{s} = 200$ and 500 GeV for two rapidity ranges, $2 < \eta < 3$ and $3 < \eta < 4$.

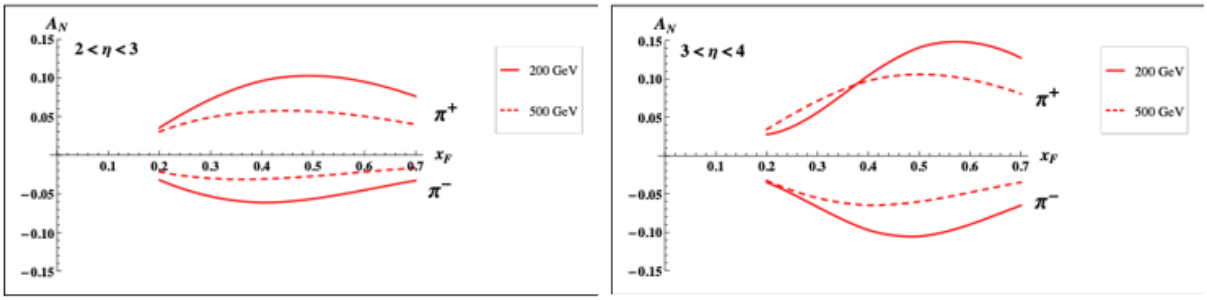

Figure 51. Predictions for AN for π^+ and π^- production over the ranges $2 < \eta < 3$ (left) and $3 < \eta < 4$ (right) at $\sqrt{s} = 200$ GeV (solid lines) and 500 GeV (dashed lines). The $\sqrt{s} = 200$ GeV BRAHMS A_N data for charged pions cover up to x_F of 0.3.

In Run-22, with the full suite of forward tracking detectors and calorimetry installed, STAR will for the first time be able to map out inclusive charged-hadron asymmetries up to the highest energies achievable at RHIC and at these forward rapidities. It would be very interesting to confirm that these asymmetries are indeed largely independent of center-of-mass energy. The measurements of A_N for charged hadrons, together with analogous data (from Run-22 as well as previous STAR runs) on A_N for direct photons and neutral pions, should provide the best data set in the world to constrain the evolution and flavor dependence of the twist-3 ETQS distributions and to determine if the 3-parton collinear fragmentation function H_{FU} is the main driver of the large forward inclusive asymmetries.

- ***Sivers and Efremov-Teryaev-Qiu-Sterman Function***

There is great theoretical interest in testing the relation between the ETQS correlation functions and the Sivers function. As discussed above, both the Sivers and the ETQS functions encapsulate partonic spin correlations within the proton, but they are formally defined in different frameworks. While the Sivers function is a TMD quantity that depends explicitly on spin-dependent transverse partonic motion k_T, the ETQS function is a twist-3 collinear distribution, in which SSAs are generated through soft collinear gluon radiation.

Measurements of forward jet production from the ANDY collaboration indicated rather small asymmetries. This was argued to be consistent with the idea that the twist-3 parton correlation functions for up and down valence quarks should cancel, because their behavior reflects the Sivers functions extracted from fits to the SIDIS data that demonstrate opposite sign, but equal magnitude, up and down quark Sivers functions. Preliminary STAR results on charge-tagged dijets at mid-rapidity support this interpretation, with the caveat that the measured observable (a spin-dependent $\langle k_T \rangle$) is defined in the TMD, and not the twist-3, framework.

To better test quantitatively the relation between the two regimes, one can measure spin asymmetries for jets which are *intentionally* biased towards up or down quark jets via detection of a high-z charged hadron within the jet. Higher-twist calculations of jet asymmetries based on the Sivers function predict sizeable effects for these flavor-enhanced jets. With the suite of new forward detectors installed at STAR, full jet reconstruction, along with identification of a high-z hadron of known charge sign, will be possible at high pseudorapidity. Using realistic jet smearing in a forward calorimeter and tracking system, and requiring a charged hadron with $z > 0.5$, the asymmetries can be separated and compared to the predictions for the Sivers function based on current SIDIS data. The expected uncertainties, plotted at the predicted values, can be seen in Figure 52. Dilutions by underlying event and beam remnants were taken into account. The simulations have assumed only an integrated luminosity of 100 pb^{-1} at $\sqrt{s} = 200$ GeV, which

is significantly lower than what is currently expected for the Run-24 200 GeV polarized $p + p$ run. The same measurement is possible at 500 GeV.

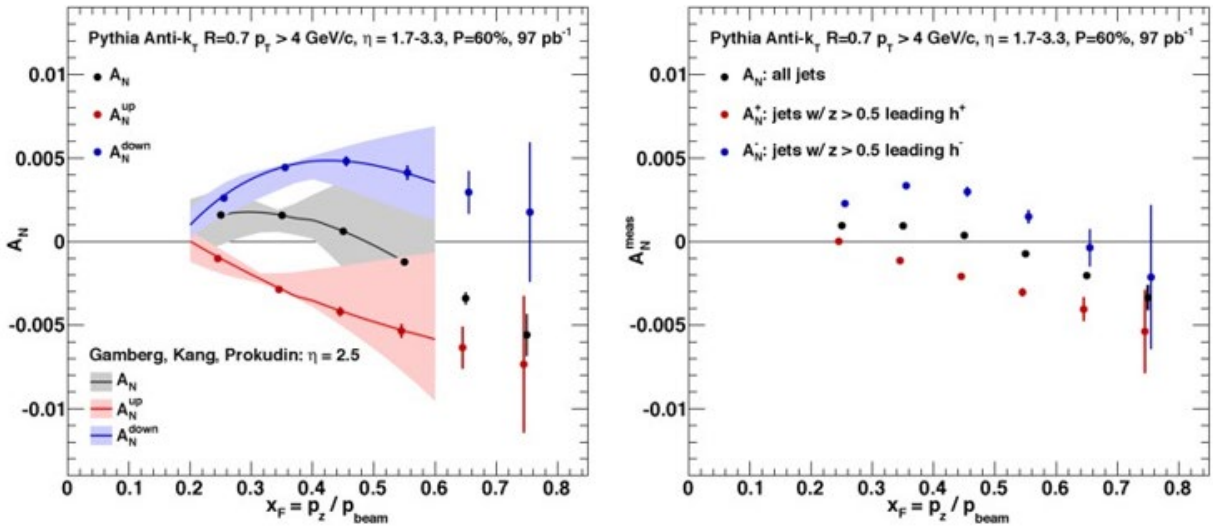

Figure 52. Left: up quark (red points), down quark (blue points) and all jet (black points) single spin asymmetries as a function of x_F as calculated by the ETQS based on the SIDIS Sivers functions. Right: Expected experimental sensitivities for jet asymmetries tagging in addition a positive hadron with z above 0.5 (red points), a negative hadron with z above 0.5 (blue points) or all jets (black) as a function of x_F. Note: these figures are for 200 GeV center-of-mass energy proton collisions – the 500 GeV results are expected to be qualitatively similar.

In a TMD framework, the Sivers effect manifests itself as a correlation (a triple product) between the transverse momentum of a parton ($\vec{k}_T$) with momentum fraction x, and the transverse spin ($\vec{S}$) of a polarized proton moving in the longitudinal ($\vec{p}$) direction. Thus, for transversely polarized protons, the Sivers effect probes whether the k_T of the constituent quarks is preferentially oriented in a direction perpendicular to both the proton momentum and its spin. Momentum conservation then implies that the two jets in the final state will not emerge back-to-back on average, but instead will 'tilt' in the direction of the summed k_T of the initial state partons. Moreover, the (average) tilt of interest will reverse direction under a 'flip' of the proton spin; a spin-dependent $\langle k_T \rangle$ can then be extracted by associating the azimuthal opening angle of the jet pair with this tilt.

STAR carried out an earlier measurement of this transverse single-spin asymmetry using a dijet dataset with ~1 pb^{-1} of integrated luminosity, and found it to be consistent with zero within 2σ. Perhaps most significantly, the jets were sorted according to their net charge Q, calculated by summing the signed momentum of all particle tracks with $p > 0.8$ GeV, to minimize underlying event contributions, yielding jet samples with enhanced contributions from u quarks (positive Q) and d quarks (negative Q), with a large set near $Q = 0$ dominated by gluons. Simple kinematics allow for conversion from the spin-dependent 'tilt' of the dijet pair to a value of k_T on an event-by-event basis; these are then sorted by the Q of the jet and binned by the summed pseudorapidities of the outgoing jets, $\eta^{\text{total}} \equiv \eta_3 + \eta_4$. Because the contributions of different partons (u, d, all else) to $\langle k_T \rangle$ vary with both Q and also η^{total}, in a way that can be estimated robustly using simulation, the data can be inverted to yield values of $\langle k_T \rangle$ for the individual partons, though with coarser binning in η^{total}.

With the new forward detectors in place, along with the enhanced reach in η afforded by the iTPC, this technique can be expanded in Run-22 to cover pseudorapidities at STAR from roughly –1

to +4, though with a gap at $1.5 < \eta < 2.5$. Despite this gap, values of $\langle k_T \rangle$ can be extracted for u and d quarks for η^{total} ranging from 1.5 to as high as 7 with reasonable statistics. This latter regime will probe $2 \rightarrow 2$ hard scattering events in which $x_1 >> x_2$, *i.e.*, a sample enriched in valence quarks interacting with low-x gluons. Such measurements, exploiting the full kinematic reach of STAR, will not only allow precise determinations of the average transverse partonic motion, $\langle k_T \rangle$, exhibited by individual partonic species in the initial state, but will provide important information on the x dependence of the proton Sivers functions.

Collisions at $\sqrt{s} = 510$ GeV will also allow STAR to continue our successful program to study the evolution and sign change of the Sivers function. By focusing on interactions in which the final state involves only weakly interacting particles, and hence the transverse partonic motion (in a TMD framework) or the collinear gluon radiation (in twist-3) must be in the initial state, one can test for the predicted sign change in AN relative to interactions in which these terms must appear in the final state, such as SIDIS measurements. The improved tracking capabilities provided by the iTPC upgrade will allow us to push our mid- rapidity $W^{\pm}$ and Z^0 measurements to larger rapidity $y_{W/Z}$, a regime where the asymmetries are expected to increase in magnitude and the anti-quark Sivers' functions remain largely unconstrained. Figure 53 demonstrates the expected precision of asymmetry measurements after data from the Run-17 has been fully analyzed. In addition to the noted extension of our kinematic reach, an additional 16 or more weeks of beam time at $\sqrt{s} = 510$ GeV in Run-22 would increase our data set by more than a factor of 2. This experimental accuracy would significantly enhance the quantitative reach of testing the limits of factorization and universality in lepton-proton and proton-proton collisions.

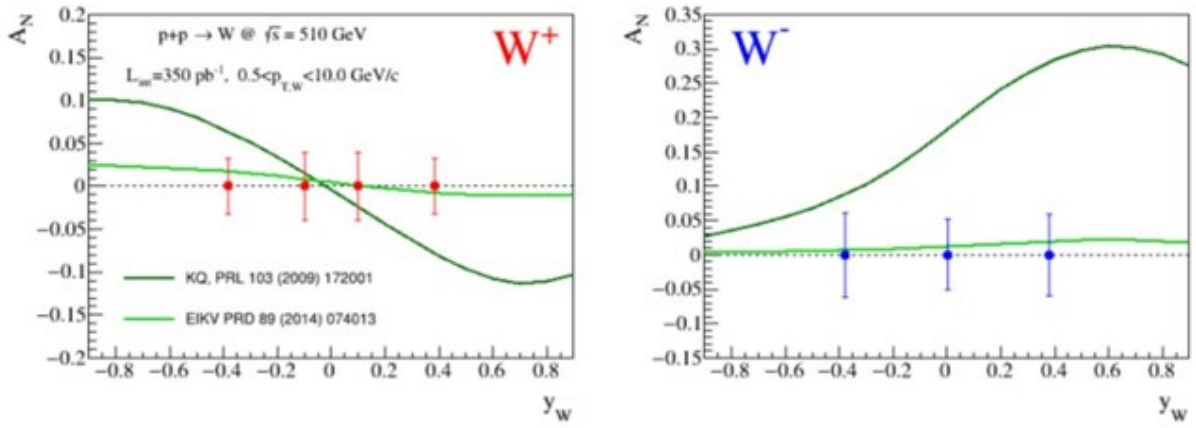

Figure 53. Projected uncertainties for transverse single-spin asymmetries of $W^{\pm}$ bosons as functions of their rapidity for a delivered integrated luminosity of 350 pb^{-1} and an average beam polarization of 55 %. The dark and light green lines are theoretical predictions from the KQ and EIKV groups, respectively, folding in data on the sea-quark Sivers functions.

- ***Transversity, Collins Function and Interference Fragmentation Function***

A complete picture of nucleon spin structure at leading twist must include contributions from the unpolarized and helicity distributions, as well as those involving transverse polarization, such as the transversity distribution. The transversity distribution can be interpreted as the net transverse polarization of quarks within a transversely polarized proton. The difference between the helicity and transversity distributions for quarks and antiquarks provides a direct, x-dependent connection to nonzero orbital angular momentum components in the wave function of the proton. Recently, the first lattice QCD calculation of the transversity distribution has been performed [C. Alexandrou et al., Phys. Rev. D 98, 091503 (2018)]. In addition, the measurement of transversity

has received substantial interest as a means to access the tensor charge of the nucleon, defined as the integral over the valence quark transversity: $\delta q^a = \int_0^1 [\delta q^a(x) - \delta \bar{q}^a(x)] dx$ [R. Jaffe and X.-D. Ji, Nucl. Phys. B 375, 527 (1992), R. Jaffe and X.-D. Ji, Phys. Rev. Lett. 67, 552 (1991)]. Measuring the tensor charge is very important for several reasons. First, it is an essential and fundamental quantity to our understanding of the spin structure of the nucleon. Also, the tensor charge can be calculated on the lattice with comparatively high precision, due to the valence nature of transversity, and hence is one of the few quantities that allow us to compare experimental results on the spin structure of the nucleon directly to ab initio QCD calculations. Finally, the tensor charge describes the sensitivity of observables in low-energy hadronic reactions to beyond the standard model physics processes with tensor couplings to hadrons. Examples are experiments with ultracold neutrons and nuclei.

Transversity is difficult to access due to its chiral-odd nature, requiring the coupling of this distribution to another chiral-odd distribution. Semi-inclusive deep-inelastic scattering (SIDIS) experiments have successfully probed transversity through two channels: asymmetric distributions of single pions, convoluting the TMD transversity distribution with the TMD Collins fragmentation function, and azimuthally asymmetric distributions of di-hadrons, coupling transversity to the so-called "interference fragmentation function" (IFF) in the framework of collinear factorization. Yet in spite of a wealth of lepton-scattering data, the kinematic reach of existing SIDIS experiments limits the precision with which the proton's transversity can be extracted, as the range of Bjorken-x values that can be accessed does not extend above $x \sim 0.3$.

In hadronic collisions, the k_T integrated quark transversity distribution may be accessed via two channels. The first is the single spin asymmetry of the azimuthal distribution of hadrons in high energy jets. In the jet + hadron channel, the collinear transversity distribution couples to the TMD Collins function. This makes $p + p$ collisions a more direct probe of the Collins fragmentation function than Collins asymmetries in SIDIS, where a convolution with the TMD transversity distribution enters. This also makes the Collins asymmetry in $p + p$ collisions an ideal tool to explore the fundamental QCD questions of TMD factorization, universality, and evolution. The second channel is the single spin asymmetry of pion pairs, where transversity couples to the collinear interference fragmentation function. STAR mid-rapidity IFF data have been included in the first extraction of transversity from SIDIS and proton-proton IFF asymmetries.

The universality of TMD PDFs and fragmentation functions in $p + p$ collisions has been an open question. General arguments have shown that factorization can be violated in hadron-hadron collisions for TMD PDFs like the Sivers function, though very recent calculations indicate the violations might be quite small. In contrast, while there is no general proof that the Collins effect in $p + p$ collisions is universal to all orders, explicit calculations have shown that diagrams like those that violate factorization of the Sivers function make no contribution to the Collins effect at the one- or two-gluon exchange level, thereby preserving its universality at least to that level.

Comparisons of the transversity distributions extracted from the Collins and IFF channels will allow STAR to study the size and nature of any factorization breaking effects for TMD observables in hadronic collisions. Likewise, comparisons with the transversity, Collins and IFF distributions extracted from SIDIS collisions will shed light on universality and constrain evolution effects. The measurement of evolution effects in TMD distributions is particularly important because, unlike the collinear case, TMD evolution contains a non-perturbative component that cannot be calculated directly. Measurements at $\sqrt{s}$ of 200 and 510 GeV will provide additional experimental

constraints on evolution effects and provide insights into the size and nature of TMD observables at the future Electron-Ion Collider.

Extending measurements of di-hadron and Collins asymmetries to the forward direction during Run-22 will allow access to transversity in the region $x > 0.3$. This valence quark region is not currently probed by any experiments and is essential for the determination of the tensor charge, which receives 70 % of its contributions from $0.1 < x < 1.0$. In addition, probing transversity in $p + p$ collisions also provides better access to the d-quark transversity than is available in SIDIS, due to the fact that there is no charge weighting in the hard scattering QCD $2 \rightarrow 2$ process in $p + p$ collisions. This is a fundamental advantage of $p + p$ collisions, as any SIDIS measurement of the d-quark transversity has to be on a bound system, *e.g.* He-3, which ultimately requires nuclear corrections to extract distributions. The high scale we can reach in 500 GeV collisions at RHIC has allowed STAR to demonstrate, for the first time, that previous SIDIS measurements at low scales are in fact accessing the nucleon at leading twist. Figure 54 shows the $x - Q^2$ coverage spanned by the RHIC measurements compared to the future EIC, JLab-12, and the current SIDIS world data.

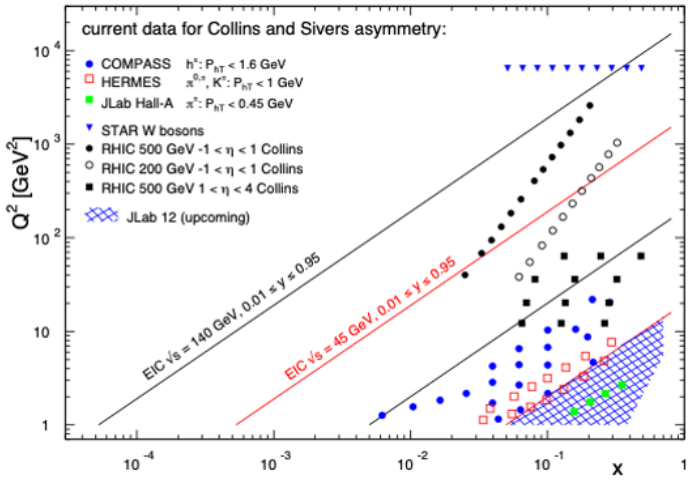

Figure 54. x–Q^2 coverage of RHIC measurements compared to existing Collins and Sivers effect measurements in SIDIS and the future coverage of the EIC.

Another fundamental advantage of $p + p$ collisions is the ability to access gluons directly. While gluons cannot be transversely polarized in a transversely polarized spin 1/2 hadron, they can be linearly polarized. Similarly, there exists an equivalent of the Collins fragmentation function for<the fragmentation of linearly polarized gluons into unpolarized hadrons. The linear polarization of gluons is a largely unexplored phenomenon, but it has been a focus of recent theoretical work, in particular due to the relevance of linearly polarized gluons in unpolarized hadrons for the p_T spectrum of the Higgs boson measured at the LHC. Polarized proton collisions with $\sqrt{s} = 510$ GeV at RHIC, in particular for asymmetric parton scattering if jets are detected in the backward direction, are an ideal place to study the linearly polarized gluon distribution in polarized protons. (Note that the distributions of linearly polarized gluons inside an unpolarized and a polarized proton provide independent information). A first measurement of the "Collins-like" effect for linearly polarized gluons has been done by STAR with data from Run-11, providing constraints on this function for the first time.

Figure 55 shows projected uncertainties for Collins asymmetries at 510 GeV with the Forward Upgrade during Run-22. As indicated on the figure, jets with $3 < \eta < 4$ and $3 < p_T < 9$ GeV/c will explore transversity in the important region $0.3 < x < 0.5$ that has not yet been probed in SIDIS.

A realistic momentum smearing of final state hadrons as well as jets in this rapidity range was assumed and dilutions due to beam remnants (which become substantial at rapidities close to the beam) and underlying event contributions have been taken into account. As no dedicated particle identification at forward rapidities will be available for these measurements, only charged hadrons were considered. This mostly reduces the expected asymmetries due to dilution by protons (10–14 %) and a moderate amount of kaons (12–13 %). As anti-protons are suppressed compared to protons in the beam remnants, especially the negative hadrons can be considered a good proxy for negative pions (78 % purity according to PYTHIA6). Given their sensitivity to the down quark transversity via favored fragmentation, they are particularly important since SIDIS measurements, due to their electromagnetic interaction, are naturally dominated by up-quarks. We have estimated our statistical uncertainties based on an accumulated luminosity of 268 pb^{-1}, which leaves nearly invisible uncertainties after smearing. These expected uncertainties are compared to the asymmetries obtained from the transversity extractions based on SIDIS and Belle data as well as from using the Soffer positivity bound for the transversity PDF. More recent global fits have slightly different central up and down quark transversity distributions. But due to the lack of any SIDIS data for $x > 0.3$, the upper uncertainties are compatible with the Soffer bounds. This high-x coverage will give important insights into the tensor charge, which is essential to understand the nucleon structure at leading twist.

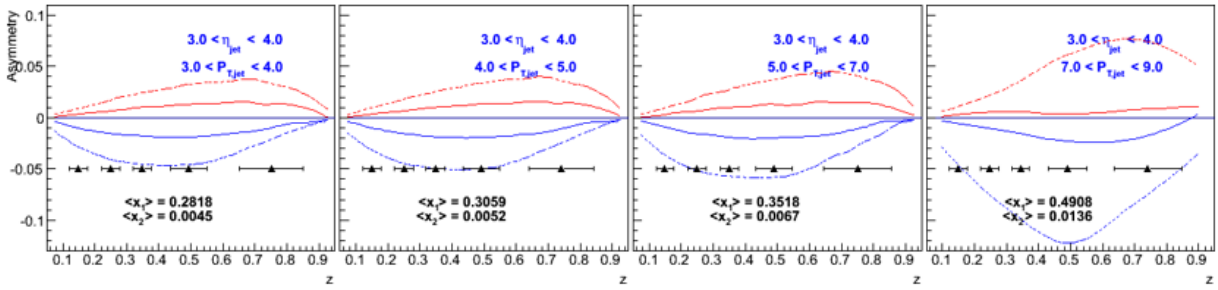

Figure 55. Expected h^- Collins asymmetry uncertainties at $3 < \eta < 4$ (black points) from a sampled luminosity of 268 pb^{-1} at $\sqrt{s} = 510$ GeV, compared to positive (red) and negative (blue) pion asymmetries based on the Torino extraction (full lines) and the Soffer bound (dashed lines) as a function of hadron z for bins in jet p_T. Most uncertainties are smaller than the height of the triangles.

Although the studies presented here are for the Collins asymmetries, the resulting statistical uncertainties will be similar for other measurements using azimuthal correlations of hadrons in jets. One important example is the measurement of "Collins-like" asymmetries to access the distribution of linearly polarized gluons. As described earlier, the best kinematic region to access this distribution is at backward angles with respect to the polarized proton and at small jet p_T. Figure 55 shows that a high precision measurement of the distribution of linearly polarized gluons down to $x \sim 0.005$ will be performed concurrently.

It is also important to recognize that these hadron-in-jet measurements with the STAR Forward Upgrade will provide very valuable experience detecting jets close to beam rapidity that will inform the planning for future jet measurements in similar kinematics at the EIC.

While the STAR Forward Upgrade will provide sensitivity to transversity to the highest x, concurrent mid-rapidity measurements (see Figure 54) will provide the most precise information as a function of x, z, j_T, and Q^2 to probe questions of TMD factorization, universality, and<evolution. The left panel of Figure 56 shows published STAR measurements of the Collins

asymmetry vs. pion z in 500 GeV $p + p$ collisions from 2011. The results, which represented the first ever observation of the Collins effect in $p + p$ collisions, are consistent at the 2-sigma level with model predictions, with and without TMD evolution, derived from fits to e^+e^- and SIDIS data. However, greater precision is clearly necessary for a detailed universality test, as well as to set the stage for the EIC.

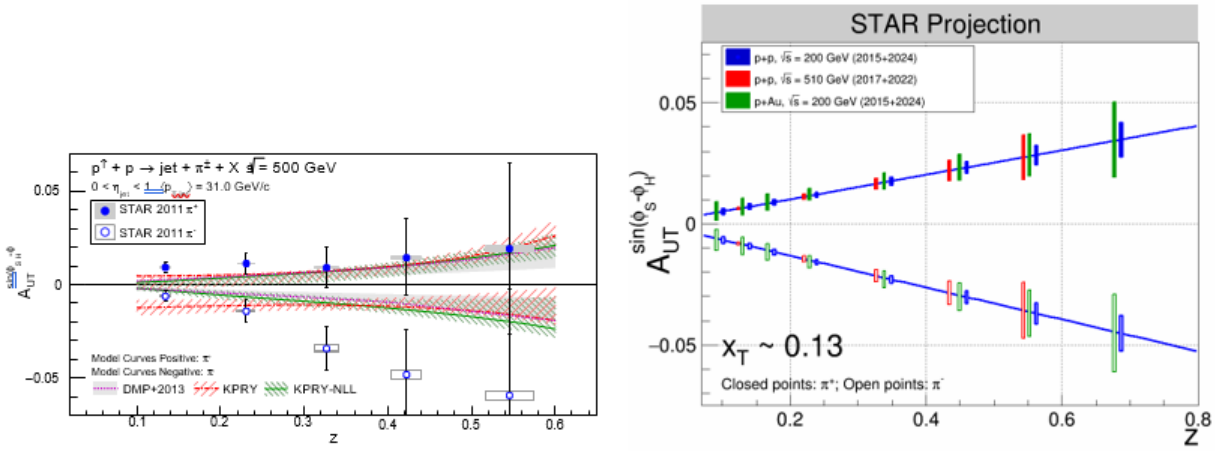

Figure 56. The left panel shows STAR measurements of the Collins asymmetry vs. pion z in 500 GeV $p + p$ collisions from Run-11, compared to several model calculations. The right panel shows projected statistical uncertainties for STAR Collins asymmetry measurements at $0 < \eta < 0.9$ in $p + p$ at $\sqrt{s} = 200$ and 510 GeV and p + Au at $\sqrt{s_{\mathrm{NN}}} = 200$ GeV. The points have arbitrarily been drawn on the solid lines, which represent simple linear fits to the STAR preliminary 200 GeV p + p Collins asymmetry measurements from 2015. (Note that only one bin is shown spanning $0.1 < z < 0.2$ for 510 GeV $p + p$, whereas three bins are shown covering the same z range for the 200 GeV measurements).

In 2017, STAR sampled about 14 times the luminosity that we recorded in 2011. In Run- 22, we propose to record another data set equivalent to 16 times the sampled luminosity from 2011. Furthermore, during Run-22 the iTPC will improve the *dE*/*dx* particle identification compared to the previous years. Studies using the *dE*/*dx* distributions seen in our 200 GeV $p + p$ data from 2015 and the actual *dE*/*dx* resolution improvements that have been achieved during BES-II indicate the iTPC will yield a 20–25 % increase in the effective figure-of- merit for pions with $\eta < 0.9$. The right-hand panel of Figure 56 shows the projected STAR statistical uncertainties for the Collins asymmetry at $0 < \eta < 0.9$ in 510 GeV $p + p$ collisions once the Run-17 and Run-22 data sets are fully analyzed. It's also important to recognize that the iTPC will also enable STAR to measure the Collins asymmetry over the region $0.9 < \eta < 1.3$ during Run-22, in addition to the projections that are shown in Figure 56.

Statistical improvements from the 2011 data to 2017+'22 data comparable to those shown for the Collins effect in Figure 56 are also expected for mid-rapidity measurements of transversity in 510 GeV $p + p$ collisions using IFF asymmetries.

7.2. Run-24 request for Polarized $p + p$ and p + A collisions at 200 GeV

Run-24, with polarized $p + p$ and p + Au collisions at $\sqrt{s_{\mathrm{NN}}} = 200$ GeV, will likely be the last RHIC spin/cold QCD run. This run will provide STAR with the unique opportunity to investigate these 200 GeV collision systems with the Forward Upgrade providing full tracking and calorimetry coverage over the region $2.5 < \eta < 4$ and the iTPC providing enhanced particle identification and expanded pseudorapidity coverage at mid-rapidity. These powerful detection capabilities,

when combined with substantially increased sampled luminosity compared to Run-15, will enable critical measurements to probe universality and factorization in transverse spin phenomena and nuclear PDFs and fragmentation functions, as well as low-x non-linear gluon dynamics characteristic of the onset of saturation. This will provide unique insights into fundamental QCD questions in the near term, and essential baseline information for precision universality tests when combined with measurements from the EIC in the future.

We therefore request at least 11 weeks of polarized $p + p$ data-taking at $\sqrt{s} = 200$ GeV and 11 weeks of polarized p + Au data-taking at $\sqrt{s_{\mathrm{NN}}}$ = 200 GeV during Run-24. All of the running will involve transversely polarized protons, with the choice between vertical or radial polarization to be determined during the coming year. Based on recent (08–21–20) C-AD guidance, we expect to sample at least 235 pb^{-1} of $p + p$ collisions and 1.3 pb^{-1} of p + Au collisions. These totals represent 4.5 times the luminosity that STAR sampled during transversely polarized $p + p$ collisions in Run-15 and 3 times the luminosity that STAR sampled during transversely polarized p + Au collisions in Run-15.

Run-24 will enable STAR to probe transversely polarized $p + p$ and p + Au collisions with a far more capable detector and much larger data sets than were available during Run-15, thereby allowing us to set the stage for related future measurements at the EIC. Here we give brief descriptions of several of the opportunities presented by Run-24.

Forward transverse spin asymmetries

STAR will publish very soon in a pair of papers discussing forward transverse spin asymmetries in $p + p$, p + Al, and p + Au collisions measured with the Forward Meson Spectrometer (FMS). One paper focuses on the dynamics that underlie the large asymmetries that have been seen to date. Data for A_N for forward π^0 production in $p + p$ collisions at 200 and 500 GeV is substantially larger when the π^0 is isolated than when it is accompanied by additional nearby photons. The same analysis also shows that A_N for inclusive electromagnetic jets (EM-jets) in 200 and 500 GeV collisions is substantially larger than that for EM-jets that contain three or more photons and that the Collins asymmetry for π^0 in EM-jets is very small. The other paper focuses on the nuclear dependence of A_N for π^0 in $\sqrt{s_{\mathrm{NN}}}$ = 200 GeV collisions. It presents a detailed mapping of A_N as functions of x_F and p_T for all three collision systems. It was found earlier that the observed nuclear dependence is very weak. The same analysis shows that isolated vs. non-isolated π^0 behave similarly in p + Al and p + Au collisions as they do in $p + p$ collisions.

These two papers will provide a wealth of new data to inform the ongoing discussion regarding the origin of the large inclusive hadron transverse spin asymmetries that have been seen in $p + p$ collisions at forward rapidity over a very broad range of collision energies. Nonetheless, the STAR Forward Upgrade will be a game changer for such investigations. It will enable measurements of A_N for $h^{+/-}$, in addition to π^0. It will enable isolation criteria to be applied to the $h^{+/-}$ and π^0 that account for nearby charged, as well as neutral, fragments. It will enable full jet asymmetry and Collins effect measurements, again for $h^{+/-}$ in addition to π^0, rather than just EM-jet measurements. It will permit all of these measurements to be performed at both 510 GeV and at 200 GeV. In addition, all of these observables can be tagged by forward protons detected in the STAR Roman pots to identify the diffractive component of the observed transverse spin asymmetries. For $p + p$ there will be considerable overlap between the kinematics at the two energies, but the 510 GeV measurements will access higher p_T, while the 200 GeV measurements will access higher x_F. Meanwhile, at 200 GeV we will also perform the full suite of measurements in p + Au to identify any nuclear effects. Predictions for the inclusive $\pi^{+/-}$ A_N in 200 and 500 GeV

$p + p$ collisions show the estimated sensitivity of one hadron-in-jet measurement that will help to isolate the Sivers effect contribution at 200 GeV.

Sivers effect

The Sivers effect in dijet production was firstly observed. Such measurements are crucial to explore questions regarding factorization of the Sivers function in dijet. Those results were derived from 200 GeV transverse spin data that STAR recorded in 2012 and 2015 (total sampled luminosity 75 pb^{-1} for the two years combined). Nonetheless, the uncertainties remain large enough. Run-24 data will reduce the uncertainties for $|\eta_3 + \eta_4| < 1$ by a factor of two. The increased acceptance from the iTPC will reduce the uncertainties at $|\eta_3 + \eta_4| \approx 2.5$ by a much larger factor, while the Forward Upgrade will enable the measurements to be extended to even larger values of $|\eta_3 + \eta_4|$. When combined with the 510 GeV data from 2017 and 2022, the results will provide a detailed mapping vs. x for comparison to results for Sivers functions extracted from SIDIS, Drell-Yan, and vector boson production.

Transversity and related quantities

Measurements of the Collins asymmetry and IFF in $p + p$ collisions at RHIC probe fundamental questions regarding TMD factorization, universality, and evolution. Data from 200 GeV $p + p$ collisions will play an essential role toward answering these questions. It was found that 200 GeV $p + p$ collisions interpolate between the coverage that we will achieve during Run-22 at high-x with the Forward Upgrade and at low-x with the STAR mid-rapidity detectors. They will also provide a significant overlapping region of x coverage, but at Q^2 values that differ by a factor of 6. This will provide valuable information about evolution effects, as well as cross-checks between the two measurements. Furthermore, for most of the overlapping x region, 200 GeV $p + p$ collisions will also provide the greatest statistical precision, thereby establishing the most precise benchmark for future comparisons to *ep* data from the EIC.

The high statistical precision of the Run-24 data will enable detailed multi-dimensional binning for the Collins asymmetry results. This is particularly valuable because hadron-in-jet measurements in $p + p$ collisions provide a direct probe of the Collins fragmentation function since they combine it with the *collinear* transversity distribution. In general, the observed asymmetries are functions of jet (p_T, η), hadron (z, j_T), and Q^2. However, the physics interpretations associated with these variables separate, with p_T and η primarily coupling to the incident quark x and the polarization transfer in the hard scattering, while z and j_T characterize the fragmentation kinematics. Thus, A_{UT} vs. p_T provides information about the transversity distribution. In parallel, the (z, j_T) dependence, integrated over a wide range of jet p_T, as shown in Figure 57 for the preliminary 2015 results, provides a detailed look at the Collins fragmentation function. Note that STAR finds the maximum value of A_{UT} shifts to higher j_T as z increases. The statistical uncertainties will be reduced by a factor of 2.5 when Run-15 and Run-24 data are combined together.

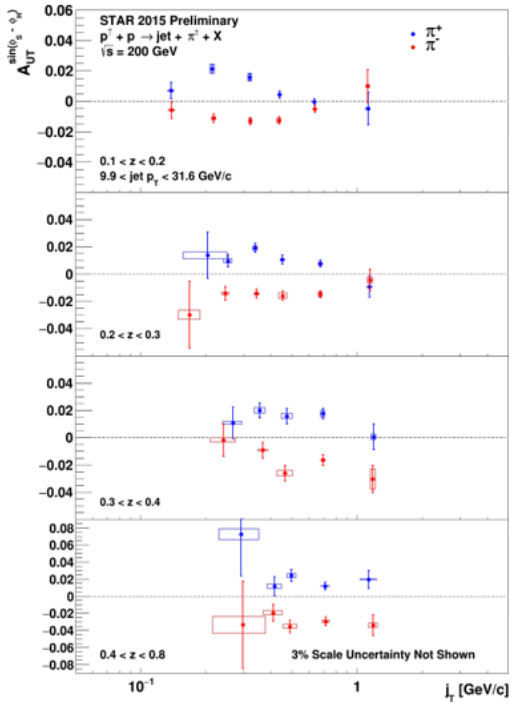

Figure 57. Preliminary 2015 results for the Collins asymmetry for charged pions in 200 GeV $p+p$ collisions as a function of z and j_T, integrated over $9.9 < p_T < 31.6$ GeV/c and $0 < \eta < 0.9$.

The 2015 Collins analysis has also, for the first time, measured the Collins effect for charged kaons in $p+p$ collisions, as shown in Figure 59. The asymmetries for K^+, which like π^+ have a contribution from favored fragmentation of u quarks, are about 1.5-sigma larger than those for π^+, while those for K^-, which can only come from unfavored fragmentation, are consistent with zero at the 1-sigma level. These trends are similar to those found in SIDIS by HERMES and COMPASS , and provide additional insight into the Collins fragmentation function. This same analysis with Run-24 data will yield statistical uncertainties a factor of 3 smaller than those in Figure 59. This is a much greater improvement than would be expected from the increase in sampled luminosity thanks to the improved dE/dx resolution provided by the iTPC. In addition, the iTPC will enable the measurements in Figure 57, Figure 58, and Figure 59 to be extended to an additional higher η bin ($0.9 < \eta < 1.3$).

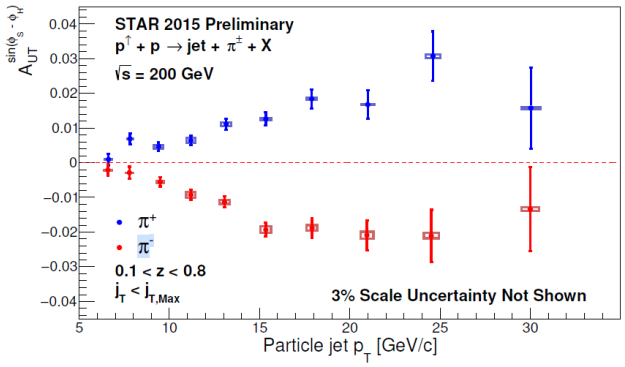

Figure 58. Preliminary results for the Collins asymmetry plotted for identified π^+ (blue) and π^- (red) particles as a function of jet p_T for jets that scatter forward to polarized beam ($x_F > 0$). The full range of both z and j_T are integrated over.

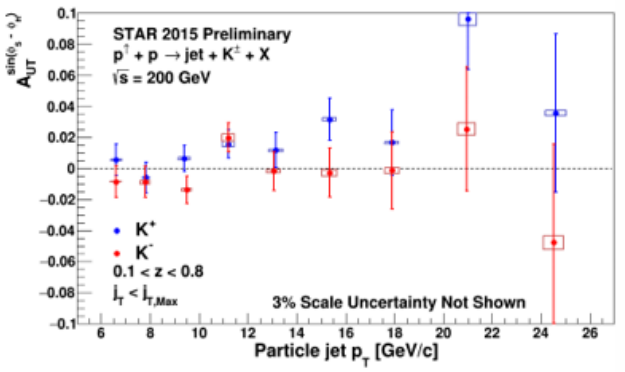

Figure 59. Preliminary 2015 results for the $K^{+/-}$ Collins asymmetries *vs.* jet p_T for $0 < \eta < 0.9$ in 200 GeV $p + p$ collisions.

RHIC has the unique opportunity to extend the Collins effect measurements to nuclei. This will provide an alternative look at the universality of the Collins effect in hadro- production by dramatically increasing the color flow options of the sort that have been predicted to break factorization for TMD PDFs like the Sivers effect. This will also explore the spin dependence of the hadronization process in cold nuclear matter. STAR collected a proof-of-principle data set during the 2015 p + Au run that is currently under analysis. Those data will provide a first estimate of medium-induced effects. However, the small nuclear effects seen by STAR for forward inclusive π^0 A_N indicate that greater precision will likely be needed. The projected 2015+'24 statistical uncertainties for the p + Au Collins asymmetry measurement at $\sqrt{s_{\mathrm{NN}}}$ = 200 GeV are found to be compared to those for the $p + p$ at the same energy.

8. Production of Strange Particles in *pp* and AuAu Collisions at RHIC Energies. Self-Similarity of Strange Particles Production

Experimental data on transverse momentum spectra of strange particles ($K_0^S, K^-, K^{*0}, \varphi, \Lambda, \Lambda^*, \Sigma^*, \Xi, \Omega$) produced in pp collisions at $\sqrt{s}$ = 200 GeV obtained by the STAR collaborations at RHIC were analyzed in the framework of z-scaling approach. The concept of the z-scaling is based on fundamental principles of self-similarity, locality, and fractality of hadron interactions at high energies. General properties of the data z-presentation are studied. Self-similarity of fractal structure of protons and fragmentation processes with strange particles is discussed. A microscopic scenario of constituent interactions developed within the z-scaling scheme is used to study the dependence of momentum fractions and recoil mass on the collision energy, transverse momentum and mass of produced inclusive particle, and to estimate the constituent energy loss. We consider that obtained results can be useful in study of strangeness origin, in searching for new physics with strange probes, and can serve for better understanding of fractality of hadron interactions at small scales.

We obtained results of new analysis concerning the strange particle production in *pp* collisions. The approach relies on a hypothesis about self-similarity of hadron interactions at a constituent

level. New indication on scaling properties of strangeness production different hadrons by the same scaling function $\psi(z)$ depending on a single variable was found. Results of data z-presentation on inclusive cross sections demonstrate "collapse" of data points onto a single curve.

The found feature supports the hypothesis on the universality of the shape of the scaling function for different hadron species ($K_0^S, K^-, K^{*0}, \varphi, \Lambda, \Lambda^*, \Sigma^*, \Xi, \Omega$). The observed regularity (the shape of $\psi(z)$ and its scaling behavior over a wide kinematic range) we treat as a manifestation of the self-similarity of fractal structure of the colliding objects, interaction mechanism of their constituents and processes of fragmentation of the constituents into registered real particles.

The performed analysis showed some tendency in the behavior of the fragmentation fractal dimension for different strange particles. It is larger for baryons than for mesons. For hyperons, the dimension increases with number of valence strange quarks.

The scaling function $\psi(z)$ preserves its shape for hadrons with different strangeness while fragmentation fractal dimension changes with the strangeness content of the inclusive hadron. We assume that the fragmentation dimension is important characteristic of the fragmentation of a given particle. We expect that the dimension should be different for different particles even in the asymptotic region ($z > 40$). The available data however do not allow to perform reliable test of this assumption for multi-strange baryons as determination of ε_F is not unique in this case.

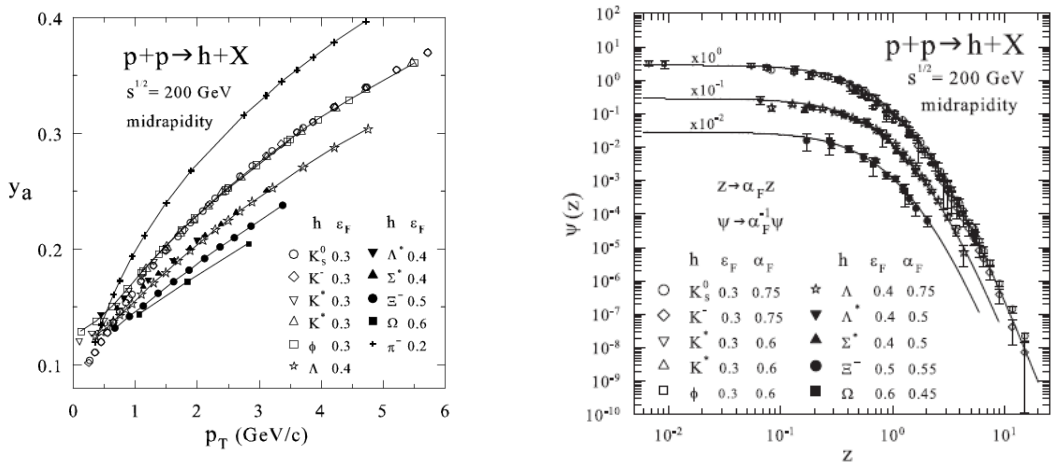

Figure 60. The z-presentation of the transverse momentum spectra and momentum fraction y_a of strange hadrons ($K_0^S, K^-, K^{*0}, \varphi, \Lambda, \Lambda^*, \Sigma^*, \Xi, \Omega$) produced in pp collisions at $\sqrt{s}$ = 200 GeV and $\theta_{cms} = 90^{\circ}$.

Publications:

1. M.V. Tokarev, I. Zborovsky,
New indication on scaling properties of strangeness production in pp collisions at RHIC, International Journal of Modern Physics A, 32, 1750029(42 pages), 2017.

2. M. Tokarev, I. Zborovsky,
Top-Quark p_T-Spectra at CMS and Flavor Independence of z-Scaling
Physics of Particles and Nuclei Letters, ISSN:1547-4771, Изд:Pleiades Publishing, 14, 5, 681–686, 2017

3. Токарев М.В., Зборовский И., Кечечян А.О., Дедович Т.Г
Проверка z-скейлинга в $p + p$, anti-$p + p$, Au + Au столкновениях на RHIC, TEVATRON и LHC». Физика элементарных частиц и атомного ядра. 2020. Т. 51. № 2. С. 221–222.

4. M.V. Tokarev, I. Zborovsky
“Self-Similarity, Fractality and Entropy Principle in Collisions of Hadrons and Nuclei at Tevatron, RHIC and LHC”, JINR Preprint E2-2020-24, Phys.Part.Nucl.Lett., 2021, v.18, №3 (accepted for publication).

Conferences:
1. M.V. Tokarev, I. Zborovsky
Self-similarity of strangeness production in pp collisions at RHIC, Journal of Physics: conference series, ISSN:1742-6588, eISSN:1742-6596, Изд:IOP Publishing Limited, 668, 012087, 2016.

2. M.V. Tokarev, I. Zborovsky, A.O. Kechechyan
“Fractality of strange particle production in pp collisions at RHIC”,
Regional STAR Meeting MEPhI, Moscow, Russia, August 23, 2017.

3. M.V. Tokarev, I. Zborovsky
“Fractality of strange particle production in pp collisions at RHIC”,
18th Lomonosov Conference on Elementary Particle Physics MSU, Moscow, Russia, August 24–30, 2017.

4. M. Tokarev, I. Zborovský, A. Kechechyan, T. Dedovich,
“*z*-Scaling from hundreds of MeV to TeV”,
Relativistic Nucler Physics from hundreds of MeV to TeV”, May 26–June 1, 2019, StaraLesna, Slovakia.

5. M.V. Tokarev, I. Zborovsky
Self-Similarity, Fractality and Entropy Principle in Collisions of Hadrons and Nuclei at Tevatron, RHIC and LHC,
Proceedings of 40th International Conference on High Energy physics – ICHEP2020, July 28–August 6, 2020, Prague, Czech Republic, Proceedings of Science, 2020. PoS (ICHEP2020) 575.

9. Development of the Software and Formation of the Infrastructure for the STAR Data Processing at JINR

The large luminosity of RHIC and high speed data acquisition system at the STAR are allowed to collect more than 24 Petabytes of information about Au + Au collisions. It is expected that by 2020 the amount of information will increase more than double. The taken data can no longer be processed only by the RHIC computer facility. Therefore, the use of the distributed data centers of different institutions of the STAR collaboration is one of the possible solutions to this problem. The Laboratory of Information Technologies of the JINR became the world's leading centers for the processing by the GRID system. Therefore, JINR resources can be used to process the STAR data. The results of this work of JINR group together with STAR software group at BNL were presented at the 7th International Conference «Distributed Computing and Grid-technologies in Science and Education» (GRID 2016, Dubna, July 2016) and XXVI International Symposium on Nuclear Electronics & Computing (NEC’2017, Becici, Budva, Montenegro, September 25–29, 2017).Technical solutions for the architecture of the Grid Software Stack and the organization of Grid Production Dataflow are shown in the two figures below.

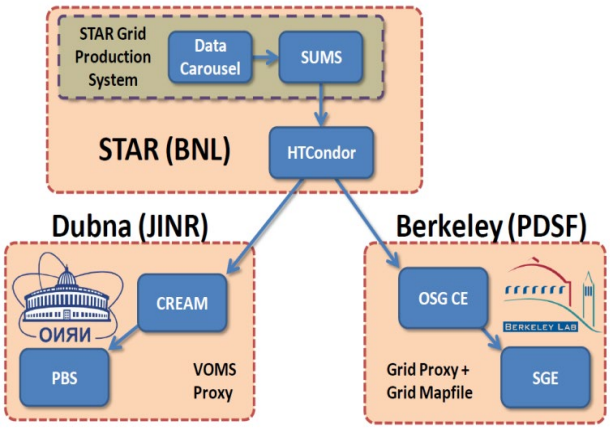

Figure 61. Grid Software Stack Architecture

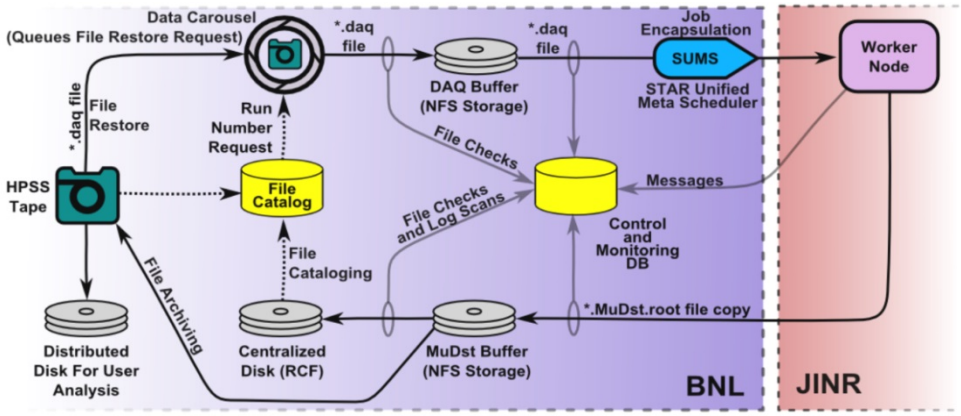

Figure 62. Current Grid Production Dataflow

- ***Analysis of computing results at JINR for the STAR***

It was created and reconstructed 23 199 files, spent 686,716 wall hours of runtime and produced a data volume of 30,367 GB.

Our framework has an excellent first pass efficiency of 93.2 %. The efficiency is comparable to, but slightly lower than, local efficiency, which is 98 %, due to the additional complexity of the added software interfaces. STAR has put a lot of thought and iterative refinement into the design of this production system. Extensive preproduction testing and a well-structured finite state system applied to each job, with retries in the event of interruption, applied to each job contributes to this high efficiency. What makes this even more remarkable is that it is running on heterogeneous nodes.

The following figures (Figure 63–Figure 67) show statistics of computing of STAR data at JINR GRID cluster.

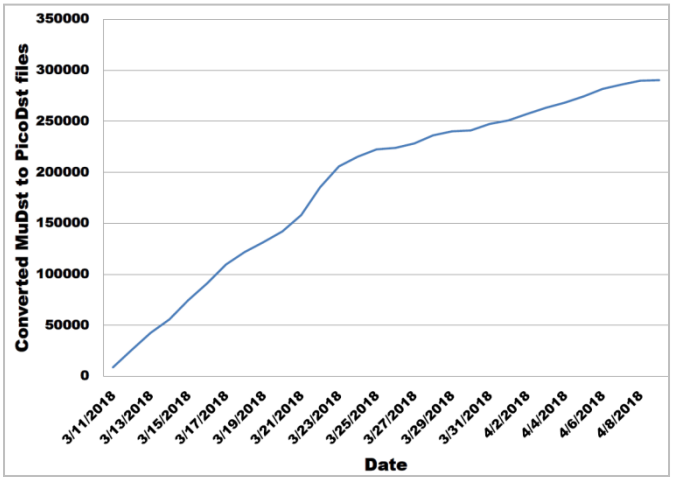

Figure 63. Files converted on JINR + Online

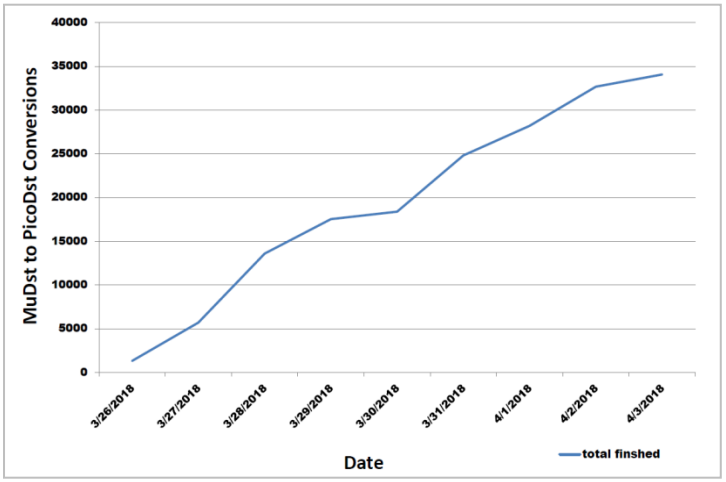

Figure 64. Total MuDst Files Finished *p*Au200_2015

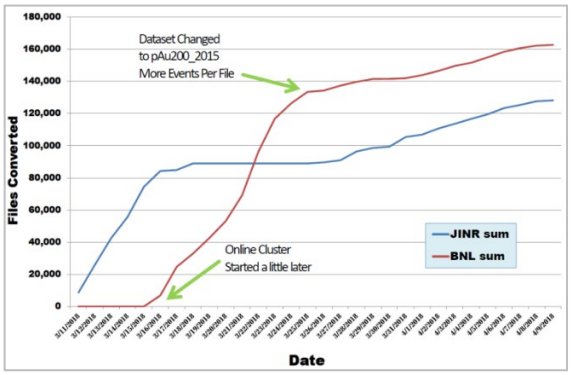

Figure 65. MuDst to PicoDst Files Converted Per Site

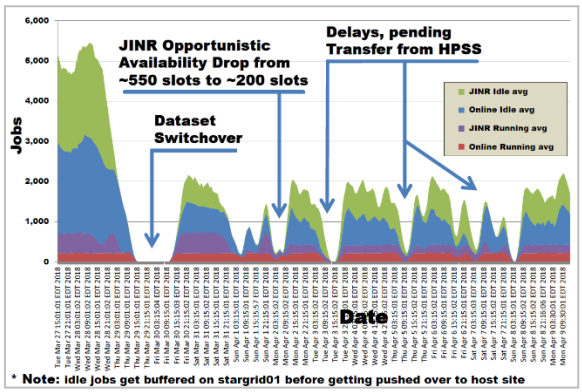

Figure 66. Running and Idle Jobs on JINR and Online site

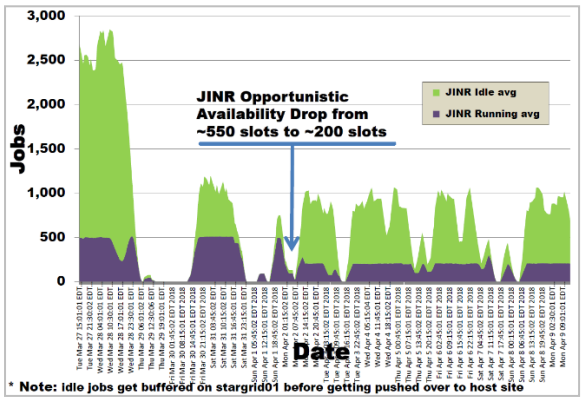

Figure 67. Running and Idle Jobs on JINR

Results of this work were presented at following conferences:

– "STAR's approach to highly efficient end-to-end grid production". XXVI International Symposium on Nuclear Electronics & Computing (NEC'2017), Becici, Budva, Montenegro, September 25–29, 2017
– "Progress report on STAR's Expansion to JINR via GRID". The 7th International Conference "Distributed Computing and GRID-technologies in Science and Education" (GRID 2016), Dubna, JINR, July 4–9, 2016

- ***MuDst to PicoDst Update***

The STAR data production plan is an evolving prioritization process based on input from the Physics Working Group (PWG) conveners, the readiness of data calibrations and the software development time invested to deliver high precision physics. Analysis of past challenges revealed that the lack of live storage was proving to be a show-stopper to either stage the MuDsts and/or store the PWG's private analysis tree necessary to pursue their analysis and publications in a timely

manner. Therefore, STAR is interested in developing newer and more compact analysis data format and in 2016 the Data Summary file format known as a "MuDST" (micro-DST) was complemented by an emerging format known as "picoDST". The picoDST related code workflows were since integrated in the STAR framework after a successful software peer-review process verifying code compliance. The PWG were actively polled for readiness and adaptation of ongoing analysis to the new file format and the picoDST was extended for a wider acceptance across all physics topics.

The generation of picoDST from Micro-DSTis a recent process by which, a more compact (and newly introduced) format could be produced from past data. The jobs are short, possibly a good match for the queue limitations at Dubna and pending a test on how many transfers we can sustain with the current infrastructure, we aim at directing the whole picoDST production at the JINR/Dubna site. Currently, over a million files production was requested from the PWG. We plan to do this work on converting MuDst to PicoDst at JINR in 2019–2021.

10. Specific Plans of JINR Group for 2022–2025

10.1. General information

Participation of the JINR group in the research program of the STAR Collaboration "Beam Energy Scan Phase II" and data analysis of results of measurements will be main goal of prolongation of the project STAR Experiment (JINR participation) for the period 2021–2023.

BES II in 2020-2023

STAR's **highest scientific priority for Run-20** is the continuation of the RHIC Beam Energy Scan II. The collaboration proposes to continue with the next two highest beam energies in collider mode (11.5 and 9.1GeV), as well as 6 FXT energies (7.7; 6.2; 5.2; 4.5; 3.94 3.5 GeV).

STAR's **highest scientific priority for Run-21** is the completion of the RHIC Beam Energy Scan II. The bulk of the 20-cryoweeks budget will be devoted to Au + Au collisions at the lowest collider energy of the program, at $\sqrt{s_{\mathrm{NN}}}$=7.7 GeV. We expect to refine our estimates of the projected run time for 7.7 GeV, currently 12 weeks, following some tests with C-AD towards the end of Run-19. The collaboration proposes to run the collider at $\sqrt{s_{\mathrm{NN}}}$= 16.7 GeV to allow collection of an important data point between 14.6 and 19.6 GeV as is pointed out earlier in this summary. We list the Run-21 proposed priorities and sequence in Table 2. Depending on the availability of cryo-weeks in Run-20 and/or Run-21 the collaboration proposes to collect data set(s) in the context of a small system run using O+O collisions. These data would allow for a direct comparison with a similarly proposed higher-energy O+O run at the LHC around 2021–2022, and further motivate the case for a small system scan complementary to ongoing efforts by the NA61/SHINE collaboration at SPS energies, and other proposed light-ion species at the LHC.

Table 9. Proposed Run-21 assuming 20 cryo-weeks, including an initial one week of cool-down and a one week set-up time for each collider energy.

Beam Energy (GeV/nucleon)	$\sqrt{s_{\mathrm{NN}}}$ (GeV)	μB (MeV)	Run time	Number Events
3.85	7.7	Au+Au	12 weeks	100M
8.35	16.7	Au+Au	5 weeks	250M
100	200	O+O	1 week	400M
				200M (central)

STAR after BES II

Under discussion now is research program of the STAR experiment after BES II period.

For Run-2022 period STAR Collaboration include a request for a dedicated 16-weeks pp run at 500 GeV. This run will take full advantage of STAR's new forward detection capabilities and further capitalize on the recent BES-II detector upgrades. We motivate a program that will use RHIC's unique ability to provide transverse and longitudinally polarized proton beams to exploit both an increased statistical power and kinematic reach from recent and planned detector upgrades.

For time period years 2022–2025 we suggest research program for Mid-rapidity $-1.5 < \eta < 1.5$ and Forward rapidity $2.8 < \eta < 4.2$.

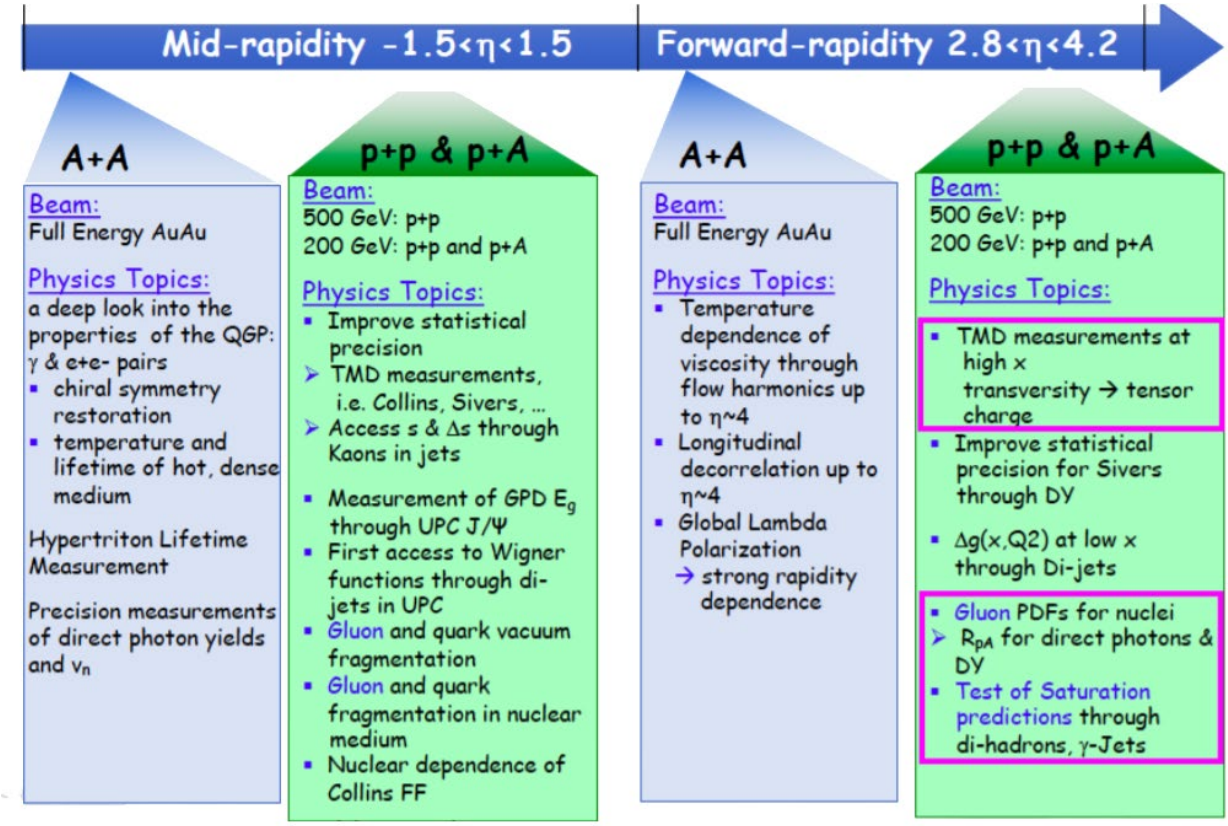

Figure 68. Physics program for mid and forward rapidities.

For realization of this research program suggested following data tacking runs schedule for years 2022–2025.

10.2. BES II – analysis of charged hadron spectra

The continuation of the Beam Energy Scan-II program at the RHIC collider includes the analysis of the spectra of charged hadrons in Au + Au collisions at energies $\sqrt{s_{NN}}$ = 9.2, 11.5, 14.6, 19.6, 27 GeV, depending on the energy and centrality of the collision and the transverse momentum of the particle.

Experimental data on the spectra of charged hadrons are an important component for studying nuclear matter formed in collisions of heavy ions, searching for signatures of phase transitions and a critical point, and establishing the phase diagram of nuclear matter. The energy range of the BES-II program and statistics that exceed the BES-I statistics by two orders of magnitude suggest that these tasks can be achieved. It should be noted that along with the study of momentum spectra, the data obtained will make it possible to carry out other data analyzes event-by-event analysis, which

will provide more detailed information about both the properties of nuclear matter and the peculiarities of the formation of various particles.

The spectra are also of interest for testing various theoretical models (transport model), approaches (hydrodynamic approach, method of statistical thermodynamics,) and for verifying new effects predicted in the framework of QCD.

The JINR group participated in the analysis of the STAR data obtained at BES-I and obtained the spectra of negatively charged hadrons depending on the energy and centrality of the collision, the momentum of an inclusive particle. The scaling properties of the spectra have been studied in the framework of the z-scaling theory, the energy losses have been estimated, and new laws have been established in the production of particles in Au + Au collisions.

The JINR group plans to continue analyzing the BES-II data to obtain impulse spectra, check the self-similarity of particle production, and use more statistics to search for signatures of new physics.

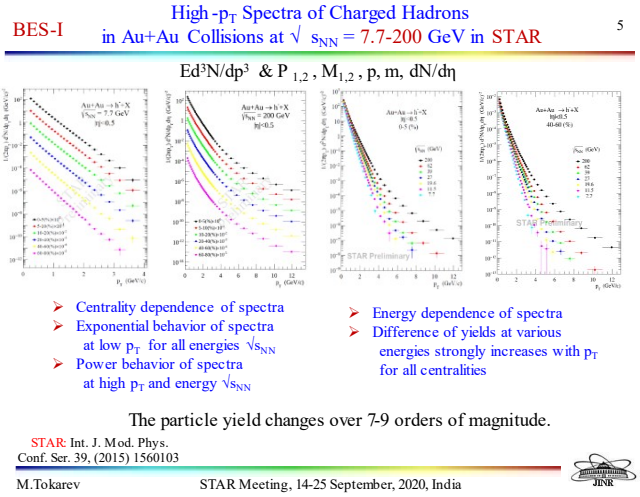

Figure 69. Invariant yields of negative hadrons in Au + Au collisions at BES-I energies and different centralities.

10.3. BES II – energy loss study

It is planned to study energy losses depending on the energy and centrality of the collision and the transverse momentum of a particle to find the features of the mechanism of particle formation in nuclear matter.

One of the important characteristics of the nuclear medium formed in collisions of heavy ions is the amount of energy loss of quarks and gluons during the passage of this medium. It is assumed that these losses in the hadronic and quark-gluon phases will be significantly different. It is expected that when the phase boundary is crossed, the value of the losses changes rather quickly and can be considered as an indicator of the phase transition. Estimates of energy losses obtained within the framework of various models and approaches are necessary to obtain a unified description and can be used to determine the phase diagram of nuclear matter.

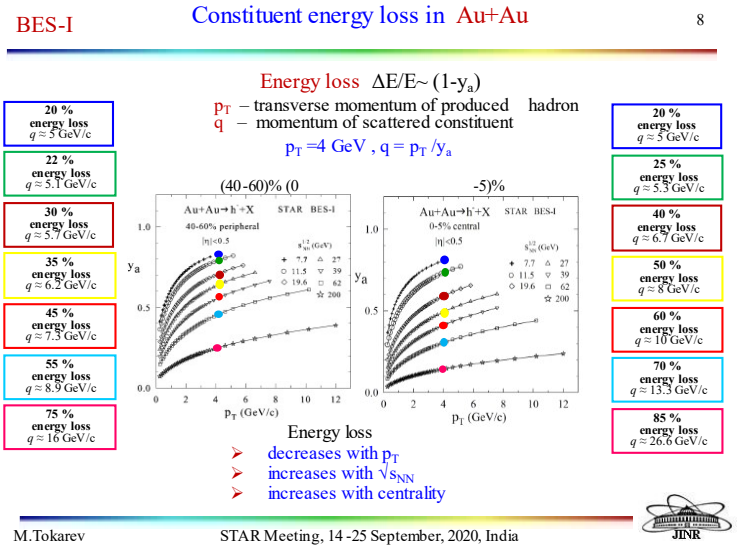

Figure 70. Constituent energy losses in Au + Au interactions at different collision energies and centralities (0–5) % and (40–60) %.

The JINR group took part in the analysis of the STAR data obtained at BES-I and determined the magnitude of energy losses depending on the energy and centrality of the collision. The results of the analysis within the framework of the *z*-scaling theory demonstrate smooth dependences of energy losses and do not reveal noticeable fluctuations.

The JINR group plans to continue analyzing the BES-II data and, using more statistics, to obtain the dependences of energy losses on the energy and centrality of the collision and the momentum of the detected particle to search for statistically significant deviations from smooth dependences.

10.4. BES II – analysis of STAR data on the cumulative production of charged hadrons

It is planned to analyze the STAR data on the cumulative production of charged hadrons in Au + Au collisions at energies $\sqrt{s_{\mathrm{NN}}}$ = 7.7 and 11.5 GeV to search for signatures of the formation mechanism of cumulative particles.

It is assumed that the cumulative trigger makes it possible to study the production of particles from compressed, or cumulated, nuclear matter. In this state, the density of nuclear matter can significantly (by an order of magnitude) exceed the density of an ordinary nuclear medium (0.16 GeV/fm^3). Therefore, the study of particle production in the cumulative region is of particular interest, since this region is located near the phase boundary and is more sensitive to the peculiarities of the rearrangement of the symmetry of the system caused by many-particle interactions of quarks and gluons than a system located far from it.

The JINR group, when analyzing the STAR BES-I data, for the first time obtained spectra of particle production in collisions of gold nuclei in the collider mode at energies $\sqrt{s_{\mathrm{NN}}}$ = 7.7 and 11.5 GeV in the cumulative region. In this region, the smooth behavior of the scaling function and other quantities (momentum fractions, recoil mass), characterizing the microscopic mechanism of hadron production, has been established.

The JINR group plans to continue the analysis of the BES-II data on the cumulative production of negatively charged hadrons using larger statistics to detect in this area the features in the behavior of model parameters (fractal dimensions, specific heat).

Preliminary results were obtained on the cumulative production of negative hadrons in Au + Au at energy $\sqrt{s_{\mathrm{NN}}}$ = 9.2 GeV.

Invariant yield of negative hadrons in Au + Au interactions at energy $\sqrt{s_{\mathrm{NN}}}$ = 9.2 GeV in the central region of pseudorapidity and various centralities.

Dependence of the Ax1 variable on the transverse momentum of a particle produced in Au + Au interactions at an energy $\sqrt{s_{\mathrm{NN}}}$ = 9.2 GeV in the central region of pseudorapidity and various centralities. The cumulative area corresponds to the range Ax_1> 1.

10.5. Verification of self-similarity in hadron production in Au + Au collisions at RHIC energies and searching for signatures of phase transitions and critical point

The search for new symmetries and the region in which they are fulfilled is one of the fundamental tasks of relativistic nuclear physics.

The JINR group is developing the theory of *z*-scaling. Based on a large amount of experimental data obtained at accelerators and colliders in scientific laboratories – IHEP (U70), CERN (ISR, SppS), FNAL (Synchrotron, Tevatron), BNL (RHIC), a new feature was established, known in the literature as *z*-scaling. It reflects the symmetry of particle formation and the principle of self-similarity. The properties of the *z*-representation of the momentum production spectra of particles with different flavor compositions from the π meson to the top quark, jets and direct photons in proton-proton and proton-antiproton collisions have been established. Experimental data on the jet and top quark production spectra obtained at the LHC confirmed the previously established properties of *z*-scaling. The field of applicability of this theory was extended to proton-nuclear interactions. With the launch of the world's first collider of relativistic nuclei RHIC at Brookhaven National Laboratory, systematic studies of the principle of self-similarity in the production of particles in heavy ion collisions have been continued.

The main task of experimental research is to establish the structure of the phase diagram of nuclear matter (the number and types of phases, phase boundaries, critical points, etc.).

The JINR group participated in the analysis of STAR data and verified the principle of self-similarity in the production of various particles (π, *K*, *p*, *J*/ψ) in collisions of protons and nuclei over a wide range of energies and centrality of collisions and transverse momenta.

The group participated in analysis of STAR BES-I data. A systematic analysis of the spectra has been carried out and important regularities in the production of particles in collisions of gold nuclei have been established. Signatures of phase transitions were proposed in the framework of the *z*-scaling theory.

The JINR group plans to continue participating in analysis of STAR BES-II data in order to search for new effects, verify and further develop the microscopic theory of *z*-scaling and the principle of self-similarity. Preliminary results have been obtained on the production spectra of negative hadrons in Au + Au collisions at an energy $\sqrt{s_{\mathrm{NN}}}$ = 9.2 GeV in *z*-representation.

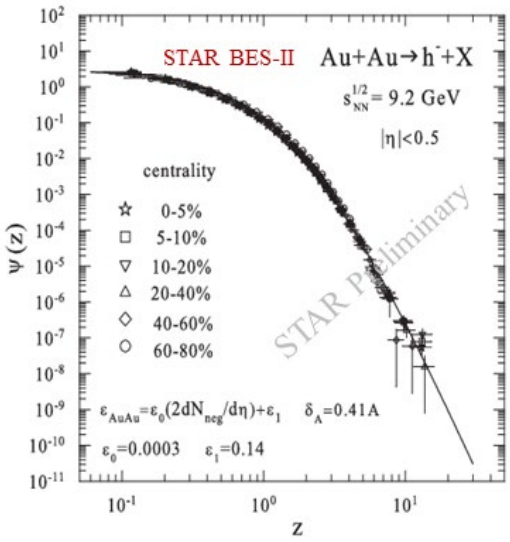

Figure 71. Scaling function of negative hadron production in Au + Au collisions at energy $\sqrt{s_{\mathrm{NN}}}$ = 9.2 GeV in the central region of pseudorapidity and different centralities.

10.6. Event-by-event analysis of Au+Au data at $\sqrt{s_{\mathrm{NN}}}$ = 200 GeV

It is assumed that the SePaC method will make it possible to distinguish events that differ in their transverse momentum distribution. Analyze the selected events considering additional criteria reflecting the mechanism of fractal formation.

The event-by-event analysis of the interactions of nuclei gives the clearest information about the mechanisms of particle formation and the properties of the nuclear medium in a collision, provided that the number of particles in the event is large enough for statistical analysis and the magnitude of the systematic error is comparable to the statistical one.

When describing the mechanism of particle formation in an event, the concept of the formation and development of a shower of quarks and gluons, which evolves and at the final stage of the fragmentation process, turns into observable particles, is widely used. It is assumed that the distribution of particles in the phase space is determined by the dynamics of interaction - the hard interaction of partons, parton shower in the initial and final states, fragmentation of partons into hadrons, and decay of resonances. This scenario is used in many Monte Carlo generators. One of the assumptions of such a scenario is a self-similar shower structure in the space of kinematic parameters (ϑ, Q^2, x ordering). In each act of parton splitting, the momentum conservation law is fulfilled. Such a self-similar process leads to a fractal distribution of particles in the phase space.

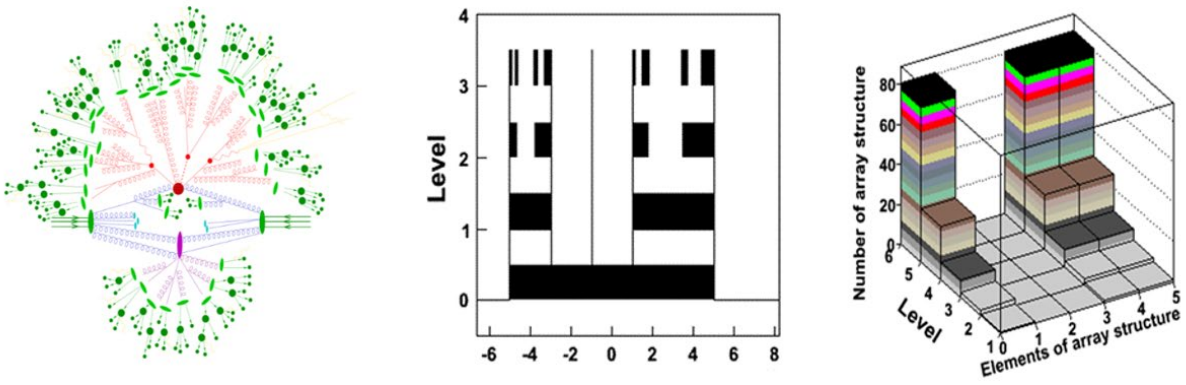

(a) (b) (c)

Figure 72. Parton shower (a), Cantor set (b) and its structure (c).

The JINR group has developed a method of fractal analysis of events – System of Equations of P-basis Coverage Method (SePaC). The method is based on the property of self-similarity at different levels of resolution in the investigated space (for example, transverse momenta). For each level, the coverage is determined, and an equation is drawn up to find the fractal dimension. The equality of dimensions for all equations of the system determines an object called a fractal. An algorithm for the reconstruction of fractals was developed, the software package was tested on a wide class of fractals, and the effectiveness of the method was estimated.

Work has begun on fractal analysis of STAR data for Au + Au collisions at energy $\sqrt{s_{\mathrm{NN}}}$ = 200 GeV.

In the JINR group, preliminary results of processing about 1 million events of different centrality were obtained: the optimal parameters of the method were determined, the distributions of events in fractal dimension were obtained, a comparison was made with different p_T-distributions of particles (power-law, exponential, random), classes of events were identified, the p_T-distributions of which were differ significantly from each other, additional criteria for selecting events are being developed in order to significantly suppress the background and obtain a cleaner set of fractal events.

The JINR group plans to continue the event-by-event analysis of Au + Au collisions at energies $\sqrt{s_{\mathrm{NN}}}$ =200 GeV and different centralities obtained by STAR at RHIC, with the aim of searching for fractal structures.

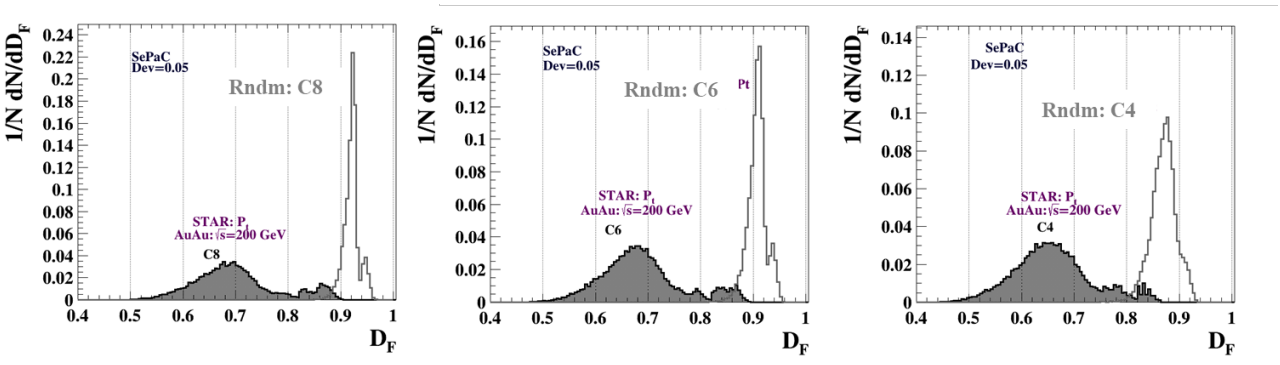

Figure 73. Fractal dimension distribution of Au + Au events (STAR – filled and Monte Carlo (random) – open areas).

10.7. Fractal analysis of Au + Au events obtained by the Monte Carlo method

It is planned to study the structure of Au + Au events obtained by the Monte Carlo method using the A Multiparticle Transport Model (AMPT) generator at a collision energy $\sqrt{s_{\mathrm{NN}}}$ = 200 GeV and different centralities.

The search for new physical laws, as a rule, relies on a comparison of the results of the analysis of experimental data with the available results of theoretical calculations. The detected difference is considered as an indication of the effects not considered in the model description and contributes to a more complete development of theoretical models and approaches.

The AMPT generator is widely used by both STAR and other collaborations to simulate ion interaction events depending on the energy, impact parameter of the collision, and to obtain different distributions of produced particles.

The JINR group plans to carry out an event-by-event analysis of Au + Au collisions at energies $\sqrt{s_{\mathrm{NN}}}$ = 200 GeV and different centralities obtained using the AMPT generator in order to find the

difference in distributions in fractal dimensions. It is assumed that such a sophisticated analysis will contribute to a deeper understanding of the mechanisms inherent in the model and the degree of their correspondence to the experimentally studied physical processes.

It is planned to compare the results of fractal analysis of events obtained by STAR at the RHIC and the Monte Carlo method to search for the peculiarities of the properties of nuclear matter formed in collisions of heavy ions.

10.8. Development of the multicriteria method of fractal analysis of events (SePaC) of nucleus-nucleus collisions at RHIC energies

The JINR group plans to further develop the SePaC method for fractal analysis of events of nucleus-nucleus interactions. It is assumed that the introduction of additional selection criteria will make it possible to create a set of purer, but rather rare, events indicating the fractal structure of nuclear matter.

10.9. Proposal of femtoscopic STAR data analysis

In high energy particle or nuclei collisions, large numbers of various particles are produced. Particle momentum correlations due to the effects of final state interaction (FSI) and quantum statistics (QS) at small relative momenta in their centre-of-mass system, as well as, – particle coalescence due to FSI, allow one to get space-time characteristics of the production processes on a femtometer level; at the same time, they provide the information on particle strong interaction hardly accessible by other means (see a review [1] and references therein).

Of particular importance is a systematic study of the production space-time parameters in the beam energy scan, together with the fluctuation characteristics, in the search for the critical endpoint and corresponding softening of the Equation of State (EoS) and increased duration of particle emission (see, e.g., [2,3]). Besides correlations of identical particles, providing information on even moments of the distribution of particle space-time separation, also the correlations of non-identical particles should be studied, the latter providing, in addition, also the information on the odd moments, including space and time shifts [1]. Obviously, correlations in various combinations of pions, kaons, nucleons and hyperons contain a rich complementary information about the production process.

The correlation measurement of strong particle interaction is especially up-to-date in connection with the so-called hyperon puzzle in neutron stars. Their radius of 10–15 km and mass of ~ 1.5–2 sun masses essentially depend on the EoS, which is softened in the presence of hyperons thus leading to a decrease of the maximal neutron star mass [4]. Unfortunately, the present knowledge of hyperon-nucleon, hyperon-hyperon, kaon-nucleon and kaon-hyperon

interactions is not sufficient for a reliable calculation of nucleon and hyperon fractions and corresponding neutron star EoS.

The measurement of the ΛΛ interaction is of particular interest in connection with a possible existence of so-called H-dibaryon. The STAR analysis of ΛΛ correlations in Au + Au collisions reported a negative singlet s-wave scattering length $f_0 \approx -1$ fm (defined as the scattering amplitude at threshold) and a large positive effective radius $d_0 \approx 8$ fm thus excluding both a near threshold s-wave resonance and a ΛΛ bound state (the latter requiring [6] $2d_0/f_0 > -1$, i.e., $d_0 < 0.5$ fm). On the contrary, a recent ALICE analysis of ΛΛ correlations in $p + p$ and p + Pb collisions is compatible with the existence of a ΛΛ bound state [7]. This discrepancy calls for a new analysis of STAR data

with higher statistics and a more refined treatment of residual correlations due to feed-down Λ's from hyperon decays (dominantly, from $\Sigma^0 \to \Lambda\gamma$).

Another possibility to extract the ΛΛ singlet scattering parameters is the analysis of Λ spin correlations using as a spin analyser the asymmetric (parity violating) decay $\Lambda \to p\pi^-$: the distribution of the cosine of the relative angle θ between the directions of the decay protons in the respective Λ rest frames allows one to determine the triplet fraction of the ΛΛ correlation function [8]. Since this technique requires no construction of the uncorrelated reference sample, it can serve as an important consistency check of the standard correlation measurements. This technique can be especially useful for the analysis of ΛΛ correlations in $p + p$ or p + A collisions, where the characteristic Gaussian source radius r_0 is rather small (~1–1.5 fm) and the correlation width $1/r_0$ ~ 200 MeV/c is sufficiently large for a statistically significant analysis.

The two-particle FSI in multiparticle production processes is usually taken into account in a similar way as in beta-decay by substituting the product of plane waves at equal times in pair rest frame (PRF) with the two-particle wave function of the corresponding scattering problem. Obviously, this assumption is not justified at very large temporal particle separation t^* in PRF, when the two-particle FSI should vanish. On the other hand, it was shown [9,10] that one can neglect the t^* separation on conditions $|t^*| << m(t^*)r^*\mathrm{Min}(r^*, 1/k^*)$, where $m(t^* > 0) = m_2$, $m(t^* < 0) = m_1$; r^* and k^* are spatial particle separation and particle momentum in PRF. These conditions are presumably well satisfied for correlations between heavy particles like kaons or protons, but their violation for correlations involving pions is not excluded (expectedly, on a level of several percent). The former statement was confirmed by the STAR correlation measurement of the proton-proton and antiproton-antiproton scattering parameters in perfect agreement with their table values [11]. As for the correlations involving pions, the validity check of the equal-time ($t^* = 0$) approximation still remains to be done. An attempt of this check was done using the NA49 $\pi^+\pi^-$ correlation data, pointing to ~20 % underestimation of the s-wave $\pi^+\pi^-$ scattering length, however, with the statistical significance of two standard deviations only [1].

Finally, presently, there is enhanced interest to the production of light ions, which surprisingly appears to be in agreement with predictions of both statistical and coalescence models. Physically, however, the former model is unjustified due to a huge difference between the temperature of chemical freeze-out of ~160 MeV and the binding energy of a few MeV. A possibility to distinguish these models has been suggested based on the yields of ^{4}Li and ^{4}He [12]. These ions have about the same masses but different spin factors (5 and 1, respectively), leading to the statistical model yield ratio of 4.3 (if one takes into account a small mass difference). As for the coalescence model, it predicts a significantly smaller ratio of yields since ^{4}He is much more compact as compared with ^{4}Li [12].

10.10. Development of new approaches to particle identification

In 2019 and 2020, the STAR collaboration carried out a major upgrade of the installation, including TPC, and collected a large amount of data under the BES II program. Since the increase in the number of points on the track and the new algorithm for calculating the energy losses of particles in the TPC gas significantly changed the detector's response function to different types of charged particles, it became necessary to obtain a new approximation of this function. A significant increase in data statistics and an increase in the efficiency of the software for searching for neutral particles makes it possible to form a new, much cleaner set of particles for determining the TPC response function to protons, pions, kaons and electrons. To do this, using the KFParticle algorithm, the distribution of energy losses of different types of particles depending on their

momentum and centrality of interaction was obtained from the data processed during the collection of collisions of gold nuclei at different energies. Now, a search is underway for a mathematical function or a set of functions that will allow describing the obtained dependencies with an accuracy better than 2%. Further, these descriptions of the response functions are planned to be applied to determine the magnitude of fluctuations of the moments of the distribution of the multiplicity of particles in collisions of gold nuclei, depending on their centrality and energy.

10.11. Turning on the event plane detector into data analysis

The work related to the inclusion of an event plane detector (EPD) in the complex of programs for processing data has been carried out. The event plane detector will increase the accuracy of event reconstruction in experiments to study global polarization and measure directed flows and other collective effects in nucleus-nucleus collisions. The results of the runs in which the event plane detector worked in the STAR experiment at RHIC since its launch in 2018 are analyzed. The software for launching the systems of codes "Event Plane with the STAR EPD code StEpdEpFinder" is installed. Within the framework of StEpdEpFinder, the data on collisions of Au + Au nuclei at energy $\sqrt{s_{NN}}$ = 27 GeV in the STAR experiment at RHIC, taking into account information from the event plane detector, have been processed. Using StEpdEpFinder, information was obtained on the plane of the event in collisions of gold nuclei at energies $\sqrt{s_{NN}}$ = 27 GeV An estimate was also obtained for the value of the forward flux (υ_1) for Au + Au collisions at an energy $\sqrt{s_{NN}}$ = 27 GeV. The analysis results indicate the presence of a nonzero value of υ_1.

In the MpdRoot repository, the algorithm developed by the Mpd thread group has been tested and the necessary functions have been selected to determine the angle of the plane of the event using the ZDC (hadron calorimeter for high rapidities). Knowing the energy release in each cell of the hadron calorimeter for high rapidity, it is possible to reconstruct the angle of the plane of the event from the forward flow. The resolution of the event plane can be calculated from the forward flow in the ZDC.

It is planned to transfer the tested and existing polarization algorithms to the online repository. The site github.com was chosen, which is positioned as a web service for hosting projects using the git version control system, as well as a social network for developers.

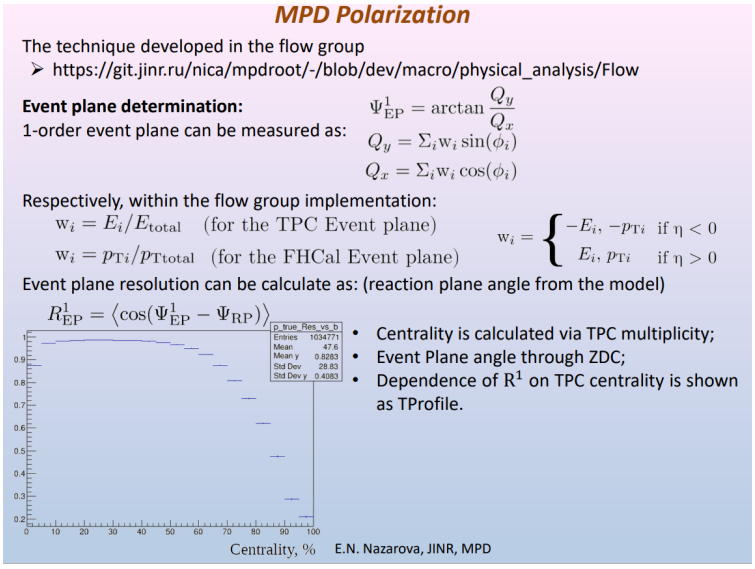

Figure 74. Using a reaction plane detector to determine polarization.

10.12. Machine learning techniques to data analysis

Given the experience with machine learning, it is planned to develop a convolutional neural network to find objects of interest in the image. It is planned to explore the possibility of machine learning in high energy physics, namely, the identification of charged particles based on machine learning. Particle identification based on trajectory geometry and TOF data analysis using a neural network. The characteristics used for identification are the particle momentum-to-charge ratio and mass-to-charge ratio, which we extract from the particle's passage through detector data, modeled using the MpdRoot software package. The parameters of the particle momentum-to-charge ratio and the mass-to-charge ratio are fed to the input layer; the output layer consists of six softmax elements, which correspond to the probabilities of identifying a particle as one of six types. For machine learning, we plan to use the open software library TensorFlow. Now there is a process of studying the literature, discussing and developing a neural network.

Given the experience with machine learning, it is planned to develop a convolutional neural network to find objects of interest in the image. It is planned to explore the possibility of machine learning in high energy physics, namely, the identification of charged particles based on machine learning. Particle identification based on trajectory geometry and TOF data analysis using a neural network. The characteristics used for identification are the particle momentum-to-charge ratio and mass-to-charge ratio, which we extract from the particle's passage through detector data, modeled using the MpdRoot software package. The parameters of the particle momentum-to-charge ratio and the mass-to-charge ratio are fed to the input layer; the output layer consists of six softmax elements, which correspond to the probabilities of identifying a particle as one of six types. For machine learning, we plan to use the open software library TensorFlow. Now there is a process of studying the literature, discussing, and developing a neural network.

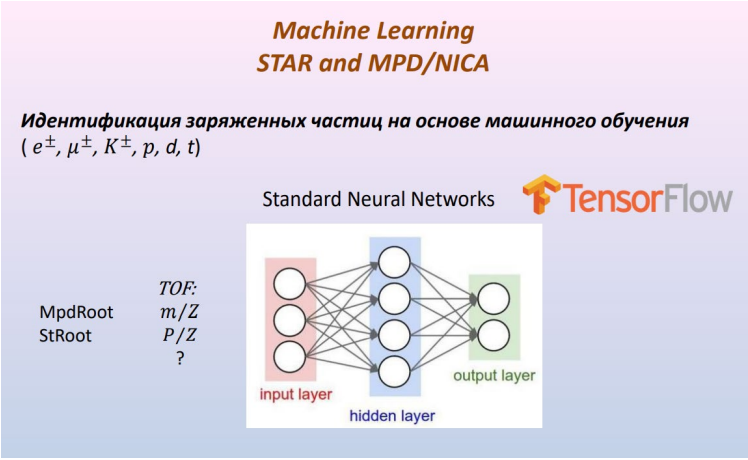

Figure 75. Possible construction of a machine learning diagram.

References

1. R. Lednicky, Phys. of Atomic Nuclei 67 (2004) 71.
2. R. Lednicky, Nucl. Phys. B (Proc. Suppl.) 198 (2010) 43.
3. P. Batyuk et al., Phys. Rev. C 96 (2017) 024911.
4. D. Lonardoni et al., Phys. Rev. Lett. 114 (2015) 092301.
5. STAR Collab. (L. Adamczyk et al.), Phys. Rev. Lett. 114 (2015) 022301.
6. P. Naidon and S. Endo, Rept. Prog. Phys. 80 (2017) 056001.
7. ALICE Collab. (S. Acharya et al.), Phys. Lett. B 797 (2019) 134822.
8. R. Lednicky and V. L. Lyuboshitz, Phys. Lett. B 508 (2001) 146.
9. R. Lednicky and V.L. Lyuboshitz, Sov. J. Nucl. Phys. 35 (1982) 770.
10. R. Lednicky, Phys. Part. Nuclei 40 (2009) 307.
11. STAR Collab. (L. Adamczyk et al.), Nature 527 (2015) 345.
12. S. Bazak and St. Mrowczynski, Eur. Phys. J. A 56 (2020) 193.

Appendix 1. List of JINR Group publications

The members of the JINR group have prepared the following publications on the research of relativistic nuclei and protons at colliders:

1. «Validation of *z*-scaling for negative particle production in Au + Au collisions from BES-I at STAR», Nucl. Phys. A993 (2020) 121646 (47 p.).
2. «*z*-Scaling in $p + p$, anti-$p + p$ and Au + Au Collisions at RHIC, Tevatron and LHC» ISSN 1063-7796, Physics of Particles and Nuclei, 2020, Vol. 51, No. 2, pp. 141–171. © Pleiades Publishing, Ltd., 2020.
3. «Критерии восстановления фракталов и подавления фоновых событий SePaC методом», Письма в ЭЧАЯ. 2021 Т. 18, № 1(233). С. 113–133
4. «Self-Similarity, Fractality and Entropy Principle in Collisions of Hadrons and Nuclei at Tevatron, RHIC and LHC», To be published in Proceedings of 40th International Conference on High Energy physics – ICHEP2020, July 28 - August 6, 2020, Prague, Czech Republic, Proceedings of Science, 2020.
5. The STAR Collaboration
   "Measurement of the mass difference andthe binding energy of the hypertriton andantihypertriton", Nature Physics, 16 (2020) 409–412.
6. M.V. Tokarev, I. Zborovsky,
   Self-similarity of hadron production: *z*-scaling
   Theoretical and Mathematical Physics, ISSN:0040-5779, eISSN:1573-9333, Изд:Springer New York, 184, 3, 1350-1360, 2016
7. T.G. Dedovich, M.V. Tokarev,
   "Incomplete fractal showers and restoration of dimension",
   EPJ Web of Conferences 204, 06003 (2019)
8. M.V. Tokarev, A.O. Kechechyan, I. Zborovský
   "Self-Similarity of Negative Particle Production in Au + Au Collisions at STAR", Physics of Particles and Nuclei Letters, 2019, Vol. 16, No. 5, pp. 510–515.
9. M.V. Tokarev, A.O. Kechechyan, I. Zborovský
   "Validation of z-scaling for negative particle production in Au + Au collisions from BES-I at STAR", Published in Nuclear Physics A 993 (2020) 121646.
10. I. Zborovsky
    "Fractality in hadron interactions: a conservation law and quantization of fractal dimensions", EPJ Web of Conf. 204, 06002 (2019).
11. M.V. Tokarev, I. Zborovsky
    Self-Similarity, Fractality and Entropy Principle in Collisions of Hadrons and Nuclei at Tevatron, RHIC and LHC, Proceedings of 40th International Conference on High Energy physics – ICHEP2020, July 28 – August 6, 2020, Prague, Czech Republic, Proceedings of Science, 2020. PoS (ICHEP2020) 575.

12. M.V. Tokarev, I. Zborovsky, A.O .Kechechyan, T.G. Dedovich
z-Scaling in $p + p$, anti-$p + p$ and Au + Au Collisions at RHIC, Tevatron and LHC
Physics of Particles and Nuclei, 2020, Vol. 51, No. 2, pp. 141–171.
13. M.V. Tokarev, I. Zborovsky
"Self-Similarity, Fractality and Entropy Principle in Collisions of Hadrons and Nuclei at Tevatron, RHIC and LHC", JINR Preprint E2-2020-24,
Phys. Part. Nucl. Lett., 2021, v.18, № 3 (accepted for publication)
14. T.G. Dedovich, M.V. Tokarev,
"Incomplete fractal showers and restoration of dimension",
EPJ Web of Conferences 204, 06003 (2019)
15. T. Dedovich and M. Tokarev,
"Analysis of fractals with combined partition," Phys. Part. Nucl. Lett. 13, 169–177 (2016)
16. T. Dedovich and M. Tokarev,
"A two-step procedure of fractal analysis," Phys. Part. Nucl. Lett. 13, 178–189(2016)
17. T. Dedovich and M. Tokarev,
"Fractal reconstruction
in the presence of background," Phys. Part. Nucl. Lett.14, 856–873 (2017)
18. T.G. Dedovich, M.V.Tokarev,
"Reconstruction of the Dimension of Complete and Incomplete Fractals", Physics of Particles and Nuclei Letters, 16, 3, 240–250, 2019
19. T.G. Dedovich, M.V. Tokarev
"Criteria of fractal reconstruction and suppression of background events by SePaC method", Physics of Particles and Nuclei Letters, 2021, Vol. 18, No. 1, pp. 93–106.
20. M.V. Tokarev, I. Zborovsky, A.A. Aparin, Phys. Part. Nucl .Lett., Vol.12, № 1, 2015, 48–58
21. M.V. Tokarev, I.Z. borovsky,
New indication on scaling properties of strangeness production in pp collisions at RHIC, International Journal of Modern Physics A, 32, 1750029(42 pages), 2017.
22. M. Tokarev, I. Zborovsky,
Top-Quark p_T-Spectra at CMS and Flavor Independence of z-Scaling
Physics of Particles and Nuclei Letters, ISSN:1547-4771, Изд:Pleiades Publishing, 14, 5, 681–686, 2017
23. Токарев М.В., Зборовский И., Кечечян А.О., Дедович Т.Г
Проверка *z*-скейлинга в $p + p$, anti-$p + p$, Au + Au столкновениях на RHIC, TEVATRON и LHC». Физика элементарных частиц и атомного ядра. 2020. Т. 51. № 2. С. 221–222.
24. M.V. Tokarev, I. Zborovsky
"Self-Similarity, Fractality and Entropy Principle in Collisions of Hadrons and Nuclei at Tevatron, RHIC and LHC", JINR Preprint E2-2020-24, Phys.Part.Nucl.Lett., 2021, v.18, №3 (accepted for publication).

Appendix 2. List of conference reports

The members of the JINR group prepared the following reports at international conferences, meetings of the STAR collaboration and seminars:

1. "z-Scaling from hundreds of MeV to TeV", Relativistic Nucler Physics from hundreds of MeV to TeV", May 26–June 1, 2019, StaraLesna, Slovakia.
2. "High-p_T spectra of h-hadrons in Au + Au collision at $\sqrt{s_{\mathrm{NN}}}$ = 9.2 GeV", STAR Collaboration Meeting, 14–25 September, 2020, Indian Institute of Science Education and Research (IISER) Tirupati, India.
3. "Search for fractal structures in Au + Au events at 200 GeV", STAR Collaboration Meeting, 14–25 September, 2020, Indian Institute of Science Education and Research (IISER) Tirupati, India
4. "Self-similarity, fractality and entropy principle in collisions of hadrons and nuclei at RHIC, Tevatron and LHC", 40th International Conference on High Energy physics – ICHEP2020, July 28 – August 6, 2020, Prague, Czech Republic
5. "Self-similarity of the proton spin", Workshop "Physics programme for the first stage of the NICA SPD experiment", JINR, Dubna, LHEP, 5–6 October 2020
6. «Методика восстановления лямбда гиперонов в ядро-ядерных столкновениях», Семинар в Национальном Центре Ядерных Исследований, г. Баку 21.01.2020
7. "STAR Recent Results on Heavy-Ion Collisions", LXX International Conference NUCLEUS-2020, online conference, 11–17 October 2020

Appendix 3. Main information about STAR–JINR Group

Большое внимание в последнее время в группе STAR в ОИЯИ и, в частности, 2020 году уделялось работе со студентами (они оформлены на работу по совместительству в ЛФВЭ или УНЦ ОИЯИ). Работу со студентами (бакалаврами и магистрами) активно ведут в Дубне старший научный сотрудник Апарин А.А. и в Кошице доцент Адели Кравчакова. Нам представляется это направление работы очень важным в контексте подготовки молодых специалистов с опытом работы в эксперименте на коллайдере для их дальнейшей работы на коллайдере NICA/MPD. Свои бакалаврские и магистерские работы человек в группе ОИЯИ в настоящее время выполняют 8 человек. В качестве научной тематики квалификационных работ сформулированы следующие задачи:

1. Анализ данных STAR для подсчета кумулянтов нэт-протонов и нэт-каонов для проверки поведения флуктуаций указанных кумулянтов в области энергии столкновения 7.7 – 27 ГэВ. Усиление флуктуаций кумулянтов и моментов распределений множественности нэт-протонов и нэт-каонов рассматривается как проявление влияния критической точки фазового перехода.
2. Работа по анализу энергетической зависимости выходов частиц на данных Монте-Карло моделирования детектора MPD. Расчет отношения выходов странных частиц к нестранным, барионов к мезонам, частиц к античастицам в зависимости от энергии в столкновениях ядер золота в диапазоне энергий 4–11 ГэВ. Проведение QA анализа треков для выбора оптимальных параметров отбора частиц. Определение функциональной зависимости выходов заряженных частиц разных типов для установления механизмов рождения в указанной энергетической области и поиска возможного влияния эффектов, связанных с фазовым переходом или наличием критической точки КХД.
3. Работа по анализу данных второго этапа программы энергетического сканирования детектора STAR. Измерение выходов частиц в зависимости от энергии столкновения при энергиях 27, 19.5 ГэВ и подсчет для оценки влияния ядерной среды на рождение заряженных частиц (jet quenching эффект). Количественные измерения влияния ядерной среды на рождение частиц (R_{CP}, R_{AA}) в центральных событиях столкновения ядер. Подбор необходимых условий отбора треков заряженных частиц для минимизации систематической погрешности.
4. Работа по анализу данных второго этапа программы энергетического сканирования детектора STAR. Измерение выходов частиц в зависимости от энергии столкновения при энергиях 7.7 – 14.5 ГэВ для оценки влияния ядерной среды на рождение заряженных частиц (jet quenching эффект). Подсчет интегральных выходов заряженных частиц.
5. Определение функциональной зависимости выходов заряженных частиц разных типов для установления механизмов рождения в указанной энергетической области и поиска возможного влияния эффектов, связанных с фазовым переходом или наличием критической точки КХД. Подготовка необходимого программного кода для работы с данными Монте-Карло моделирования и экспериментальными данными STAR.
6. Освоение необходимого программного и физического минимума. Работа с модельными данными (UrQMD) для подсчета объемных характеристик среды, образующейся в

столкновениях тяжелых ионов (закрученность, киральность). Подсчет скоростных характеристик рождения странных частиц: поляризация, вортисити, на примере лямбда гиперонов. Обучение подсчету указанных характеристик на экспериментальных данных установки STAR.

7. Освоение необходимого программного и физического минимума. Анализ данных программы энергетического сканирования установки STAR для восстановления импульсных спектров заряженных частиц. Количественные измерения влияния ядерной среды на рождение частиц (R_{CP}) в центральных событиях столкновения ядер. Подбор необходимых условий отбора треков заряженных частиц для минимизации систематической погрешности. Освоение систем распределенного написания программного кода GitHub и администрирование проектов группы на данной платформе.
8. Следует отметить, что уже подготовлено несколько докладов на конференциях для молодых ученых и планируется доклад по анализу спектров и измерению R_{CP} на совещании коллаборации STAR в марте 2021 года.

На 2021 год запланированы следующие работы:

- Участие в проведении сеанса по программе энергетического сканирования BES II в коллайдерной моде и в экспериментах с фиксированной мишенью. Анализ данных и поиск сигнатур фазовых переходов и критической точки КХД.
- Исследование фемтоскопических корреляций, структуры событий и скейлинговых свойств ядерных взаимодействий, глобальной поляризации, событий с большими p_T.
- В качестве задачи по фемтоскопическим корреляциям предполагается начать изучение пространственно-временных характеристик рождения частиц, включая пространственно-временные характеристики асимметрий в $\pi^+\pi^-$, πK и πp системах.